T.C.
AYDIN ADNAN MENDERES UNIVERSITY
GRADUATE SCHOOL OF NATURAL AND APPLIED SCIENCES
MASTER'S PROGRAMME IN ORGANIC CHEMISTRY

PREPARATION OF NEW BIO-BASED EPOXY-NANOCOMPOSITE COATINGS REPLACMENT OF BPA (BISPHENOL A)

SAMER OBAID HASAN HASAN

MASTER'S THESIS

SUPERVISOR

Assoc. Prof. Dr. Ilknur BABAHAN BIRCAN

This thesis was supported by Aydın Adnan Menderes University Scientific Research Projects Unit (Project number FEF20021)

AYDIN -2021

ACKNOWLEDGEMENTS

First of all, I would like to thank ALLAH who helped me and made it easy for me. I would like to thank my supervisor, **Assoc. Prof. Dr. Ilknur BABAHAN BIRCAN,** for her dedicated support and guidance, whose encouragement has been invaluable throughout this study.

As a special thanks, I must express my very profound gratitude to my parents, who set me off on the road to this MSc a long time ago, for providing me with unfailing support and continuous encouragement throughout my years of study, this accomplishment would not have been possible without them.

Most importantly, I wish to thank my loving and supportive wife, who provides me with unending inspiration.

TABLE OF CONTENTS

LIST OF SYMBOLS AND ABBREVAITIONS

^{13}C-NMR : Carbon NMR Spectroscopy

^{1}H-NMR : Proton NMR Spectroscopy

AHEW : Amin H Equivalent Weight

AR : Androgen Receptor

BHMF : 2,5-bis(hydroxmethyl)furan

BOB : 2,5-Bis[(2-oxiranylmethoxy)methyl]-benzene

BOF : 2,5-bis(oxiran-2-ylmethoxymethyl)furan diepoxy resin

BPA : Bisphenol A

BPF : Bisphenol F

BPS : Bisphenol S

BTCA : 1,2,4- Benzene Tricarboxylic Anhydride

CHDA : 1,2- Cyclohexane Dicarboxylic Anhydride

CNFs : Carbon Nanofibers

CNTs : Carbon Nanotubes

D230 : Poly(propyleneglycol)-bis (2-aminopropyl ether)

DDA : Dicyandiamide

DGEBA: Diglycidyle Ether of Bisphenol A

DGEBF: Diglycidyle Ether of Bisphenol F

DGF : 2,5-Furandicarboxylic Acid

DGFA : N,N-diglycidyl-furfurylamine

DGT : Terephthalic Acid

DSC : Differential Scanning Calorimetry

ECAs : Electrically Conductive Adhesive

ECH : Epichlorohydrine

ECN : Epoxy Cresol Novolac

EEW : Epoxy Equivalent Weight

EMI : Electromagnetic Interference

EPN : Epoxy Phenol Novolac

ER : Estrogen Receptor

ERs : Epoxy Resins

ESO: Epoxidized Soyabean Oil

ETO: Epoxidized Tung Oil

FDCA: Furan Dicarboxylic Acid

GMA : Glycidyl Methacrylate

GNPs : Graphene Nanoparticules

GO : Graphene Oxide

H_2O_2 : Hydrogen Peroxide

HMF : 5-hydroxymethylfurfural

IR : Infrared Spectroscopy

JEFFAMINE ED900: Difunctional Polyetheramine

JEFFAMINE T403: Trifunctional Polyetheramine

MBCBE: Mannich Base of Cardanol Butyl Ether

MHHPA: Methylhexahydrophthalic Anhydride

MRI : Magnetic Resonance Imaging

MWCNTs: Multi-Wall Carbon-Nanotubes

OBCA : Oxabicyclodicarboxylic Anhydride

PACM : 4,4-methylene bis cyclohexamine

PANI : Polyaniline

PBO : Poly (p-phenylene-2,6-benzobisoxazole)

PCB : Printed Circuit Board

PNP : Polynuclear Phenol Epoxy

SWCNTs: Single-Wall Carbon Nanotubes

Tg : Glass Transition Temperatures

TGA : Thermogravimetry Analysis

TGMDA: Tetraglycidyl Methylene Dianiline Epoxy

UV : Ultraviolet Radiation

LIST OF FIGURES

LIST OF SCHEMES

LIST OF TABLES

ÖZET

BPA (BİSFENOL-A)'A ALTERNATİF YENİ BİYO-BAZLI EPOKSİ-NANOKOMPOZİT KAPLAMALARIN ELDE EDİLMESİ

HASAN.S.O.H. Aydın Adnan Menderes Üniversitesi, Fen Bilimleri Enstitüsü, Organik Kimya Programı, Yüksek Lisans Tezi, Aydın, 2021.

Amaç: Bu çalışmanın amacı, alüminyum tabanlı metalik yüzeyler için Bisfenol-A(BPA)'ya alternatif olarak yeni biyobazlı epoksi-nanokompozit kaplamaların elde edilmesi.

Materyal ve Yöntem: Bu çalışma, Ocak-Aralık 2020 tarihleri arasında Aydın Adnan Menderes Üniversitesi, Kimya Bölümünde (Aydın, Türkiye) gerçekleştirilmiştir. İlk aşamada, epoksi fonksiyonelleştirilmiş tung yağı (ETO), tung yağının, glisidil metakrilat (GMA) ile 2,4,6-tris (dimetilaminometil)fenol ve fenotiyazin varlığında Diels-Alder reaksiyonu ile sentezlenmiştir.

Daha sonra, yeni epoksi-nanokompozit kaplamalar, epoksi fonksiyonelleştirilmiş tung yağı'nın (ETO) çapraz bağlama ajanı olan iki farklı polieteramin ile (Jeffamine T403 ve ED900) reaksiyonundan, nanopartikül olarak grafen, fulleren ve karbon nanotüpler (CNT'ler) kullanılarak başarıyla elde edilmiştir. Kürlenme sıcaklığı olarak 4 farklı sıcaklık kullanılmıştır.

Bulgular: Epoksi reçine ve yeni nanokompozitlerin karakter analizleri IR, ^{1}H NMR, ^{13}C NMR, DSC ve TGA teknikleri kullanılarak yapılmıştır. Epoksi-amin nanokompozitlerin 420 ^{o}C'ye kadar termal karaklılık gösterdiği TGA analizi ile tesbit edilirken, bu sertleşmiş filmlerin, DSC analizlerinde camsı geçiş sıcaklıkları (Tg) gözlenmemiştir. Elde edilen yeni epoksi-nano kaplamaların mekanik özellikleri, sarkaç sertliği, kalem sertliği, çapraz yapışma, çekme yapışma ve darbe direnci gibi farklı testlerle tesbit edilmiştir. Genel olarak, epoksi-amin nanokompozitlerden 120 $^{\circ}$C'de CNT ile hazırlanan kaplamalar en yüksek sarkaç sertliği değerlerine sahip olurken, diğer mekanik özellikler açısından herhangibir farklılık gözlenmemiştir. Tüm sistemler, ASTM standartlarına göre iyi çapraz yapışma (5B), kalem sertliği (> 6H), çekme yapışması (> 2 lb/in^{2}) ve darbe dirence (> 40) özelliklerine sahiptir.

Sonuç: Yeni epoksi-amin nanokompozit kaplamalar mükemmel termal kararlılık sergilemiştir. Ayrıca, tüm kürlenmiş filmler, iyi yapışma, sertlik ve darbe direnci özelliklerine sahiptir. Mükemmel termal kararlılık ve iyi mekanik özelliklerinden dolayı yiyecek ve içecek kutularının iç yüzeylerinde kullanılan BPA esaslı epoksi kaplamalara alternatif olabilirler.

Anahtar Kelimeler: Tung yağı, Biyo bazlı epoksi kaplamalar, Nano kompozitler, Jeffamine T403 ve Jeffamine-ED900, BPA.

ABSTRACT

PREPARATION OF NEW BIO-BASED EPOXY- NANOCOMPOSITE COATINGS REPLACMENT OF BPA (BISPHENOL A)

S.O.H. HASAN. Aydın Adnan Menderes University, Graduate School of Natural and Applied Sciences, Organic Chemistry Program, Master Thesis, Aydın, 2020.

Objective: The aim of this study is to synthesize new biobased epoxide-nanocomposite coatings as an alternative to BPA for aluminum surfaces.

Material and Methods: The study was conducted in Aydin, Turkey, between January-December 2020. In the first step, epoxy functionalized tung oil (ETO) was prepared from the reaction of tung oil with glycidyl methacrylate (GMA) in the presence of phenothiazine as a catalyst via the Diels-Alder reaction. Subsequently, these new epoxide-nanocomposite coatings were successfully synthesized from the reaction of an epoxy functionalized tung oil (ETO) and two different polyether amines (Jeffamines T403 and ED900) as cross-linking agents, catalized by 2,4,6-tris (dimethylamino-methyl) phenol, premixed with graphene, fullerene, and carbon nanotubes (CNTs) as nanoparticles. Four different curing temperatures were applied.

Results: Epoxide resin and the new nanocomposites were identified via ^{1}H NMR, ^{13}C NMR, IR, DSC and TGA analyses. While thermal stability of epoxide-amine nanocomposites are observed up to 420 °C according to TGA analysis, these cured films are displayed no glass transition points (Tgs) by DSC. The determination of the mechanical properties of the resulting nano coatings was accomplished by pendulum hardness, pencil hardness, cross-hatch adhesion, pull-off adhesion, impact and reverse impact resistance tests. Whereas, the epoxide-amine nanocomposite systems at 120 °C with CNT have the highest pendulum hardness values, there are no big differences in terms of the other mechanical properties. The all systems display good crosshatch adhesion (5B), pencil hardness (> 6H), pull-off adhesion (> 2 lb/in^2), impact and reverse impact resistance (> 40) according to the ASTM standards.

Conclusion: New epoxide-amine nanocomposite coatings exhibit excellent thermal stability. All the cured films showed good adhesion, hardness, and impact resistance properties. They can be used as alternative coatings instead of BPA based epoxy resins in various coating systems in food and beverage industries due to their excellent thermal stability and good mechanical properties.

Keywords: Tung oil, Bio-based epoxide coatings, Nano composites, Jeffamine T403 and Jeffamine-ED900, BPA.

.

1. INTRODUCTION

Epoxy coatings have gained great importance in recent years due to their versatility in various industrial fields due to their unique properties such as chemical and mechanical resistance, thermal stability, excellent adhesion property, conductivity, electrical insulation, high wear resistance, low shrinkage, low toxicity and low price as well (May, 1988; Ellis, 1993).

Accordingly, these coatings have been used in many fields of industry such as the automobile, ships and aerospace industries as distinct coatings (Guo, 2012). In addition to being used in the manufacture of electronic and electrical circuits, it has also been used in the civil engineering sector in building bridges, coating factory floors, and adhesives for all metals and stones. Finally, it has been widely used in the medical field in the manufacture of dental fillings and prostheses for people with special needs.

One of the negative aspects of these coatings is that they contain BPA in the backbone for the installation of these coatings, which in turn causes many risks to human health and environmental pollution due to exposure that occurs when using these coatings, which made polymer scientists and researchers in this field work to find Bio-based alternatives to Bisphenol A are harmless to the environment and human health (Ortiz et al., 2019).

Bisphenol A is considered a toxic substance that causes various human diseases such as endocrine disruption, cancers, heart disease and obesity, male and female hormonal imbalance, type II diabetes if a person is exposed to it in large proportions according to reports issued by the World Health Organization and the Health and Drug Organization American and European (Meli et al., 2020).

Recently, many nanomaterials have been added to these coatings such as carbon fibers, carbon nanotubes, fullerene, graphene, as well as inorganic nanomaterials in order to improve their properties due to the structure that these nanomaterials give to epoxy coatings (Ahmadi, 2019).

1.1. Epoxy Resins

Epoxy is a prefix refers to a three-membered heterocyclic ring consist of two carbon atoms bonded to an oxygen atom in such away to from a planar bridge molecule which is the functional group of chemical compounds known as oxirane, ethoxyline or glycidyl group (Hartman, 1984).

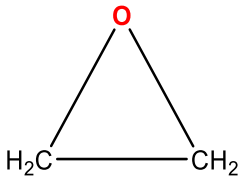

Figure 1. Structure of Oxirane

Oxirane was discovered by Wurtz in 1859 from the reaction of chlorohydrin aqueous alkali as given scheme 1. (Ellis, 1993).

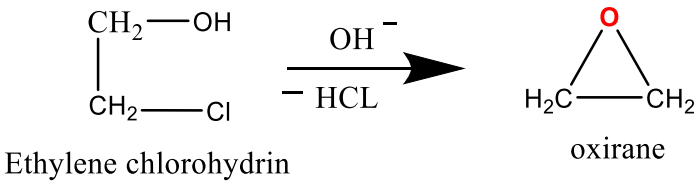

Scheme 1. Reaction of Ethylene Chlorohydrin with Aqueous Alkali

This epoxy group represents apart of an aliphatic, cycloaliphatic, aromatic and or heterocyclics molucular structure of the epoxy resin oligomers (monomers), which are fairly reactive chemical structures.

In general, epoxy resins contain two or more sets of epoxide groups which are reacting with the curing agents molecules to give a three-dimensional network in the curing process (Meijer, 1989).

The non-epoxy part of the oligomers molecules is a hydrocarbon residue such as an aliphatic, cyclic-aliphatic, aromatic group, or it might also be non-hydrocarbon and polar group (May, 1988).

The cured epoxy resins or poly epoxides are insoluble and intractable solid thermosetting chemical substances of two components, resin backbone and hardener, characterized by the inability to be reformed by heating after turning into thermoset solid due to the formation of long polymeric chains intertwined with each other (May, 1988).

The reaction of the epoxy group of epichlorohydrine with bisphenol A produces diglycidyle ether of bisphenol A (DGEBA), which is the reactive monomers, scheme 2. (Brydson, 1999).

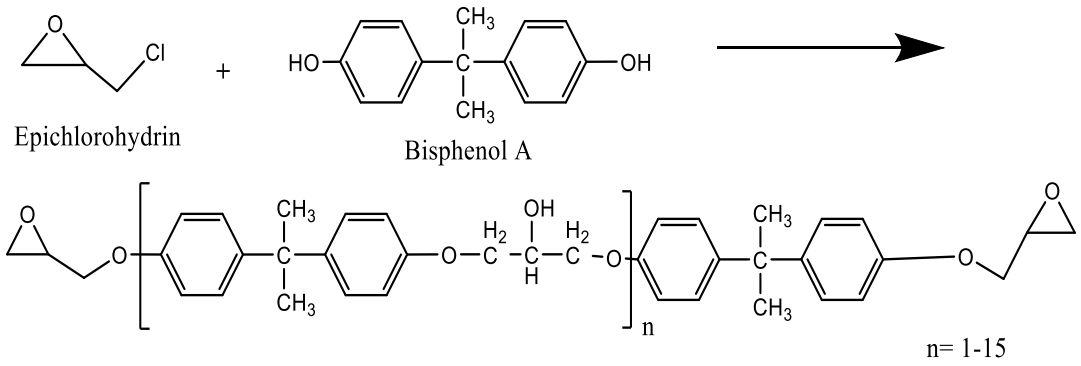

Scheme 2. The Formation of Diglycidyl Ether of Bisphenol A (DGEBA) From The Reaction of Epichlorohydrin with Bisphenol A

The first attempted preparation of resins from epichlorohydrin was reported by the German chemist Schrade in 1927. Later on, the condensation of epoxies with amine was patented by I.G. Farben in 1939, (German patent NO.676117). P. Castan described the condensation of epoxy resin with dibasic acid in 1943, (US patent NO. 2324483) (Pradhan et al., 2016). The most important class of commercial epoxy resins is firstly produced from the reaction of Bisphenol A (BPA) and epichlorohydrin in the presence of NaOH, which is called diglycidyl ether of bisphenol A (DGEBA), which represents approximately more than 75% of the commercially produced thermosetting plastics (Auvergne et al, 2014; Muroi, 1988).

(DGEBA) resin undergoes a wide range of chemical reactions with variety of reactive molecules as curing agents such as amines, polyamides, phenoles, polymercaptans, imidazole, carboxylic acid and anhydrides to produce the cured products of different chemical, physical, mechanical and reological properties, via ring opening reaction of the reactive epoxy group (Ellis, 1993).

1.2. Properties of Epoxy Resins

Epoxy resins have relatively high resistance to friction, acidic and basic chemicals, or solvents, excellent electrical insulation properties and ambient moisture resistance. In addition, they have a distinctive adhesion characteristic, low shrinkage, low prices, low toxicity, significant corrosion resistance, optimal and durable resistance to chemically aggressive environment such as seawater (Ebnesajjad, 2011; Unnikrishnan, 2006).

Owing to their exceptional hardness, distinctive adhesion, significant toughness, dimensional stability and strength due to the presence of ethers and hydroxyl group, they were used in various applications that require high functional performance (Adachi et al., 2002).

The addition of other ingredients in the formulations, such as solvents, thinners, elastic plasticizers and accelerators are modifying the properties of the resin (Kwan, 1998). Although epoxy resins are more expensive than polyester and vinyl ester resins but they possess better mechanical properties, higher resistance to moisture absorption, corrosive media and environments (Mezzenga, 2001).

They have high electrical sensitivity, heat resistant, optimal adhesion properties to several substances and to fibers of the reinforce in composite material (Camille François et al., 2017). Moreover, epoxy resins are showing low shrinkage through the curing process, their volumetric shrinkage is less than 5% whereas the shrinkage to polyester and vinyl ester is in the range 5-12% and 5-10% respectively (Zarrelli et al., 2002).

They have great versatility to adapt physical, mechanical processing properties via modification of the resin or addition of specific agent such as fire retardant, toughening agent, carbon nanotubes or metal ions. Hence epoxy coatings are used as protective material, adhesives and fiber-reinforced polymer composites, however, the disadvantage aspects of these resins are included in their poor resistance to crack growth, brittleness, low UV resistance and post-cure requirement at high temperature (Kotnarowska, 1999; Jana and Zhong, 2007; Liu et al., 2012).

1.3. Types of Epoxy Resins

Epoxy resins are divided into Petro-based and bio-based resins according to their original precursors of the epoxy groups.

The Petro-based epoxy resins are divided according to their molecular structure and fields of application to glycidyl resins, in particular glycidyl ether, glycidyl ester and glycidyl amine and/ or nonglycidyl resins particularly aliphatic and cyclic resins (Boyle et al., 2001; Gibson, 2017; Tripathi, 2011).

1.3.1. Glycidyl Ether Epoxy Resins

Epichlorohydrin reacts with polyhydroxy compounds to produce glycidyl ether resins. A number of other polyhydroxy compounds have been used in addition to the prevalent application of bisphenol A.

There are many types of commercially produced glycidyl ether resins of bisphenol A (DGEBA). Which are used in a wide range of applications. The monomers of (DGEBA) a**r**e synthesized via the reaction of epichlorohydrin with bisphenol A in presence of stoichiometric amount of sodium hydroxide at ca 75 °C as shown in scheme 3) (Brydson, 1999; Gannon, 1986; Gonza´lez et al., 2011).

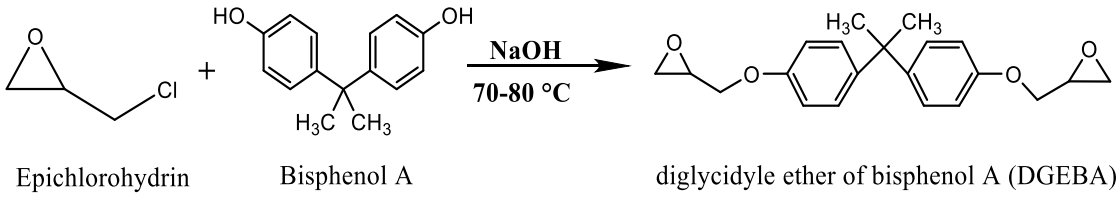

Epichlorohydrin Bisphenol A diglycidyle ether of bisphenol A (DGEBA)

Scheme 3. Synthesis of Diglycidyl Ether of Bisphenol A (DGEBA) From The Reaction of Epichlorohydrin with Bisphenol A

The higher molecular weight DGEBA resins are produced when further reaction of bisphenol A with the resulting DGEBA monomers is proceeds if limited amount of epichlorohydrin is supplied in the reaction system.

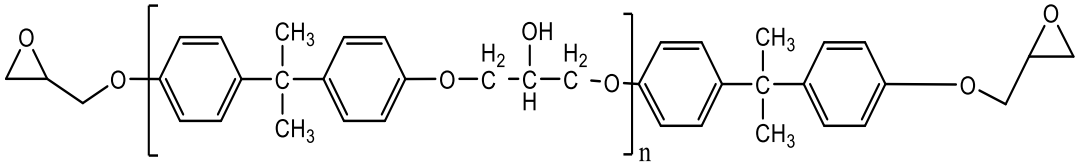

Figure 1. Diglycidyl Ether of Bisphenol A (DGEBA) Resin

Another bifunctional phenol such as bisphenol F, bis (4-hydroxyphenyl) sulfone is used to produce specific glycidyl ether resins analogues to DGEBA by the reaction of epichlorohydrin with them (Figure 3).

Both bisphenol F, and Bisphenol S can be used in the formation of epoxy resins to obtained several advantages such as low viscosity and higher mean epoxy content than that of the ERs produced through bisphenol A.

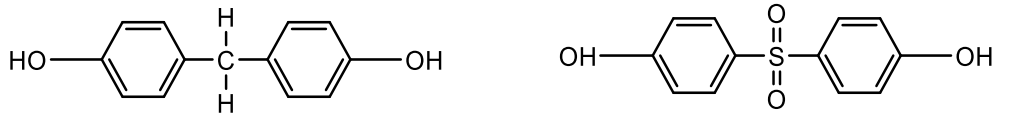

4,4'-methylenediphenol (Bisphenol F)

4,4'-sulfonyldiphenol (Bisphenol S)

Figure 3. Structures of Bisphenol F, and Bisphenol S Epoxy Resin is Similar to Bisphenol A

In order to produce a higher density cross-linked glycidyl ether epoxy resin, polyphenol which is the product of the reaction of phenol and excess formaldehyde, is used instead of BPA. Therefore, the reaction of polyphenol with excess of ECH produces stiff resin of high viscosity, excellent chemical resistance and high heat properties, known as epoxy phenol novolac resin (EPN). The excess amount of ECH is needed to minimize the side reaction of the hydroxyl group with the resulted epoxy group as given in scheme 4 (Fiore and Valenza, 2013).

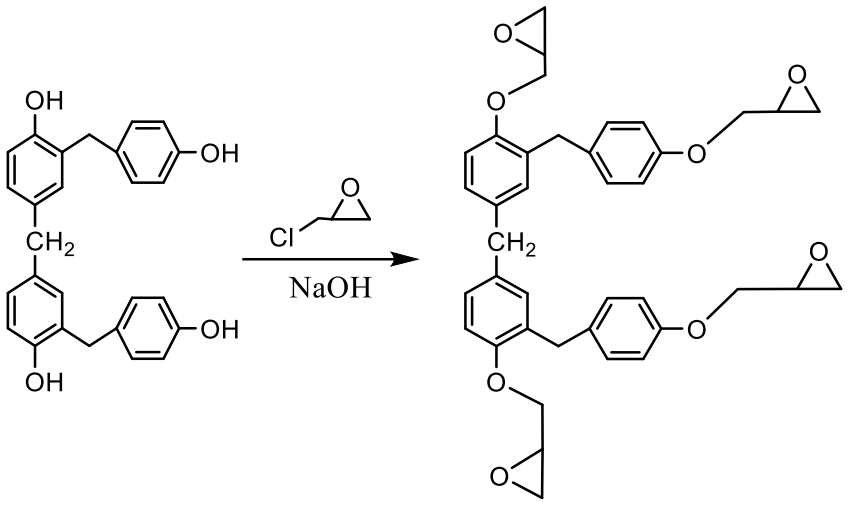

Scheme 4. Synthesis of Epoxy Phenol Novolac (EPN) Resin from Poly Phenol with Epichlorohydrin

Similarly, polynuclear phenol epoxy resins (PNP) with four epoxy groups are produced via reaction of excess ECH with tetrakis(4-hydroxyphenyl) ethane. (Figure 4) (Fiore and Valenza, 2013).

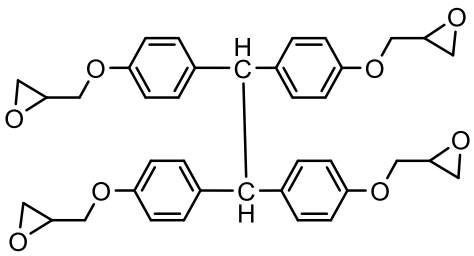

Figure 4. Structure of Polynuclear Phenol Epoxy (PNP)

Epoxy novolac resins such as epoxy phenol novolac (EPN) and epoxy cresol novolac (ECN) are produced via the reaction of excess ECH with phenol and/or cresol in some process of bisphenol A synthesis as given scheme 5. (Green Lee, 1950; Fiore and Valenza, 2013).

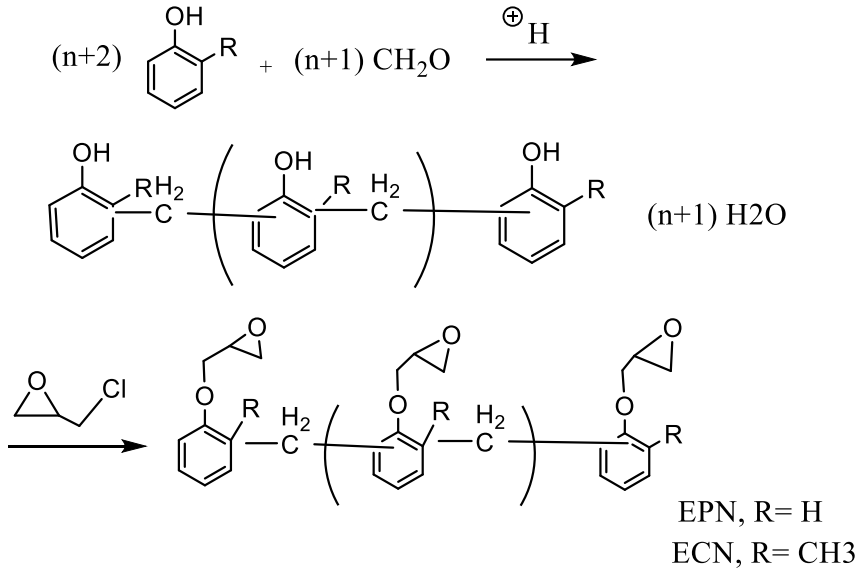

Scheme 5. Synthesis of Epoxy Phenol Novolac and Epoxy Cresol Novolac

One of the glycidyl ether resin is the product of epoxidation of tetrakis(4-hydroxyphenyl) ethane which is a product of glyoxal reaction with phenol (Schwartzer, 1957).

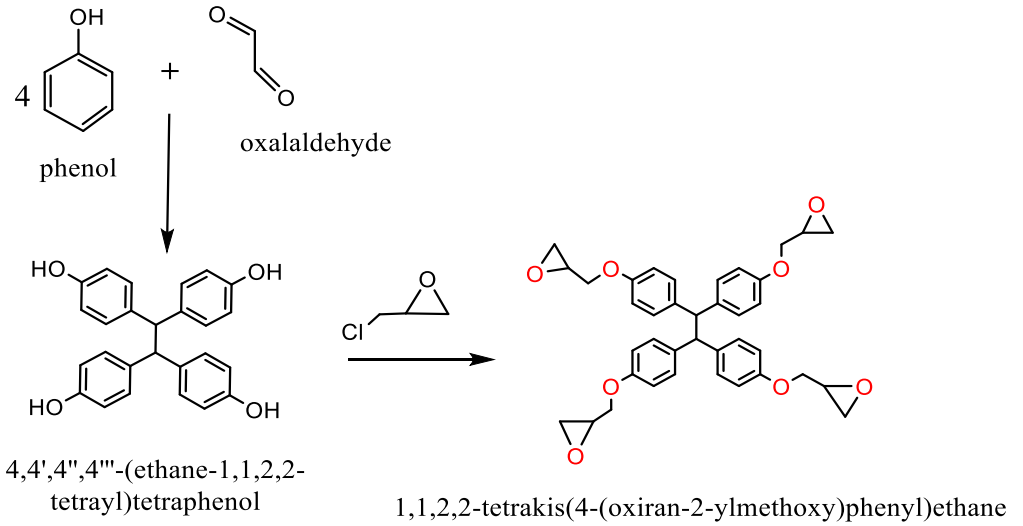

Scheme 6. Synthesis of Tetraglycidyl Ether of 1,1,2,2-Tetrakis(4-(Oxiran-2-Ylmethoxy)Phenyl) Ethane

1.3.2. Glycidyl Amine Epoxy Resin

Aromatic glycidyl amine resins are containing an aromatic amine residue in their structure, of these commercially available resins are triglycidyl ether of P- amino phenol and methylene dianiline resins, (Reinking et al., 1960).

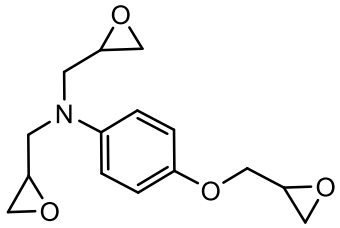

Figure 5. Structure of Triglycidyl – P-Aminophenol

In addition, an epoxy resins with higher functionality compared with DGEBA and DGEBF can be synthesized by the reaction of ECH with variety aromatic amines (Campbell, 2010) For example, in (Scheme 7) reacts with ECH to produce tetraglycidyl methylene dianiline epoxy (TGMDA).

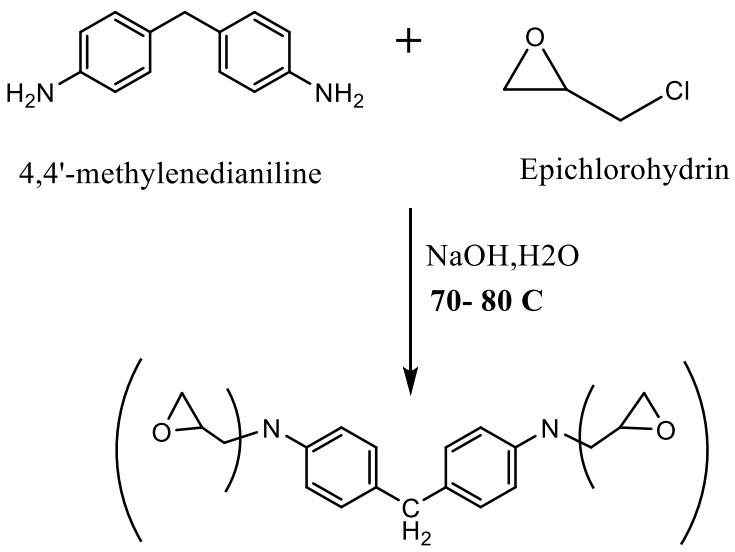

Scheme 7. Synthesis of Tetraglycidyl Methylene Dianiline Epoxy (TGMDA)

1.3.3. Epoxy Glycidyl Ester

Glycidyl esters are synthesized via the reaction of various carboxylic acid and epichlorohydrin and dehydrohalogenation of the resulting product by sodium hydroxide, as illustrated by the reaction of hexahydrophthalic anhydride, scheme 8 (Pham, 2011).

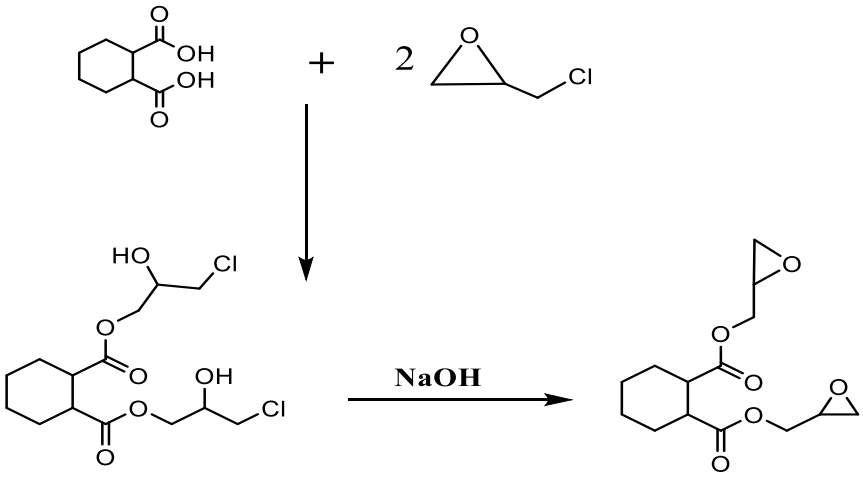

Scheme 8. Synthesis of Diglycidyl Ester of Hexahydrophthalic Acid

Epoxy vinyl esters are developed by Dow chemical a Shell chemical in the 1970s, particularly those with high properties such as chemical resistance and good mechanical properties, (Anderson et al., 1980). The prepolymers are made from the reaction of acrylic acid with DGEBA and/or epoxy novolac. The required epoxy resins are produced via free radical polymerization reaction of the double bonds of prepolymer and styrene using peroxide as initiator. The following reaction of DGEBA with acrylic acid and them with styrene in presence of peroxide is an example of these reactions as shown scheme 9.

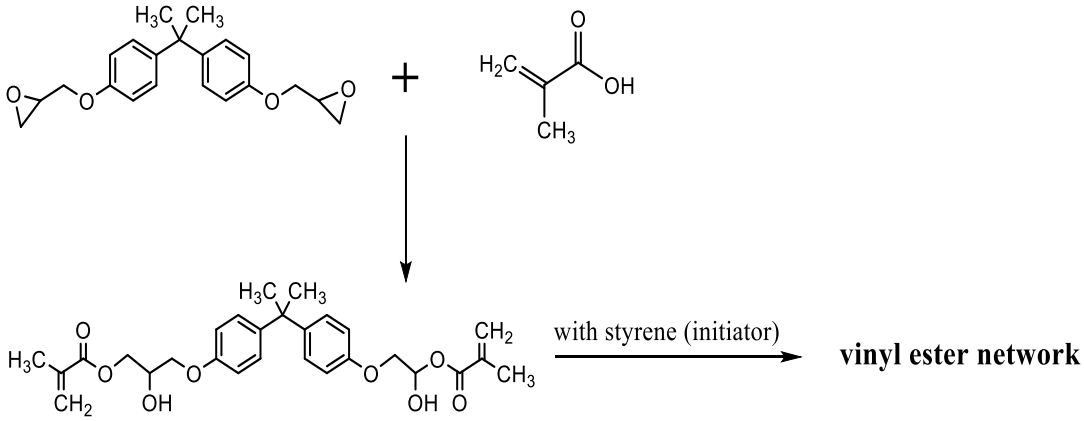

Scheme 9. Synthesis of Epoxy Vinyl Ester

Glycidyl methacrylate (GMA) resins is a dual functionality monomer, the terminal epoxy and the double bond of the acrylic molecule is an important commercially available product. This resin is resulted from the reaction of ECH with acrylic acid.

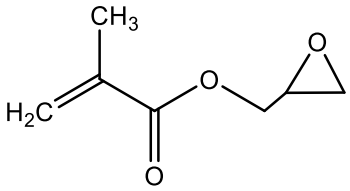

Figure 6. Structure of Glycidyl Methacrylate (GMA)

Epoxy acrylate resins is the precursors of the epoxy acrylate oligomers, which undergo free radical polymerization of the acrylate C=C bonds (Webster, 1997). (DGEBA) is almost always used to produce epoxy acrylate by the reaction of the hydroxyl group of bisphenol A with the epoxy group of the acrylate monomers, as given in figure 7.

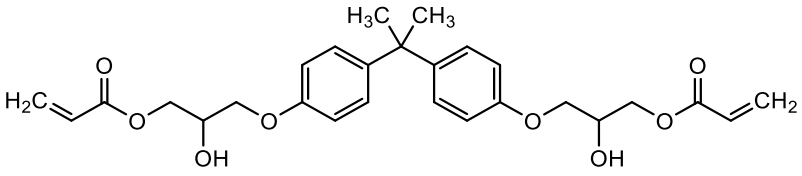

Figure 7. Structure of Epoxy Acrylate

1.3.4. Non Glycidyl (Cycloaliphatic) Epoxy Resin

Cycloaliphatic epoxy resins, with high heat aberration and excellent electrical properties at high temperatures, were used in printed circuit board (PCB) industries. In recent years, and they are used as significant out door electrical insulation for outdoor and indoor power equipment such as motors and switchgears (Kumagai and Yoshimura, 2000).

Furthermore, when compared to other epoxy resins on the market, these resins have a low viscosity, a high chemical resistance, and good mechanical properties. As an example of these resins is given in Scheme 10 (Fiore and Valenza, 2013).

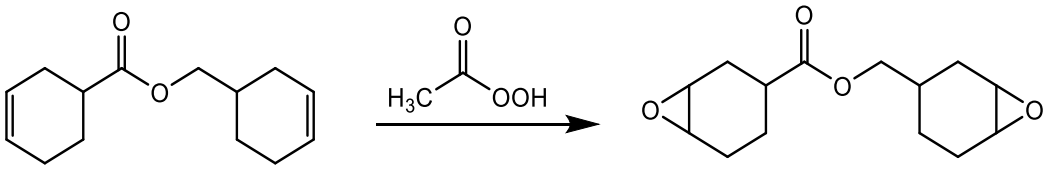

Scheme 10. Structure of 3,4-Epoxycyclohexylmethyl-3,4-Epoxycyclohexane Carboxylate

1.4. Curing Agents of Epoxy Resins

Curing agents (hardeners or crosslinkers) is a term referring to the reactive materials which undergo easy and fruitful reactions with the epoxy groups incorporated in the epoxy resins monomers to produce hard infusible thermoset polymers. The characteristic properties of the thermosets such as, mechanical, chemical, electrical, flame retardant and heat resistance are greatly depending on the nature and amount of the curing agents in addition to the pot life, curing temperature, rate of curing reaction, and the number and location of the epoxy groups in the structure of the epoxy prepolymers (Capricho et al., 2020).

Curing epoxy resins may be achieved at room temperature or, more frequently, with moderate heating to speed up and boost the reaction. The curing process of epoxy resins is an exothermic reaction that, if not regulated, can generate enough heat to cause thermal degradation. (Pham, 2011).

According to their origin the curing agent can be divided to either Petro-based compounds or bio-based natural renewable products. On the other hand, hardeners are classified according to their chemical structure and elemental constitution. Duo to the exceeding concern over sustainability environmental considerations and wast disposal a great interst and attention was given to explore a natural and renewable resources as alternatives to both epoxies derived from BPA as petrochemical materials and the Petro-based curing agents to satisfy the requirement for restorable cost and eco-friendliness. (Ma, 2016).

1.4.1. Nitrogen- Containing Curing Agents

Various nitrogen-containing compounds are widely employed as curing agents such as primary, secondary and tertiary aliphatic amines, aromatic amines, imidazole, urea, hydrazine and hydrazides (Sabu Thomas, 2014).

1.4.1.1. Amines

Primary and secondary amines are widely used as highly reactive curing agents at ambient temperature. Their reactivity is owing to the presence of unshared electron pair possessing potent nucleophilicity towards the electrophilic methylene site of the epoxy group and the presence of the active hydrogen to protonate the oxygen atom (Sabu Thomas, 2014).

On the other hand, at room temperature, most tertiary amines have slow reaction rates with epoxy resins. As a result, tertiary amines are commonly used as acceleration catalysts for the curing at elevated temperature cured systems. The hydroxy group of phenolic compounds played an important role in the curing process. The most widely used tertiary amines, such as dimethylaminomethyl phenol and Tris(dimethylaminomethyl) phenol (Ellis, 1993; Pham, 2011). Also, there are other types of amine derivatives that are used as treatments in the manufacture of epoxy coatings such as polyaminoimidazoline, polyamide, Mannich bases, ketimines, acrylonitrile adducts, polyetheramines, alicyclic aliphatic amines, biguanide and dicyandiamide,

1.4.2. Curing Agents Containing Oxygen

The second most common form of curing agent for epoxy resins is carboxylic acid functional polyesters and anhydrides. The first curing agents used for epoxy resins were dicarboxylic acid anhydrides, they have gained widespread commercial significance uses. When acid anhydrides are used as curing agents, however, crosslinking temperatures as high as >200 ˚C are needed, and the mechanism is very complex (Capricho et al., 2020).

1.4.3. Curing Agents Containing Sulphur

In an addition reaction, the thiol group (-SH) can react with epoxy resin. This necessitates the use of amines to catalyze the production of reactive mercaptide ions at room temperature as shown in the Scheme 11.

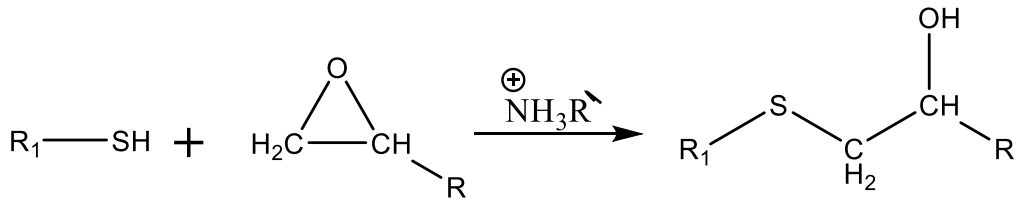

Scheme 11. Reaction of Epoxy with Thiol

The primary and tertiary amines are used as initiators with mercaptan curing agents for the cross-linking of di-functional bisphenol A epoxy resins (Ellis, 1993). Polysulphides with low mercaptan content were found to be effective curing agents for epoxy resins. Epoxy-polysulphide solutions are primarily used in construction adhesives. Several attempts have been made to commercialize other mercaptan-curing agents due to the mercaptan group's appealing reactivity characteristics with epoxy resins. Diamond Chemicals (1968) produced a number of tri-functional polymercaptans for specific applications. At low temperatures and in thin films, the inherent beta-hydroxy groups stimulate the mercaptan groups, resulting in high reactivity. These polymercaptans also provide the high lap shear adhesion needed for patch repair adhesive and structural concrete bonding applications when used at high loadings relative to the tertiary-amine co-catalyst (Ellis, 1993).

1.5. Bio-Based Curing Agents

Renewable materials such as plant oils, imidoamino, tung oil, acids and acid anhydrides, phenol, lignin, rosin acid and terpenes are known as bio-based curing agents and have been used extensively in the hardening of both Petro-based and bio-based epoxy resins (Ding and Matharu, 2014).

1.5.1. Cardanol- Based Curing Agents

Cardanol- based curing agent is a Mannich base of cardanol butyl ether (MBCBE) was used for efficient curing of the DGEBA associated with significant improvement of impact strength lab shear strength and viscosity compared with phenalkamine- curing agent (Huang et al., 2012).

1.5.2. Citric Acid-Based Curing Agents

Unique curing of epoxidized soyabean oil (ESO) was achieved by using aqueous solution of citric acid without co-catalyst to produce completely green polymers (Alltuna et al., 2013).

1.5.3. Rosin- Based Curing Agents

Maleopimaric acid and methyl Maleopimaric acid have been synthesized from rosin acid and were used as environmentally friendly curing agents to cure epoxy resins. The rosin- cured thermosets exhibit higher Tg and lower thermal degradation compared with those cured by 1,2-cyclohexane dicarboxylic anhydride (CHDA) or 1,2,4- benzene tricarboxylic anhydride (BTCA). (Wang et al., 2008). Hence it is clear that rosin- based curing agent is an excellent eco- friendliness alternative hardener for the aromatic Petro-based hardeners (Chrysanthos et al., 2011).

1.5.4. Furan- Based Curing Agents

Furfural is naturally produced from corncobs has been used as a precursor to produce oxabicyclodicarboxylic anhydride (OBCA) as a bio- based curing agent via series of chemical reactions as given in Scheme 12.

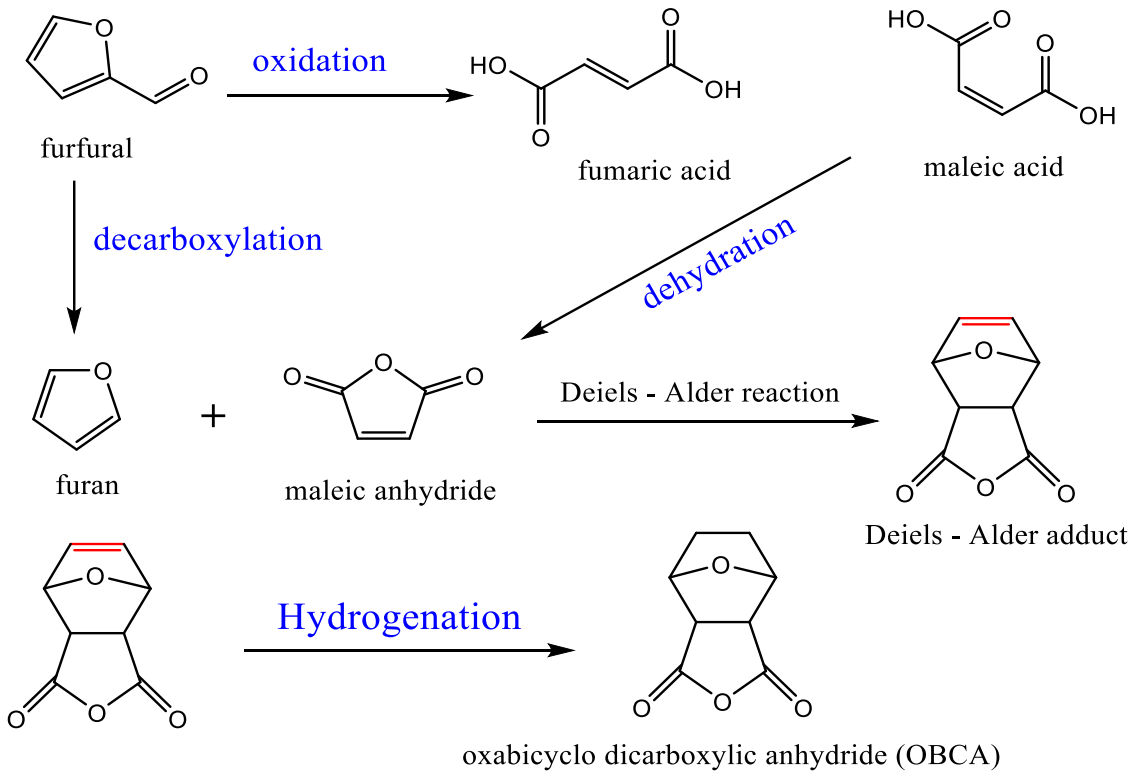

Scheme 12. Synthesis of Furfural-Based Curing Agent (OBCA)

The OBCA is consider as excellent curing agent for epoxy resins if compared with Petro-based cyclohexanedicarboxylic anhydride which is more suitable for industrial applications (Tachibana et al., 2014).

1.6. Curing Process

The concept of curing is defined as the process of changing the prepolymer (monomer) into thermosetting polymers via chemical reaction with reactive substances called the hardener (curing agent), since both the prepolymer and the hardeners are chemically stable before mixing, but the

one-part system is also existing. One part epoxy systems are a mixture of epoxy resins, dicyandiamide (DDA) as a latent curing agent and N-(4-chlorophenyl)-N'N'-dimethylurea as accelerator. The curing of these system is accomplished at around 100-120 °C instead of 180-200 °C (Sharma, 2011).

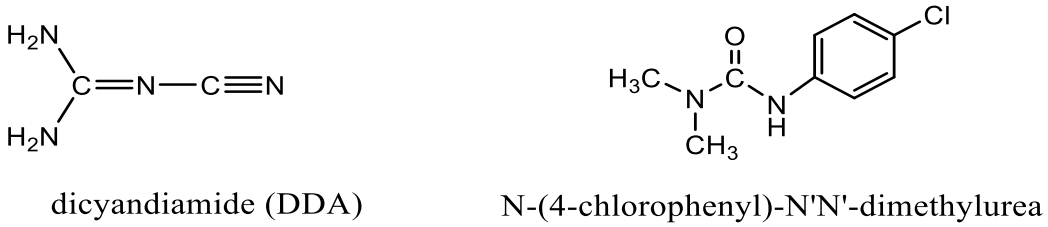

Figure 8. Structure of Epoxy/DDA/ Monuron (One-Part Epoxy System)

The curing process of epoxy resins takes place through a fruitful reaction between the terminally or internally located reactive epoxy groups of the epoxy resin monomers with variety of nucleophilic and electrophilic reagents such as amines, carboxylic acids and anhydrides, phenol, imidazole, polymercaptans, urea, isocyanate. The presence of the highly strained three- membered epoxy ring imparts potent role to the curing reaction and the required curing temperature (Pritchard, 1998; Sharma, 2006).

Catalytic initiation for homopolymerization is accomplished by addition of boron trihalides and tertiary amines as catalysts to produce insoluble and intractable thermoset polymers, as depicted in the following examples, Scheme 13.

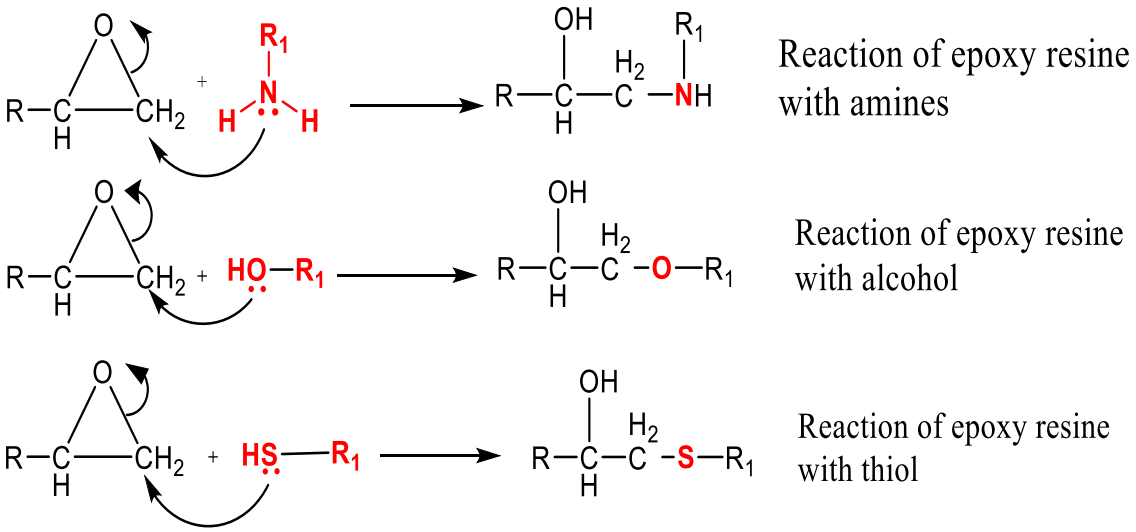

Scheme 13. Opening The Epoxide Ring by Adding Nucleophiles as Amines, Alcohols and Thiols

The selection of a curing agents is governed by various factors such as cost, curing methods, curing conditions, environmental limitations, pot life, gel time and the needed chemical, physical, mechanical, electrical and thermal properties of the produced thermosetting polymers (Raju Thomas et al., 2014).

The rate and temperature of curing reaction of the epoxy monomers are limited to the reactivity and nature of both the curing agents and the epoxy monomers, which plays significant role in the curing process as well as the steric hindrance associated with geometrical structure of both the monomers and the curing agent. For example, polyfunctional amines (diethyleneamine or triethyleneamine) and poly amido-amines are good reagents for curing at ambient- temperature (T>80˚C), which are associated with partial curing at room temperature, whereas both trialkyl amines, cycloaliphatic amines and aromatic amines are less reactive curing agents due to their sterically hindered structures (curing occurred at 150-170 ˚C) (Pham, 2011; Weinmann et al., 1996; Fiore and Valenza).

The highly stressed state associated with the planer geometrical structure of the epoxy group in which the bond angle is 60˚ instead of 109.5˚ of the tetrahedral carbon and the number of epoxy groups and other substituents in the oligomer structure play effective role on the curing temperature. In some cases, curing catalyst is required to enhance the curing process, for this reasons Lewis acids and bases are used as reactive curing catalyst to initiate the homopolymerization of epoxy resins (Pham, 2011).

1.7. Applications of Epoxy Resins

Due to their chemical nature, crosslinking density and dimensional stability, the cured epoxy resins possess an excellent chemical, mechanical, electrical and thermal properties (May, 1988). They are engaged in a wide range of applications, particularly in engineering field, adhesives, coatings, electrical insulation, anticorrosion coatings for marine and other industries that need treatment such as foods containers and piping systems in petroleum industry (Sharmin et al., 2010; Gibson, 2017).

Epoxy resins can be used in the field of dentistry either directly or indirectly. The most commonly used composites in dentistry may be compounds based on the (DGEBA) resins (Garcia et al., 2009).

On the other hand, thermosetting polymers are characterized by firm adhesion properties, excellent strengthening effects and good resistance to mechanical stress, therefor these distinctive properties encouraged their applications to various construction systems, stone materials adhesion, sealing cavities or cracks and structural adhesives in repair and conservation of concrete structure (Sharmin et al., 2010; Lakshmi et al., 2010).

These composite polymers in turn are widely in engineering fields applications, as aircraft, trains, ships components, manufacturing of automotive, and aerospace industries (Guo, 2012; Prolongo et al., 2009).

Epoxy resins are used as music's tools, skateboards and sport instruments all over the world (Krauklis and Chtermeyer, 2018).

As with other classes of thermoset polymer materials, blending different grades of epoxy resin, as well as use of additives, plasticizers or fillers is common to achieve the desired processing or final properties, or to reduce cost. Use of blending, additives and fillers is often referred to as formulating. Likewise, distinctive flame-retardant epoxy resins are synthesized by addition of metal-containing compounds, halogens, organophosphorus compounds, silicon-containing compounds, and nanocomposites, the composite epoxy resins are produced by the incorporation of numerous stiff phase materials of specific characteristics as reinforcement components such as glass wool, aramid fiber, carbon fiber, ceramic nanofiller, titanate nanotubes (Jin et al., 2015; Yeasmin et al., 2021).

1.8. Bisphenol A

The Russian chemist A.P. Dianin synthesized bisphenol A (BPA: 4,4′-isopropylidenediphenol) in 1891 by the reaction of phenol with acetone in the presence of a strongly acidic ion exchange resin as a catalyst. BPA is typically synthesized via an acid catalyzed condensation reaction of two molecules of phenol with one molecule of acetone in using of hydrogen chloride or cross-linked polystyrenes that act as catalysts, although a large excess of phenol is needed in the process to reduce the formation of higher molecular weight oligomers (Corrales et al., 2015).

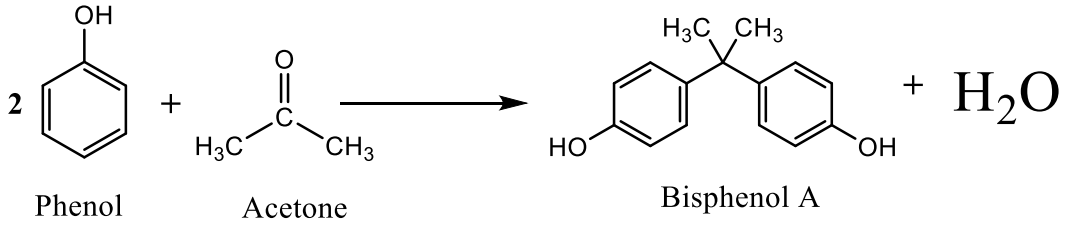

Scheme 14. Preparation of BPA By Condensation Reaction

It is an organic compound with two hydroxyphenyl groups and at ambient- temperature, it is a white solid with a mild phenolic odor, and has well solubility in acetic acid, aqueous alkaline solutions and organic solvents such as acetone, benzene and ether, and poor solubility in water (120-300 mg/L at 25°C) (O´Neil, 2006; Lide and Milne, 1994).

BPA is a precursor to produce variety of thermosetting plastic products which are used in a wide range of applications such as manufacturing of kitchen appliances, toys, baby's bottles, container, eye glasses, computers and dental equipment. (Guo et al., 2017). It is used as basic component in the flam-retardants thermosets, laminates, for printed circuit boards, color developers in thermal receipt papers. BPA is considered to be an environmental chemical pollutant which has been detected in soil, air, water, landfill leachate and human body. Obviously, BPA reach the human body through skin contact, inhalation, dental fillings, and occupational exposure, in addition to food contamination caused by leaching of food containers (Meli et al., 2020).

The ubiquitous detection of BPA in the environment (air, water, and soil) and human body draws the attention to its dangerous health effects. BPA is structurally capable to fit in the estrogen

receptor (ER) binding pocket, act as endocrine disruptor, androgen receptor (AR) antagonist, interact with the thyroid receptor (Moriyama, 2002) and act as nuclear and cell membranes binder. Animal and human research confirmed many health problems, such as infertility, obesity problems (Masuno et al., 2005), behavior changes, early onset-puberty, prostate (Liu et al., 2012) and mammary gland cancers, metabolic syndrome, (Teppala, 2012), cardiovascular effects, disease, altered liver enzymes, diabetes and hypertension. The epidemiological studies on health effects associated with BPA exposure reveal that increment of BPA levels in urine causes alteration in hormone levels, small reduction in free testosterone and a decrease in the sexual capability of men, and a decrease in the number of retrieved oocytes in women (Omran et al., 2017).

1.9. Bio-Based Epoxy Resins

The Petro-based molecule, BPA is substantially incorporated in wide range of epoxy monomers and variety of synthetic thermosets and as modifying materials for polyurethane and unsaturated polyesters. The significant toxicity of BPA on human lives is fairly established, since it is known as carcinogenic agent, reprotoxic and endocrine disruptor, in addition to being environmental pollutants (Ortiz et al., 2019).

The superiority of bio-based epoxies to those of Petro-based is due to the readily available and low prices natural oils with respect to the availability and prices of fossil oils, which in turn affects the final products prices. In addition, bio-based epoxies are environmentally green chemicals due to their nontoxicity, nondegradability, nonvolatility and biodegradability. Hence the natural chemicals such as vegetable oils, lignin (Liu, 2014), sugar (Niedermann, 2015), furan (Hu, 2014), starch (Zhao, 2008), cellulose (Kalia, 2011), rosin (Ma, 2013) itaconic acid (Ma, 2013), tannins (Liu, 2014) are used as alternative sources to get epoxies.

1.9.1. Vegetable Oils-Based Epoxies

There are variety of vegetable oils such as soyabean oil (Saho, 2015), tung oil, rapeseed oil (Babahan et al., 2020), linseed oil (Pin, 2011), palm oil (Hirose, 2011), castor oil (Sudha, 2017),

Karanja oil (Kadam, 2015), mahua oil (Goud et al., 2006) mustard oil (Ravindra, 2013), cotton oil (Srikanta, 2008), hemp oil (Manthey, 2013), safflower oil (Pan, 2011), canola oil (Omonov, 2014), cashew nut oil (Maiorana, 2015), khaya seed oil (Okieimen, 2000), sunflower oil (Schneider, 2009), fish oil (Marks, 2002), grapeseed oil (Stemmelen, 2011).

The predominant components of these oil are triglycerides (triacylglycerol) and fatty acids molecules which in consist of unsaturated C=C double bonds in their structures, that undergo oxidative reaction to give the required epoxy group in the monomeric structures, which in turn undergo polymerization reaction to produce thermoset plastic. For example, epoxies from castor oil, soyabean oil and many other plant oils are commercially supplied to produce epoxy resins for various application. As a model epoxidation of oleic acid is achieved by oxidation of the C=C double bond by hydrogen peroxide (H_2O_2) in formic acid or acetic acid at 55 $^{\circ}$C (Stemmelen, 2011).

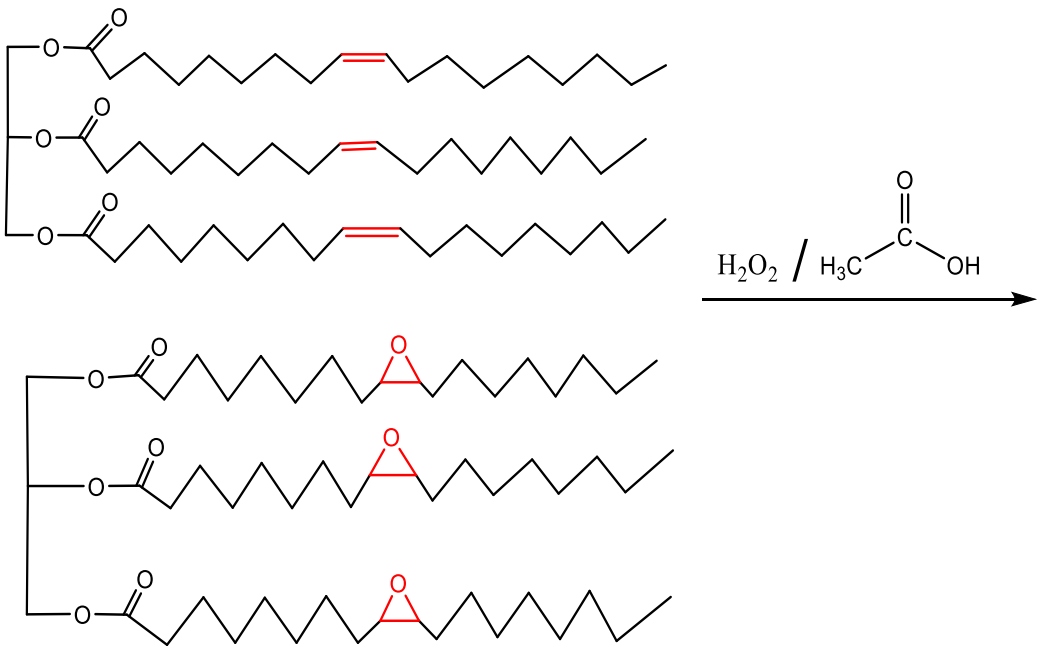

Scheme 15. Epoxidation of Oleic Acid by Oxidation of The C=C Double Bond By Hydrogen Peroxide in Formic Acid or Acetic Acid

In addition, fatty acid- derived oxazoline epoxies were synthesized via oxazoline synthesis from unsaturated fatty acid followed by epoxidation of the C=C double bond to get epoxy group (Trumbo, 2008), as shown in the following reaction (Scheme 16).

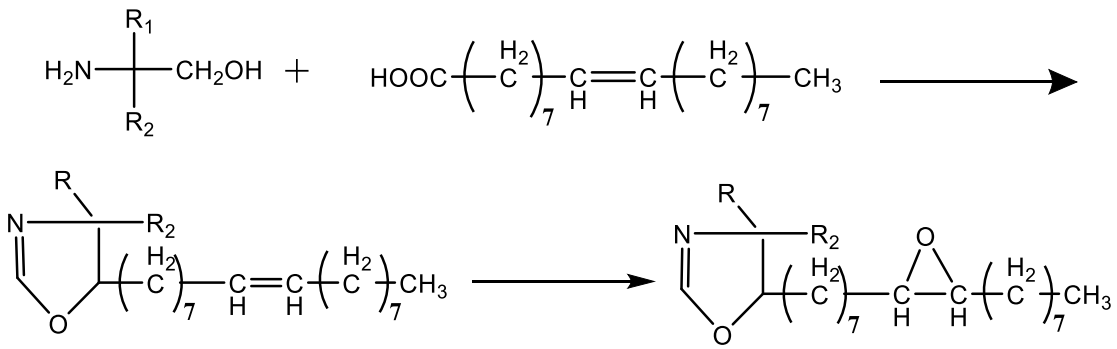

Scheme 16. Synthesis of Fatty Acid- Derived Oxazoline and Its Epoxidation.

Cardanol bio-based epoxies is another type vegetable oil epoxy. (Unnikrishnan, 2008).

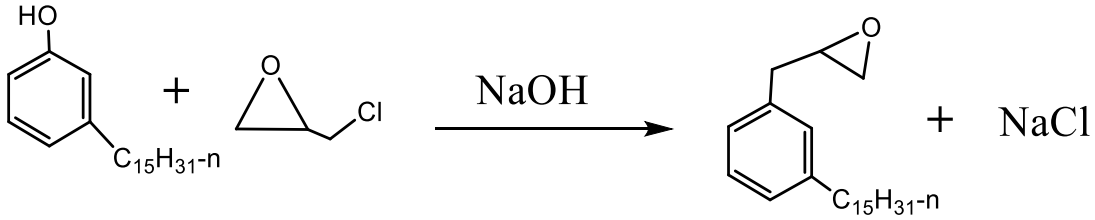

Scheme 17. Epoxidation of Cardanol

1.9.2. Furan- based epoxy

The five- membered heterocyclic compound furan is a unique substance synthesized from celluloses obtained from agricultural sources such as baggas, corn cobs, and rice or oats hulls.

Furan derivative such as furfural, 5-methylfurfural, furfuryl alcohol, 2,5-bis(hydroxmethyl)furan (BHMF), 2,5-furandicarboxylic acid, 5-hydroxymethylfurfural (HMF) and furan-2-ylmethanamine are the most importance precursors for the synthesis of furan-based resins (Fink, 2013)

The synthesis of 2,5-Bis [(2-oxiranylmethoxy) methyl]-furan diepoxy resin (BOF) was synthesized by heating 2,5-bis (hydroxymethyl) furan and epichlorohydrin at 65 °C, via a ring opening nucleophilic addition reaction as depicted in Scheme 18 (Hu et al., 2015).

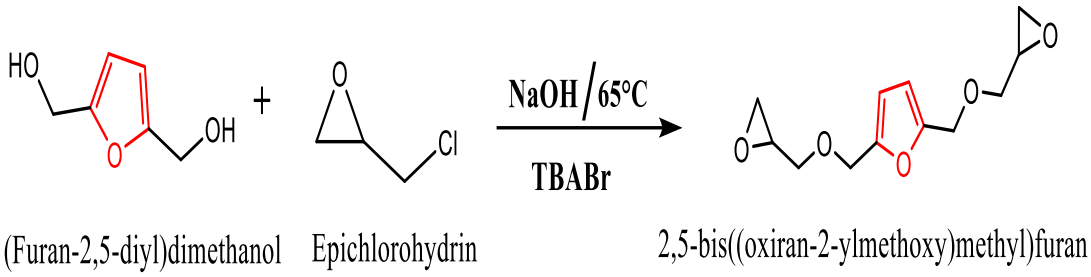

Scheme 18. Synthesis of 2,5-Bis((Oxiran-2-Ylmethoxy)Methyl)Furan

The 2,5-Bis[(2-oxiranylmethoxy)methyl]-benzene (BOB) resin and its analogues 2,5bis[(2-oxiranylmethoxy) methyl] benzene was reacted with 4,4-methylene bis cyclohexamine (PACM) and diethyl toluene diamine **(**Li et al., 2016).

The furan based-epoxy thermoset process high T_g and storage modulus with respect to those of benzene- based resin, therefor furan ring is considered a good replacement to benzene ring. Another furan- based epoxy resin is diglycidyl ester of 2,5-furandicarboxylic acid (DGF), which is a monomer analogue to the diglycidyl ester of terephthalic acid (DGT), obtained from the reaction between furan dicarboxylic acid (FDCA) and 3-bromopropene (allyl bromide) followed by epoxidation by m-chloroproperbenzoic acid. Both DGF and DGT are reacted with methylhexahydrophthalic anhydride (MHHPA) and poly (propylene glycol)-bis (2-aminopropyl ether) D230 amine- cured agent. The thermoset of DGF possess higher glass transition temperature (Tg), excellent curing reactivity and comparable mechanical properties in comparison with those of DGT (Deng et al., 2015).

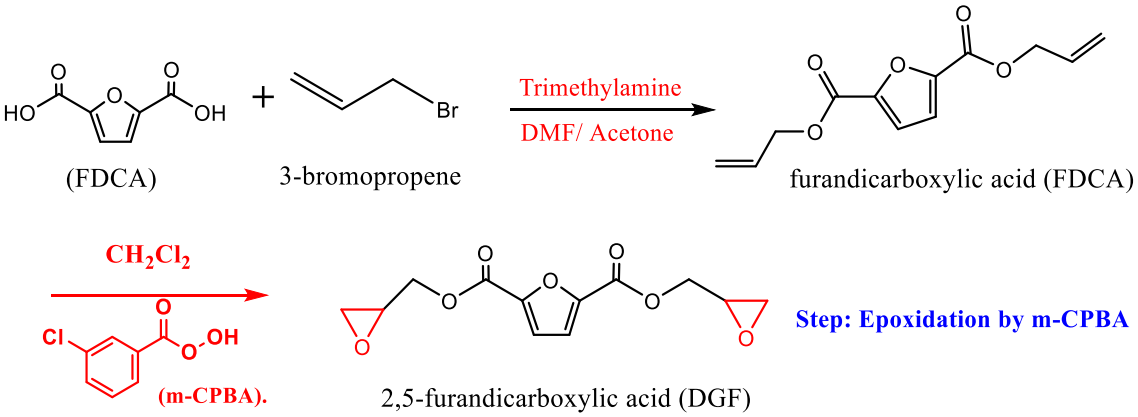

Scheme 19. Synthesis of Diglycidyl Ester of 2,5-Furandicarboxylic Acid (DGF) Epoxy Resin.

Novel N, N-diglycidyl-furfurylamine (DGFA) epoxy resin was synthesized by ring-opening nucleophilic addition of furan-2-ylmethanamine to the epoxy group of epichlorohydrin followed by dehydrogenation using aqueous sodium hydroxide to get the epoxy group as given scheme 20 (Tian, 2009).

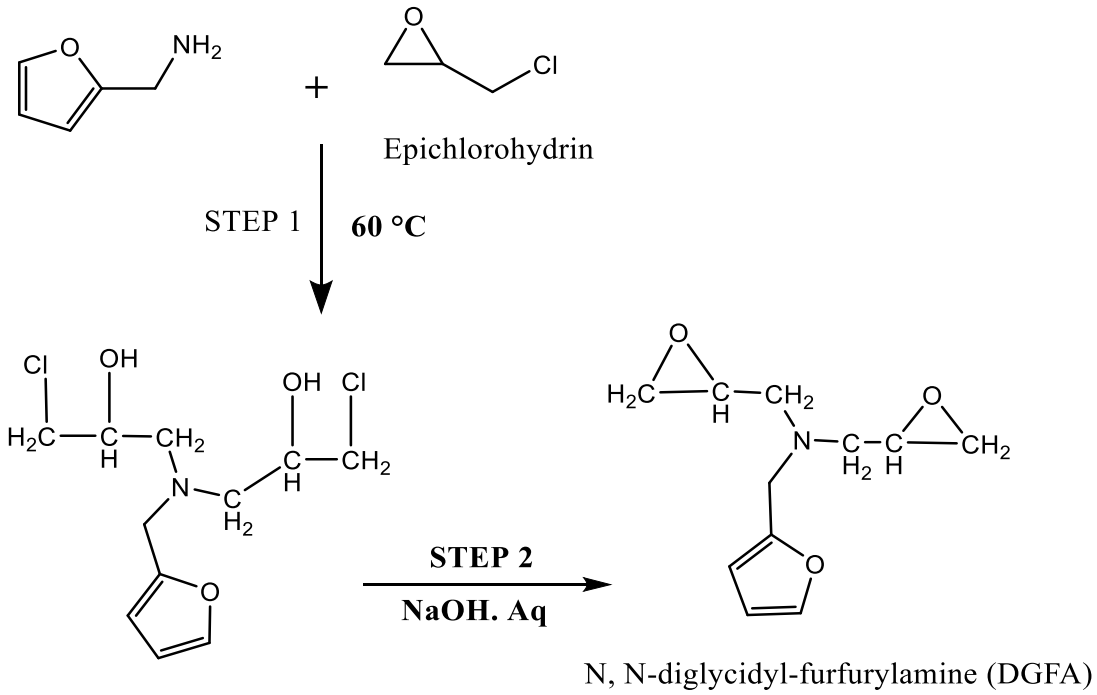

Scheme 20. Synthesis of N, N-Diglycidyl-Furfurylamine (DGFA) By 2 Steps.

1.10. Epoxy Nano Composites

The importance of epoxy nano composite thermosets is a result of the combined physic-chemical properties of both the epoxy resins and the nanoparticles of very small size and high specific area in the skeleton of the final structure (Guo, 2013), an extra ordinary improvement of the mechanical, electrical conductivity (Guo, 2016), magnetic (Wang, 2010), optical, heat retardation. Also, good mechanical strength and stiffness, anticorrosive properties **(**May, 1989; Olad, 2012) have been obtained by using various nanoparticles as main constituents in structure of the thermosetting.

Epoxy composites of these nanoparticles are carbon nanofibers (CNFs) (Zhu, 2010), carbon nanotubes (CNTs) (Qing, 2014), graphene (Zaman, 2011), nanoclay (Wang, 2005), alumina

(Mcgrath, 2008), silica (Park, 2006), polyaniline (PANI) (Jang, 2005), and metal oxides such as iron (Zhu, 2010), zinc (Liu, 2012) and aluminum oxides (Goyat et al., 2011). The epoxy nano composites are used in a wide range of application due to their unique characteristics properties to meet special requirements, such as adhesives and coatings, matrices to produce fiber-reinforced composites, electrical components, and insulators (Ellis, 1993). With the addition of one or more nanosized phases, epoxy resins already excellent properties can be further improved, yielding a nanocomposite (Mascia, 1998).

Epoxy resins have a variety of disadvantages, including poor durability (they are brittle by default, like other thermosetting polymers) and other shortcomings that restrict their use in certain more challenging applications (nano-electronic, medical devices, aeronautical applications). The featuring of preformed nano-constructors, i.e., the nanofillers, can be modified, improved or adapted on request to meet specific requirements. Nanosubstances of different chemical nature can be defined as materials of one dimension from 1 to 100 nm, produced as nanomaterials 0D, 1D, 2D and 3D of these nanocomposites for example are following categories (Shehzad, 2016).

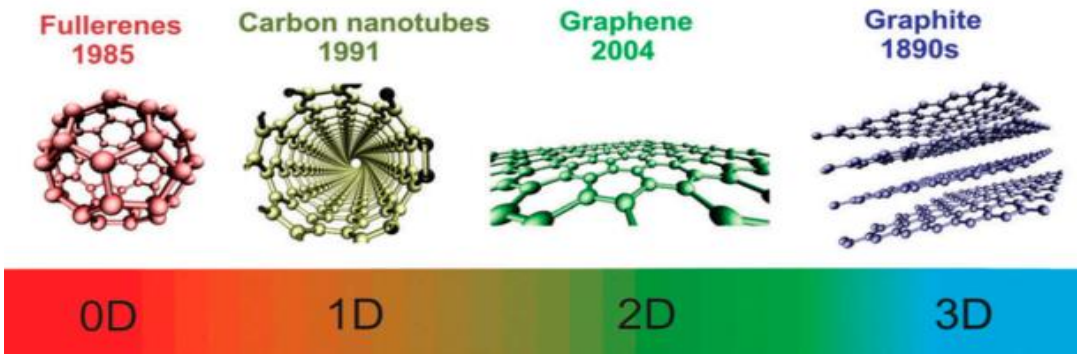

Figure 9. Nanomaterials of 0D, 1D, 2D and 3D Structures Classification and Examples

1. Epoxy nanocomposites with magnatic properties. In corporation of magnetic nanoparticles into the thermosets structures offer abroad engineering applications of these products, such as microwaves absorption (Zhu, 2011), magnetic resonance imaging (MRI) (Guo, 2006), electromagnetic interference (EMI) shielding and flexible electronics (Gu, 2012).

2. Epoxy nanocomposites with thermal electrical conductivity both electrical and thermal conductivity are very effective properties of the epoxy nanocomposites meet the requirements of the semiconductor electronic devices, in addition to the environmentally issues and low-cost faction (Gu, 2016). Many kinds improved electrical conductivity of epoxy nanocomposites are manufactured and used. Based on using different nanoparticles such as Graphene, CNTs, CNFs, and metal nanoparticles (Chen et al., 2015). The production of nanocomposites with improved thermal properties have been achieved by providing Al_2O_3 (Yu, 2011), boron nitride (Huang, 2013), graphene and CNTs as nanoparticles to the epoxy resins. As a conclusion, graphene, fullerene, CNTs and CNFs nanoparticles are considered to be the most efficient additives to improve the electrical conductivity and the epoxy resins are recognized as the most electrically conductive adhesive (ECAs) for electronic industry due to their excellent adhesive strength, good chemical and corrosion resistance and low cost (Rosca, 2011).
3. Epoxy nanocomposites flam retardancy since the ordinary epoxy thermosetting polymer is highly inflammable material, their applications are significantly limited (Hergenrother, 2005). Therefore, serious modification of the polymers are needed of this modification is using flame retardant polymers such polyamide, poly (p-phenylene-2,6-benzobisoxazole) (PBO) (Bourbigot and Duquesne, 2007).

1.10.1. Types of Nanomaterials for Epoxy Resins

Various nanomaterials were investigated as fillers capable of improving/modifying epoxy resin properties and properties. They come from various chemical families, namely carbon fillers, metal oxides and clay nanoparticles (Al-Saleh and Sundararaj, 2009; Ray and Okomoto, 2003).

1.10.1.1. Carbon nanotubes

Theoretically, carbon nanotube is distinguished as a rolling graphene sheet cylinder. It can be separated into one well or several wells. Single-wall carbon nanotubes (SWCNTs) are described as single well nanotubes and first reported on in 1993. (Iijima and Ichihashi, 1993) Multi-wall carbon-nanotubes (MWCNT), with more than one well, were discovered in Iijima for the first time in 1991(Iijima S, 1991). They have different and interesting chemical and physical characteristics

and are used extensively in biomedicine, nanotechnology, construction, electronics (Eatemadi et al., 2014; Devitt et al., 2007; Liu et al., 2009). Moreover, they are favorable for many technical and engineering applications due to the mechanical characteristics and flexibility of carbon fiber reinforced polymer matrix composites (Argon and Cohen, 2003).

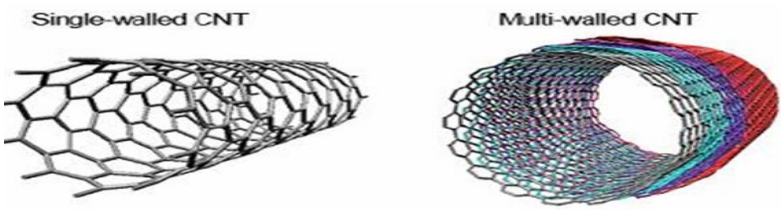

Figure 10. Structures Types of Carbon Nanotubes (CNT).

1.10.1.2. Graphene

Graphene is a two-faced carbon nanomaterial with unique physical and chemical properties, which include high surface area, good thermal and electric conductivity, mechanical resistance and ease of functioning (Nguyen and Nguyen, 2016). Graphene and graphene Oxide (GO) are among the most common graphene forms used in a wide range of different applications, alongside reduced graphene oxide (Figure 11). It can enhance the epoxy-matrix as well as multifunctionality for a wide range of applications of engineering (adhesives, thermal conductors and insulators, anticorrosive coatings) which cost less than the costly carbon nanotubes, to produce electrical and electronic devices as well as in the field of fiber-reinforced polymers (Rafiei Hashjin et al., 2018; Yuan et al., 2020; Jojibabu et al., 2020).

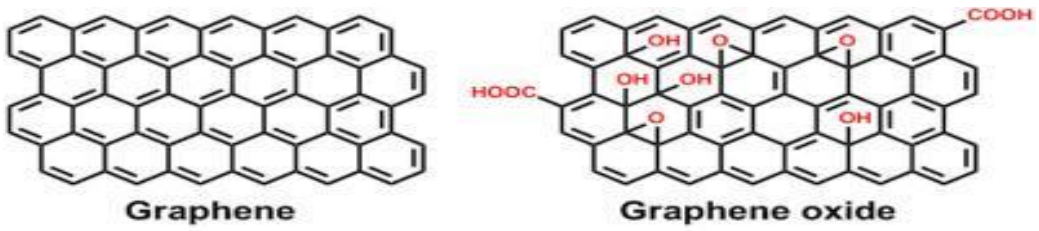

Figure 11. Structure of Graphene and Graphene Oxide

1.10.1.3. Fullerene

Fullerenes are a class of fully carbon-composed molecules. Buckminsterfullerene was the first of these molecules found in 1985 and contains 60 carbons in a spherical hollow cage consisted of 12 pentagonal and 20 hexagonal faces. Since then, other spherical fullerenes, have been synthesized (Figure 12) (Kroto et al., 1985). Fullerenes have been suggested as the basis for new technologies in environmental engineering for the development of nanomaterial-compatible disinfection, oxidation, improved membrane processes, adsorbents and biofilm-resistant surfaces (Bottero et al., 2006). Fullerene-based nanomaterials appear in a number of applications, such as cosmetics, energy generation (Kamat et al., 2004), semiconductors (Saran et al., 2004) and medicines (Ros and Prato, 1999).

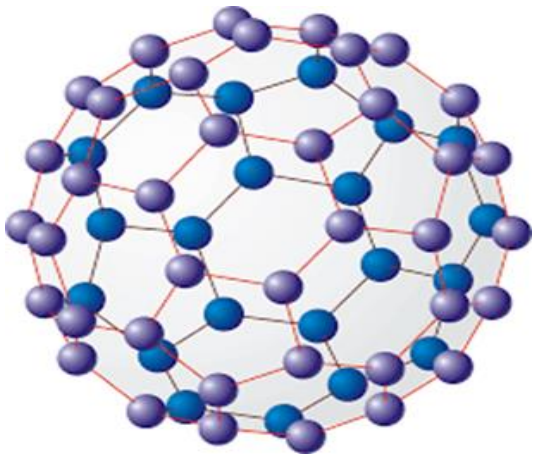

Figure 12. Structure of Fullerene C60.

2. LITERATURE REVIEW

Epoxy resin has been used to screen carbon fiber/epoxy adhesive joints (Figure 13). Carbon nanofibers, various surface treatments, and plasma have been used to improve adhesive connections. Plasma therapy significantly enhances surface energy, resulting in a significant improvement in joint strength (Prolongo et al., 2013).

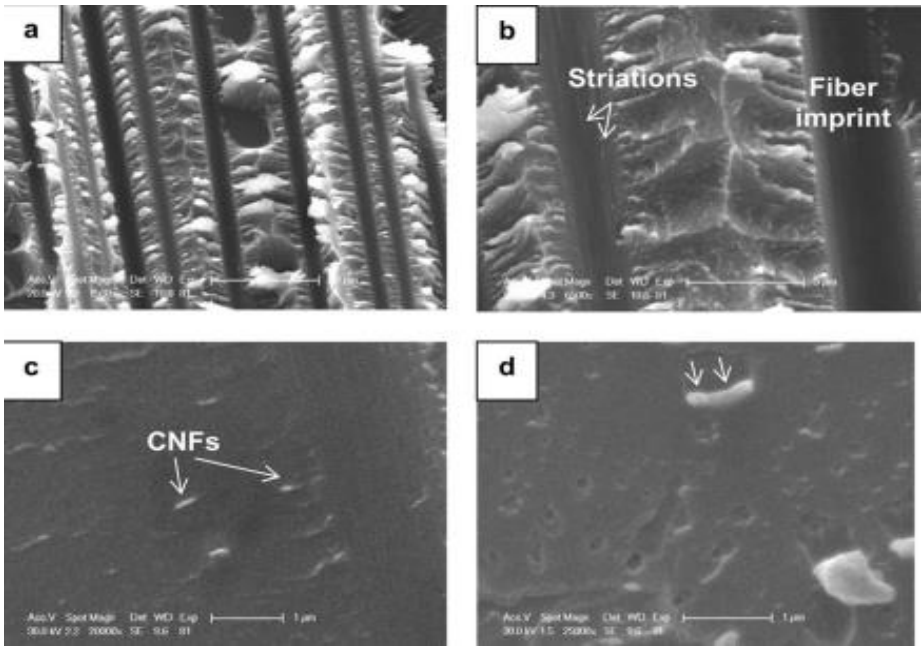

Figure 13. SEM Micrographs of Joints Treated with Plasma.

The enhanced E-glass/epoxy-nanocomposite sheet of graphene nanosheets (GNPs) was evaluated. The measured (GNPs) content was between 1% wt. and 5% with another 1% step. To produce the tested nanocomposites, they used two distinct types of E-glass fabrics, i.e., Twill 2 da2 and Uni-Directional (Seretis et al., 2018).

F. Yaesmin et al. incorporated microporous silica as a filler in epoxy resin with the aim of introducing the polymer into the pores of silica in a paper published in 2021 (Figure 14). As expected, the thermal stability of the composite was significantly increased (Yaesmin et al., 2021).

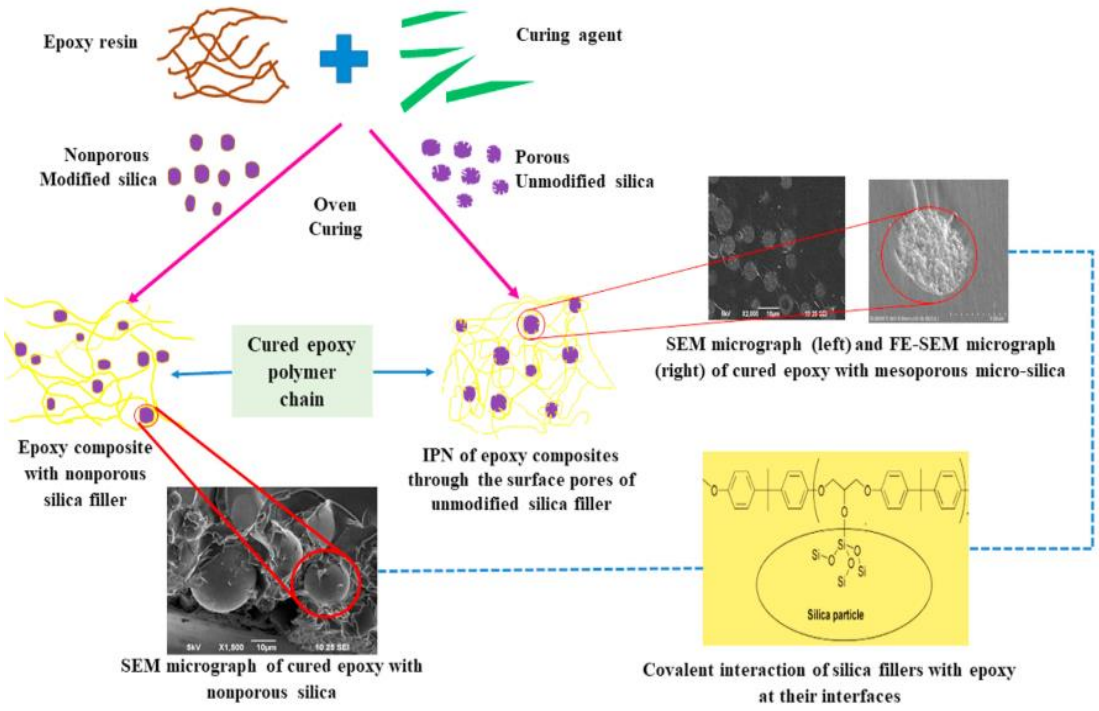

Figure 14. Schematic Description by Including Nano/Micro Filler of The Production of The Polymeric Resin Composite Epoxy.

Graphene is quite interesting in different areas of biomedical science. The utilization of graphene-based materials has been of tremendous interest in the development of neural tissue regeneration scaffolds (Figure 15). Graphene is employed with its particular topographical and chemical characteristics as a pantry that can connect regenerative nerves (Aydin et al., 2018).

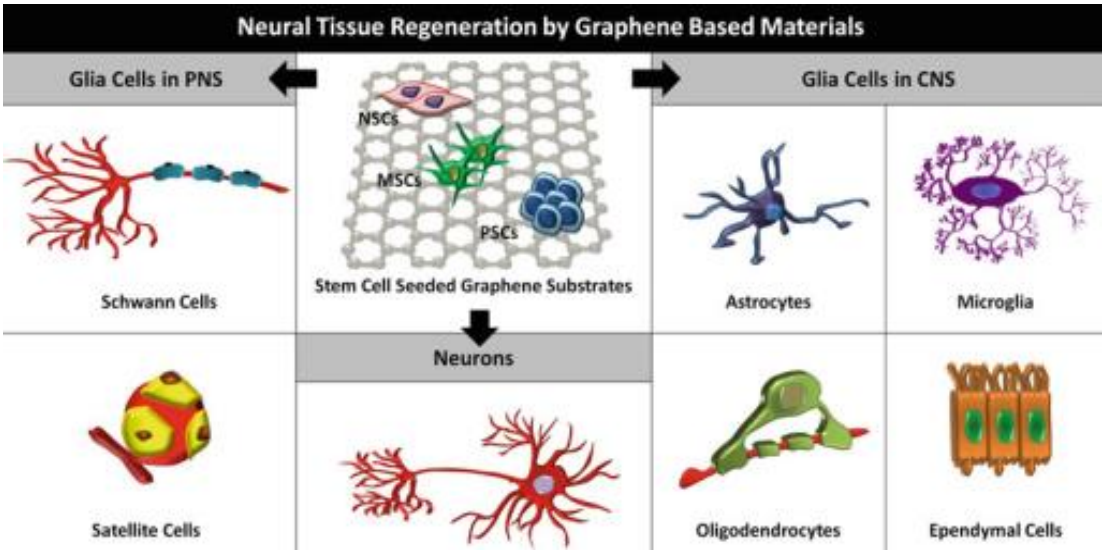

Figure 15. Pictures of Neural Tissue Renovation by Graphene Nanomaterials

Based on the research published in the Journal of Advanced Engineering Materials, it was concluded that the modification of epoxy resins with nanoparticles could endow the materials with some superior properties. This includes modest increases in the glassy modulus, low dielectric constant and significant increases in key mechanical properties (Njuguna et al., 2007).

Graphene is a new class of nano-fillers with excellent qualities (the most compatible with most polymers). Graphene has been used as a substrate to improve the mechanical properties of epoxy. Compared with the two nanocomposites, the cured epoxy exhibited outstanding mechanical properties due to changes in material properties upon introduction of the fillers. This made the matrix more flexible (Berhanuddin et al., 2017).

Nanocellulose has been used as a biodegradable nanomaterial for renewable, lightweight, a daptable, high performing, and safe electrochemical energy-storage devices. The nanocellulose derived porous structure Carbon has a three-dimensional structure made up of linked nanofibers. They can carry ions and electrons even with a thick (as to several hundred micrometers). However, they also have a lot of active sites (micropores) for charge storage. As a result, it provides a sensible architecture for sustainable electrochemical sensors other than supercapacitors (Figure16), (Zhang et al., 2019).

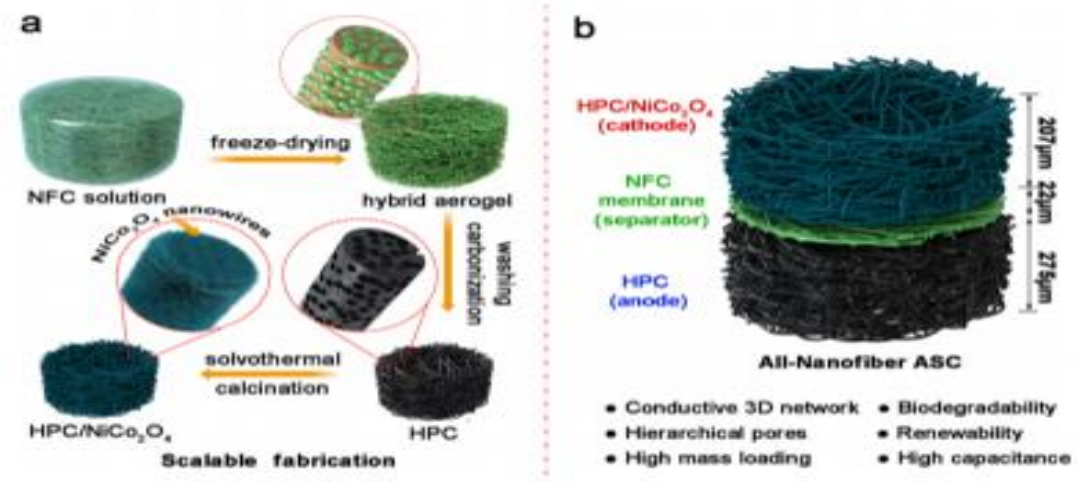

Figure 16. (A) Nanocellulose-Derived Aerogels for Nanocellulose Manufacturing (HPC / $Nico_2o_4$).

(B) Assembling Them into An All-Nanofibre System.

This study was published in Composites Part B: Engineering, with the aim of clarifying the function of polyaniline as an effective polyelectrolyte modification for the surface treatment of mesoporous materials. To accomplish both barrier and active protection, metal nanoparticles treated with zinc cations (Zn^{2+}) can also be embedded in a polymeric covering. The polyaniline coated nanoparticles and the epoxy matrix had strong interfacial and chemical interaction, according to the researchers. Epoxide/nanocomposite coatings are an example of a double barrier/active protection system. (Haddadi et al., 2021).

3. MATERIAL AND METHOD

3.1. Material and Chemicals

Tung oil, glycidylmethacrylate (97 %), phenothiazine (98 %) and 2,4,6-tris(dimethyl aminomethyl)phenol were supplied by Sigma-Aldrich chemical company. Trifunctional polyetheramine Jeffamine T403 and difunctional polyetheramine Jeffamine ED900 were supplied by Sigma-Aldrich (Figures 17 a-b). Graphene Nanoplatelet (Purity: 99.9+% Size: 3 nm S.A: 320 m2/g Dia: 1.5 μ), Multi Walled Carbon Nanotubes (Purity:> 96% Outside Diameter: 4-16 nm) and Fullerene C60 (Purity: 95%) were purchased from Nanografi company in Turkey.

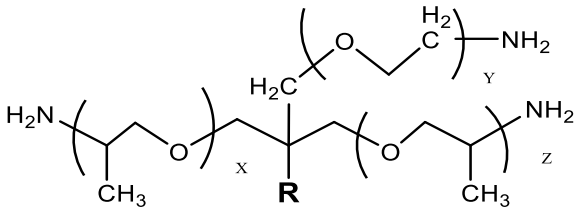

Figures 17a. Structure of Polyetheramine Jeffamine T403 (R:C_2H_5, X + Y + Z = 5 - 6)

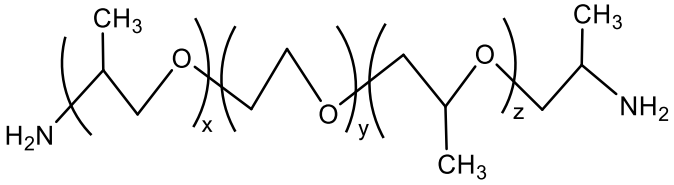

Figures 17b. Structure of Polyetheramine Jeffamine ED900

3.2. Instruments

FTIR spectra are recorded by Nicolet™ 50 FTIR spectrophotometer. Both ^{1}H-NMR and ^{13}C NMR are determined by Mercury-400 spectrophotometer (Varian). The DSC Q200 from TA instruments is used to determine the (TGs) values of the synthesized polymers and the Thermogravimetry (TGA) values are recorded by Q50 TGA from TA instrument.

3.3. Coating Tests

All general coating properties were tested according to the ASTM standard: pendulum hardness (D4366), pencil hardness (D3363), crosshatch adhesion (D3359), pull- off adhesion (D4541), Impact and reverse impact resistance (D2794). Pull-off adhesion tests were used to evaluate the adhesion strength of the cured systems to the substrate by using two different epoxy glues. At least five samples were used to measure the pendulum hardness, pencil hardness, pull off adhesion, impact resistance, reverse resistance, and chemical resistance.

3.4. Method

In this study, epoxy-amine nanocomposites as replacement of bisphenol A (BPA) based epoxy coatings for aluminum surfaces. The nanocomposite coatings were prepared from the reaction of epoxidized tung oil resins (ETO) with polyetheramines (Jeffamine T403 and Jeffamine ED900) and nanoparticles. Carbon nanotubes, graphenes, fullerenes are specifically used as additives to get the targeted properties for the epoxy nanoporous coatings. In addition, mechanical properties such as hardness, adhesion, impact resistance and thermal properties of the new bio-based nanocoatings in this study were investigated. The first step epoxidation product (ETO) of tung oil was carried out using the Diels-Alder reaction of glycidyl methacrylate (GMA) with tung oil (Scheme 21). The bio-based resin (ETO) is cured with polyetheramine with different amine functionality (JeffamineT403 and JeffamineED900) and carbon nanoparticles (carbon nanotubes, graphene and fullerenes).

New epoxide-nanocomposite coatings were prepared by curing with carbon nanoparticles at different temperatures (25-150 $^{\circ}$C), (Scheme 22). As a result, as shown in Scheme 22, the epoxide-amine network attached to the surface of carbon nanostructures provides for aluminum metallic substrates to be coated with Graphene/CNT/Fullerene based nanoparticle doped nanocomposites.

Character analysis of the new nanocomposite coatings were performed by using IR, differential scanning calorimetry (DSC), thermogravimetric analysis (TGA), and gel content tests.

3.4.1. Step: Epoxidation of Tung Oil

An acetone mixture of tung oil (60 g) and phenothiazine (0.6 g) was reacted with glycidyl methacrylate (19.47 g, 0.14 mol) in a 250 ml three-necked round flask equipped with mechanical stirrer, nitrogen inlet and condenser (Scheme 21). The mixture was heated an oil bath for 6 hours up to 150 °C with continuous stirring. The acetone solvent was evaporated by rotary evaporator and the product was identified by structure of the product was identified ^{1}H-NMR and ^{13}C-NMR spectroscopy (Babahan et al., 2020).

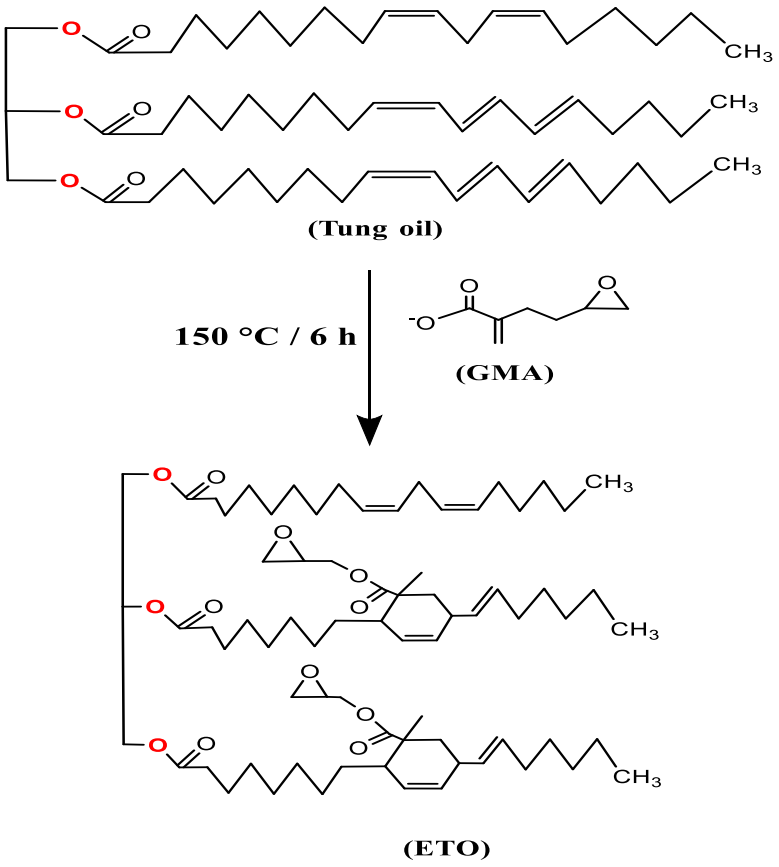

Scheme 21. Epoxidation of Tung Oil Via Deils-Alder Reaction.

3.4.2. Step: Preparation of Formulations

a) Preparation of ETO-ETO Formulations

ETO-ETO systems were prepared without any hardeners as a control sample. Epoxide resins (ETO) were mixed strongly with 2% of 2,4,6 tris(dimethylaminomethyl)phenol and stired by magnetic stirrer for 2 h. Then the mixtures were applied on aluminum test panels (10 cmx 15 cm) and the mechanical performance properties for each formulation were evaluated.

ETO-ETO system didn't cure at 25°C. The coatings also were cured at 80 ˚C for 4 h, and at 120 ˚C and 150 ˚C for 2 h and 1 h, respectively. The cured systems were removed by scratching the panels by razor blade for characterization and mechanical performance testings.

b) Preparation of Epoxide-Nanocomposite Formulations

The procedures for preparing carbon-based (nano/epoxy) coatings are schematically shown in Figure 18, and the machinery equipment and experimental setups used are shown in detail. Carbon-based nanoparticles (Graphene, CNT and Fullerene) were used to prepare nanocomposites. In order not to accumulate carbon-based nanoparticles and to ensure their dispersal in the epoxy matrix, they were first mixed in acetone for (2 h) in a sonication bath at 25°C. After the nanoparticles were added to the prepared epoxy matrix at 0.10% by mass, in the solvent in a sonication bath, they were mixed again for 2 h using a mechanical mixer. This process was carried out by adding epoxy resin (ETO) to the mixture (solvent/nanoparticles) for a certain time and under temperature control. The amount of nanoparticles to be added to the epoxy matrix in order to prepare the nanocomposites at the required mass was calculated with the help of equation (3.1). For example, for 0.10% carbon-based nanoparticles/epoxy, the amount of carbon-based nanoparticles to be added to 10 ml of epoxy is calculated from (equation 3.1).

$$\frac{X}{100} = \frac{m_{nm}}{m_{nm} + (V_t * \rho_t)}$$ **equation (3.1)**

X: desired mass
m_{nm}: nanomaterial mass
Vt: epoxy volume
ρ_t: epoxy density

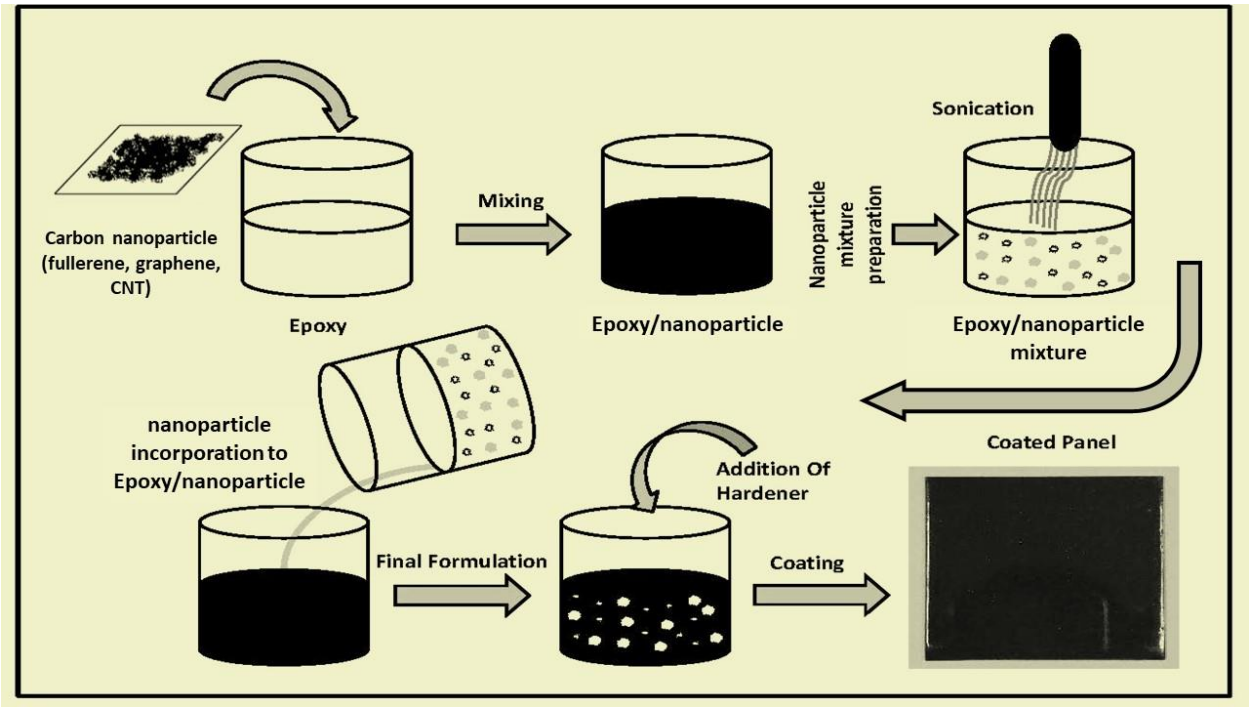

Figure 18. Preparation of Epoxide-Nanocomposite Coatings

3.4.3. Step: Polymerization

The polymerization process of the nanoparticle/epoxide mixture was carried out using epoxide resin (ETO) and JeffamineT403 and ED900 as its hardeners.

Nanoparticle/epoxide mixture keep is overnight at room conditions to remove from the solvent. Subsequently, Jeffamine hardeners were added into the nanoparticle/epoxide mixture at a ratio of 1:1 by mass, epoxy: amine, and it was allowed to react well with the magnetic stirrer for

about 2 hours. Various formulations were obtained with epoxy nanoparticles mixture reagents with a 1:1 epoxy amine ratio from polyetheramine (Figure 18).

Theoretically, all formulations should be prepared according to the equation (3.2) given below, according to the active H amine ratio of 1:1 M epoxy group in order to obtain the maximum cross-linking density of the cured epoxy resins, (Babahan et al., 2020).

The formulations were made without the use of solvents.

Amine Amount(g)= (AHEW)/(EEW) …… (Equation 3.2)

2% of 2,4,6 tris(dimethylaminomethyl)phenol was added as a catalyst to all formulations. As a result of ring opening reactions, cross-linking of epoxidized tung oil (ETO) with polyetheramines with different amine functionality was obtained. It will be used to show that the epoxy resin also performs the homopolymerization reaction by preparing only ETO systems from the same test conditions without adding as a control sample.

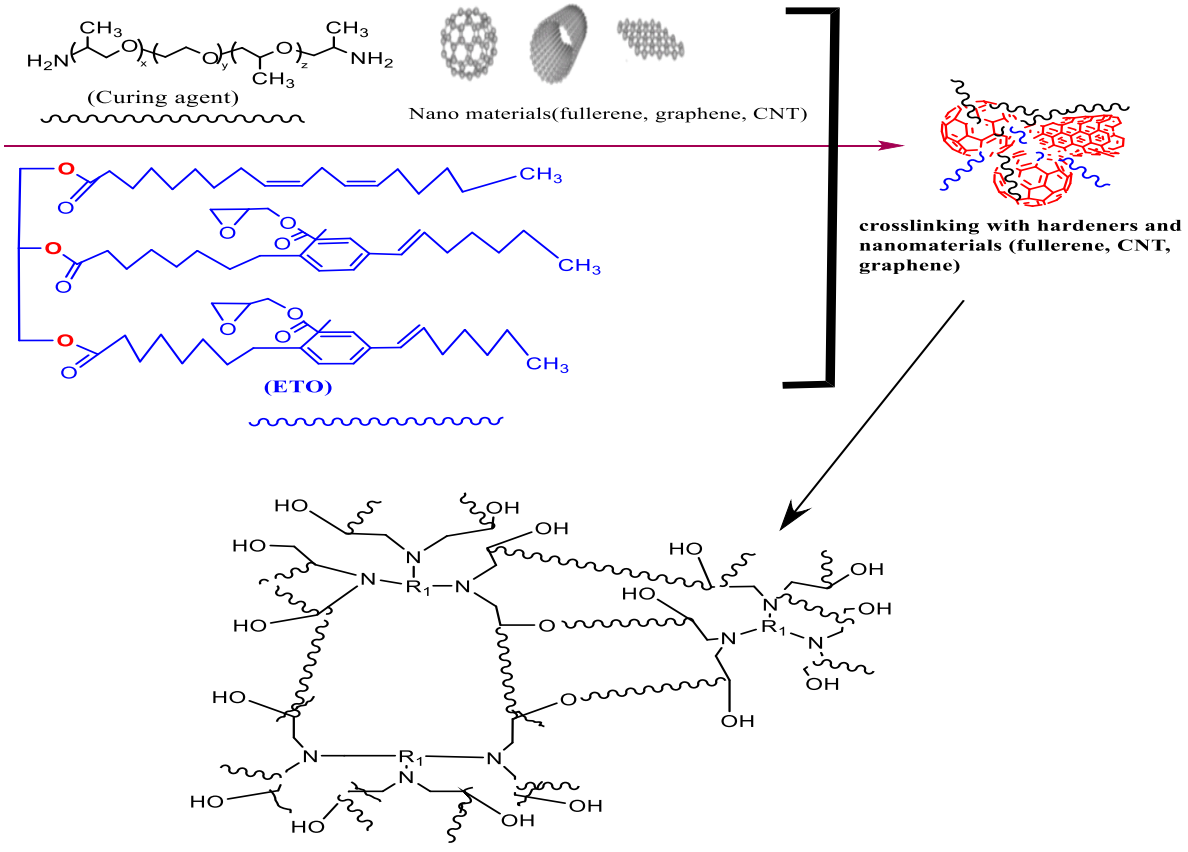

Scheme 22. Preparation of New Epoxide-Nanocomposite Coatings

3.4.4. Step: Application

After the sonication process (ultrasonic bath) and mixing processes of the mixture consisting of nanoparticles added to the epoxy matrix and the hardener added to it, the mixtures are poured onto the metal plates by means of a drawing device, and films are prepared for each composition on the aluminum plates. For this purpose, aluminum plates, which were washed and dried with acetone, were coated with a thickness of 0.5 mm with the classical coating method using a drawing apparatus (Figure 19).

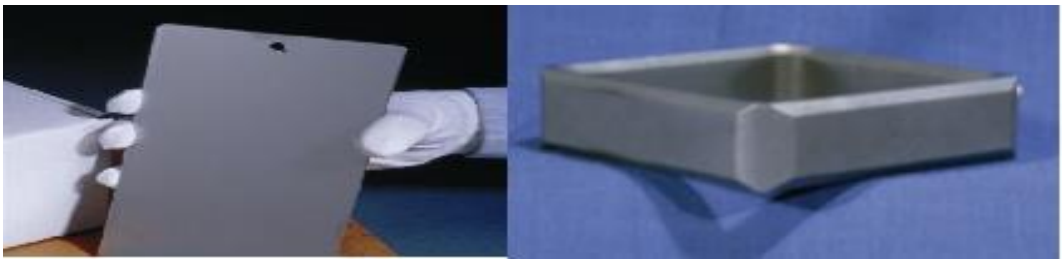

Figure 19. Aluminum Plate and Drawing Apparatus Used In The Coating Stage

3.4.5. Step: Curing Process

Curing stage is the last step. After addition of Jeffamines to the epoxide-nanofiller mixture as given in the method section, curing procedure was carried out at four different temperatures (25°C, 80°C, 120°C and 150°C).

The coatings were kept for 3 days at 25°C, 4 hours at 80°C in an oven, 2 hours at 120°C and 1 hour at 150°C to complete the curing process. Fully cured stable coatings were obtained in 3 days at 25°C, 4 hours at 80 °C, 2 hours at 120°C and 1 hour at 150°C. Some pictures of expoxide-diamine nanocomposite coatings are given in (Figure 20). The others are given in supplementary section.

Figure 20. Pictures of ETO-ED900 Coatings (Views of Graphene-Doped Nanocomposite Coatings from Left to Right, at 25°C, 80 °C, 120 °C and 150 °C, Respectively)

3.5. Coating Tests and Characterization

Cured epoxide-nanocomposites were characterized by IR, differential scanning calorimetry (DSC), thermogravimetry (TGA) and gel content test.

Their mechanical properties were determined by using pendulum hardness, pencil hardness, cross-cut adhesion, pull-off adhesion test, impact resistance and reverse impact resistance tests. ETO-ETO systems were prepared without hardener and nanoparticle as a control group.

3.5.1. Thermal Analysis

Thermogravimetry (TGA) and differential scanning calorimetry (DSC) were used to determine thermal properties of the new epoxide-nanocomposite coatings.

3.5.2. Gel Content Test

Gel content test is used to determine the crosslinking density of the polymers and to compare the polymerization rate by performing the gel content test. The test was performed as

follows in accordance with ASTM D-2765 standards. Approximately 10 mg of coating sample was scraped from the metallic surface and the exact amount is weighed on a precision balance. Then, extraction procedure was carried out by using Soxhlet device for 24 hours with the appropriate solvent. After extraction, the sample was dried thoroughly, and the remaining amount was determined by weighing again in a sensitive scale. Gel content test result is calculated according to the formula below (Babahan et al., 2020).

Gel content (%) = [A_{end} /Ao] *100…… (Equation 3.3)

A_o: Weighed Amount of Coating Before Soxhelet (g)

A_{end}: Weighed Amount of Coating After Soxhlet (g)

3.6. Mechanical Tests

Mechanical performance properties of cured systems were investigated by pendulum hardness, pencil hardness, cross-cut adhesion, pull-off adhesion test, impact resistance, reverse impact resistance tests.

3.6.1. Pendulum Hardness Test

Pendulum hardness is used to measure the hardness of the coating and is also known as pendulum hardness. Simply attach the pendulum to the loading pins, load the sample and start the instrument. The pendulum automatically moves to its initial position, the sample table rises, and the test begins. The stopping point of the pendulum oscillation indicates the hardness value. Pendulum stiffness is measured by the number of swings a pendulum makes between two predetermined angles. Angles are 12° for the Persoz test and 6° for the König test. The standard product is equipped with a fastening system. König pendulum can be included as an option. There is an electronic control box that enables easy operation with both pendulums. Although the device is programmed to work in both systems, the König pendulum is offered as an option. The device complies with ISO 1522, DIN 53157, ASTM D4366 standards.

3.6.2 Pencil Hardness Test

The pencil hardness test uses varying hardness values of graphite pencils to evaluate the hardness of a coating. Pencil hardness testing is perhaps the simplest form of hardness testing. The pens are pushed into the hand-guided device and the coating hardness is defined by the trace produced on the surface. The pencil, which was prepared by rubbing on thin sandpaper beforehand, is held at an angle of 45 degrees according to the Wolff Wilborn method and leaves a superficial mark or gives it to the substrate by applying equal pressure to the sample. The pencil hardness test is performed with a stand and a set of 14 pencils varying between 6B-6H hardness. The test is performed in accordance with ASTM D 3363 standards.

3.6.3 Cross Cut Adhesion Test

Cross Hatch or Cross Cut Adhesion test is a measurement method that test the adhesion of coatings to the surface. The adhesion of the coatings to the surface is easily tested by checking the cuts made diagonally to the surface and checking these cuts with test tapes. The Cross Cut adhesion test is used to test the adhesion strength by making a series of cuts on the dry paint films on the applied surface. A pattern consisting of 25 or 100 squares is created with 2 series of parallel scratches drawn at right angles to each other. The drawn area is treated with a brush or adhesive tape for hard surfaces and then classified by Comparison with the rubric. The coating is divided into small squares, thus reducing lateral adhesion and adhesion is evaluated according to ISO 2409, ASTM D3359 and DIN53151 standards.

3.6.4 Pull-Off Adhesion Test

Adhesion tests (tensile) are used to classify the adhesion forces of different coatings to the substrate. Two different epoxy glues are preferred for application. A dolly is attached to the surface to be tested and a cut is made all around the dolly to isolate the film. The tool is placed on the surface and, by turning the wheel, a gradually higher initial force is applied. At the moment of separation, the electronic display shows the applied force. An electric drill is used to remove the

coating around the stud. The tensile test is performed using a tensile equipment with a velocity unit of 1 $mm.min^{-1}$. The force required to separate the coating from the substrate at a 90° angle is tracked as a function of the stud. Standards such as ASTM D4541/D7234, ISO 4624/16276-1, AS/NZS 1580.408.5 are used in the tests.

3.6.5 Impact Resistance Test (Resistance to Rapid Deformation)

It is used to measure the resistance of coatings against impacts. In this way, it can simulate the formation of cracks and peeling, resistance to shocks, flexibility, adhesion and elongation of coatings. Impact strength is evaluated to examine the load distribution characteristic of pavement systems. The impact test is used to determine the impact resistance and flexibility of coatings. Impact test apparatus is an apparatus for determining the impact resistance and flexibility of paints and coatings. The double scale apparatus has a guide tube that ensures that the impact distance always remains the same in accordance with the relevant norm. The dual scale instrument is equipped with a special guide that ensures that the distance between each impact is always according to the standard. Each impact test is performed in accordance with DIN/ISO 6272, ASTM D2794 and ASTM G14.

4. RESULTS AND DISCUSSION

4.1. Epoxidation of Tung Oil

A mixture of equimolar ratio of commercially grade tung oil and glycidyl methacrylate (GMA) was heated up to 150 ˚C in an oil bath, and reacted in the presence of phenothiazine for approximately 6 h (Scheme 21). Epoxidation of tung oil (ETO) proceeds according to the Diels-Alder reaction (Babahan et al., 2020 and Zheng, 2014). In this study, functionalized epoxy tung oil (ETO) was prepared by a Diels-Alder reaction in which tung oil reacted with glycidyl methacrylate to activate tung oil by epoxy groups (Scheme 21).

Characterization of both tung oil and ETO is accomplished by ^{1}H-NMR and ^{13}C-NMR (Zheng, 2014). Tung oil is known to consist of 82.0% α-eleostearic acid, 8.5% linolenic acid, 5.5% palmitic acid and oleic acid 4.0%. The signals of the backbone proton of tung oil labeled 1,2 and 3 at δ 4.13-4.19, δ 4.28-4.34, and δ 5.22-5.25 ppm (Zheng, 2014; Wutticharoenwong, 2010; Gallart-Sirvent et al., 2017). Most of the conjugated double bonds of the fatty acid side chain related to α-eleostearic acid. Their resonance at 8,9,10,11,12 and 13in Figure 21a are seen in the range of 5.60-6.44 ppm. Whereas unconjugated double bonds were detected at δ 5.31-5.44 ppm (4, 5, 6 and 7; Figure 21a). The recorded ^{1}H-NMR signals of ETO are fairly consistent with the NMR values of GMA and tung oil in the literature (Figures 21a-b) (Zheng, 2014; Wutticharoenwong, 2010; Gallart-Sirvent et al., 2017).

For ETO, the new peak (δ 1.11 ppm) seen in the new six-membered ring-linked methacrylate monomer produced via the Diels-Alder reaction belongs to methyl (CH_3) group, while the peaks at δ 5.60-6.44 ppm is related to the conjugated double bonds in (ETO), It decreased to 5.60-6.22 ppm. Protons of the oxirane ring showed clear peaks at δ 2.70-2.80 and 3.35 ppm, marked 1a-1b and 2 in Figure 21b, (Okieiman, 2000; Singh, 2015).

In the ^{13}C-NMR spectrum, peaks are observed at δ 65.3 and δ 72.4 ppm, which are shown as 1,2 and 3 in Figure 22a, is resulting from the resonance of carbon in the triglyceride backbone for tung oil. Understanding carbons for tung oil showed significant peaks at 127.3-139.7 ppm (Wutticharoenwong, 2010).

The ^{13}C-NMR spectrum of GMA, give significant peaks related to oxirane group, the oxirane group (–OCH_2 –) resonated at δ 44.27, the glycidyl group (O (CH_2) CH-CH_2) δ 49.08, and the ester group at (–OCH_2 –) δ 64.88 ppm. Other observed peaks are related to methacrylate group (CH_2=C) at δ 125.82 and 135.61 ppm, and the (C=O) group at δ 166.66 ppm (Wıcks Jr et al., 2007). As shown in Figure 22b, the expected oxirane resonance of ^{13}C- NMR of ETO is [(–OCH_2 –) ;(1)] δ 44.50 ppm and glycidyl ester resonances are [(O (CH_2) CH-CH_2 -); 2] δ at 49.22 ppm and [(–OCH_2 -); 3] δ at 65.04 ppm. Peaks of δ 125.090-135.79 ppm for the unsaturation (CH_2=C) and δ 166.96 ppm for the (C=O) group were determined due to the unreacted parts of tung oil (Saithai, 2013).

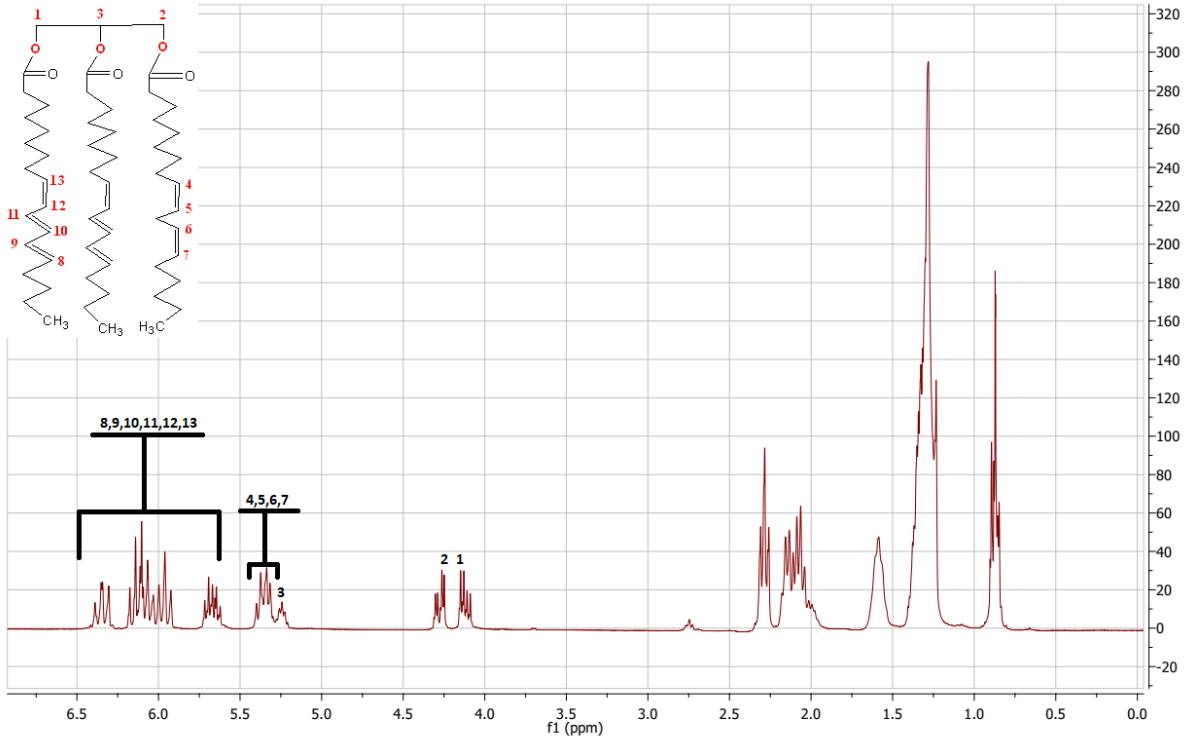

Figure 21a. ^{1}H-NMR Spectra of Tung Oil

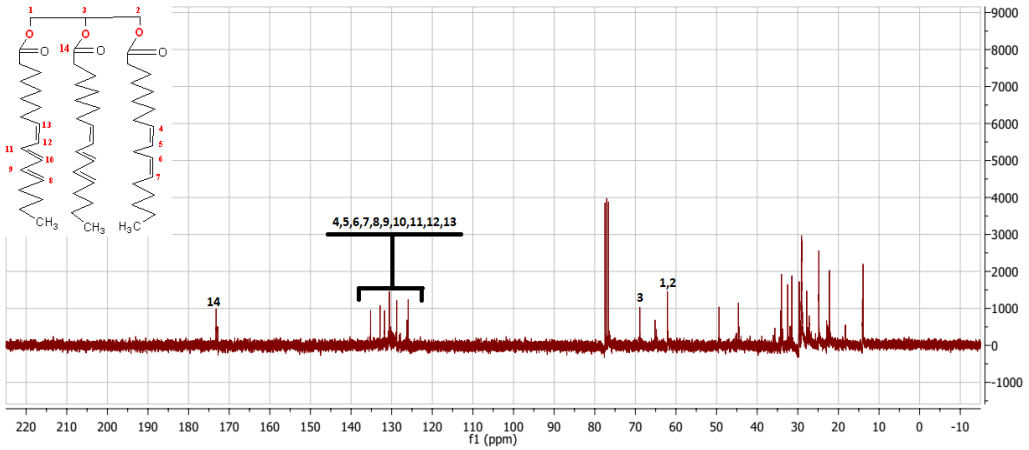

Figure 21b. ^{13}C-NMR Spectra of Tung Oil

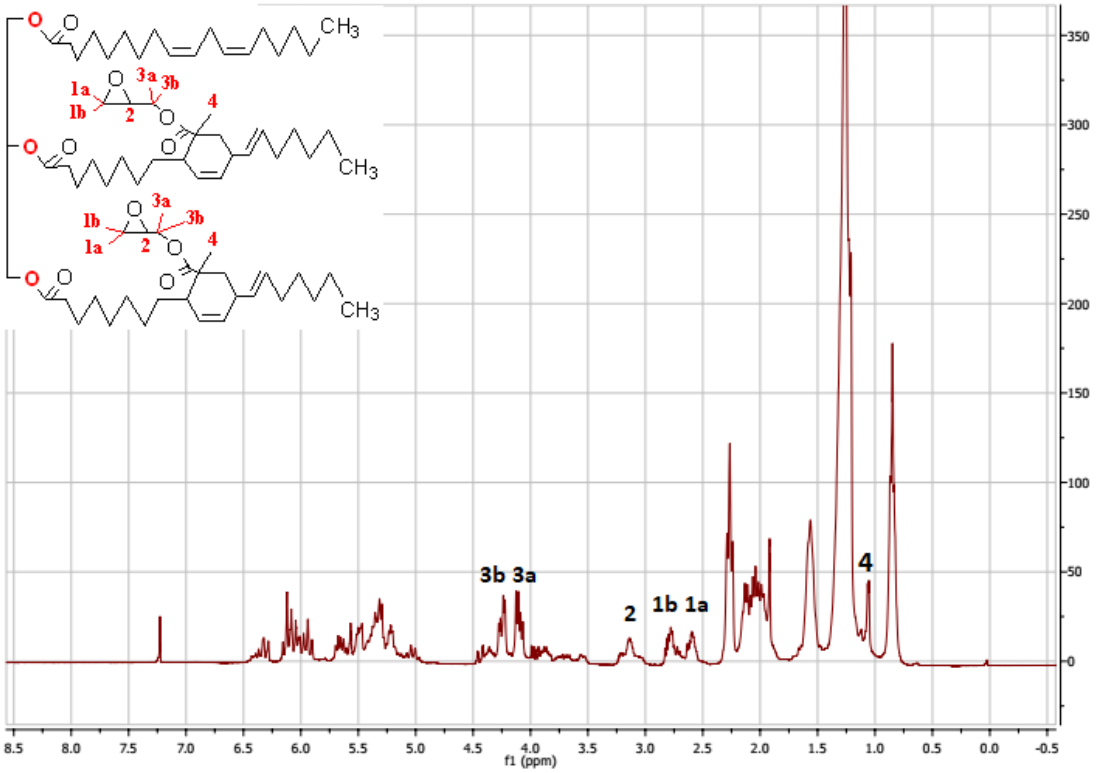

Figure 22a. ^{1}H-NMR Spectra of Epoxized-Tung Oil (ETO)

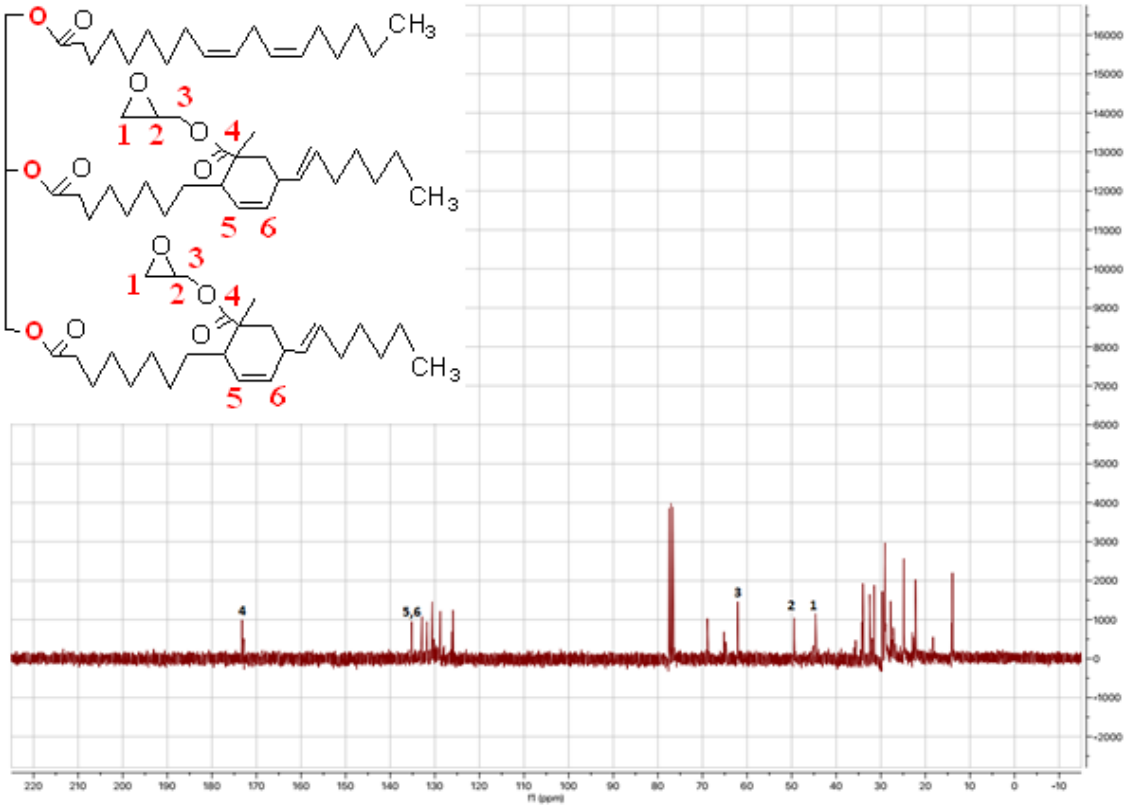

Figure 22b. ^{13}C-NMR Spectra of Epoxized-Tung Oil (ETO)

4.2. Results of ETO-ETO Coatings

4.2.1. IR Results of ETO-ETO Coatings

The -OH groups are formed as a result of expected ring opening with homopolymerization of epoxide resin (Scheme 23). These groups are seen in the range of 3459-3467 cm^{-1}. While sp^2 CH vibrations were observed in the range of 3008-3015 cm^{-1}, sp^3 CH vibrations were detected in the range of 2854-2927 cm^{-1}. The IR bands seen at 726 cm^{-1} confirm the epoxy homopolymerization (Table 1, and figure S1) shows the IR values of ETO-ETO coatings. (Ferdosian, 2016; Patil, 2017; Vijayan, 2017; Zahra, 2014)

Table 1. IR of ETO-ETO Systems

ER-ER SYSTEMS	-OH	sp^2(CH)	sp^3 (CH)	(C=O)	sp^3(CH)	(C-O) ether	(C-O) ester	C O-C/CH_2 (Rocking)
ETO-ETO (25°C)	-	-	-	-	-	-	-	-
ETO-ETO (80 ^{0}C)	3466	3009	2855-2927	1732	1456	238	1099	726
ETO-ETO (120 ^{0}C)	3467	3015	2854-2925	1735	1458	1241	1104	726
ETO-ETO (150 ^{0}C)	3459	3008	2858-2927	1735	1455	1230	1092	726

*ETO-ETO (25°C) Systems didn't Work.

ETO-ETO systems prepared without any hardeners, display homopolimerization reaction of epoxy resin. The homopolimerization reaction of epoxy resin are shown in Scheme 23.

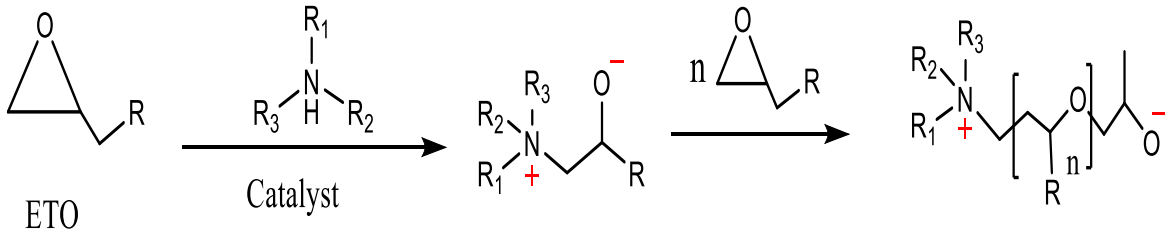

Scheme 23. Homopolymerization of ETO-ETO Systems

4.2.2. DSC Results of ETO-ETO Coatings

Since the polymerization occurred as a result of the expected ring opening with the homopolymerization of the epoxy resin (Scheme 23), Tg points were determined by performing DSC measurements of the resulting coatings. It is observed that there is no significant difference between the Tg points of the coating between 80-150 ˚C, and the Tg points are located in the range of 82-85 ˚C. Figure 23 shows the DSC values for ETO-ETO coatings.

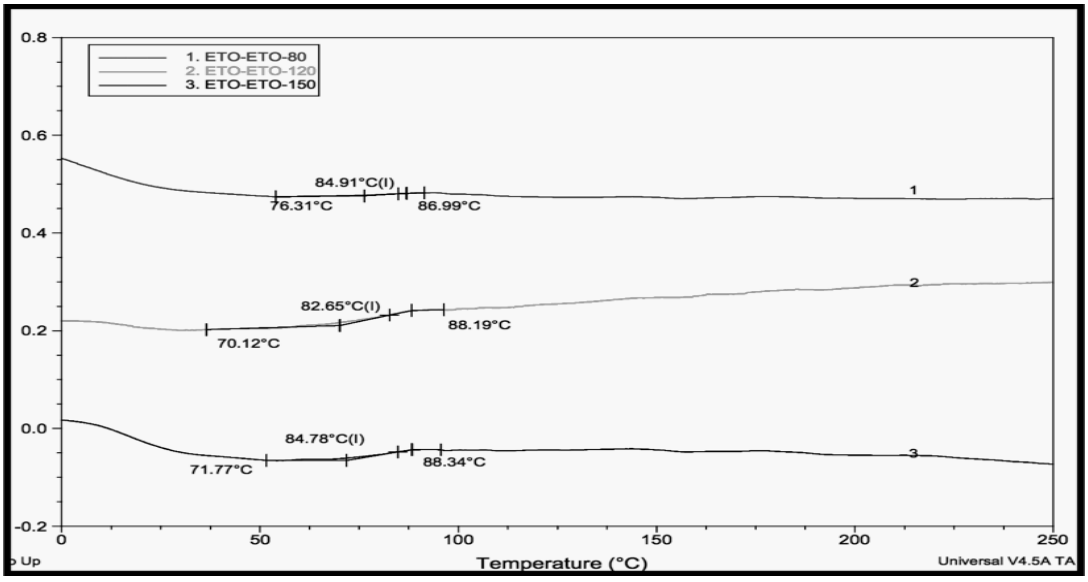

Figure 23. Values of DSC for ETO-ETO Coatings.

4.2.3. TGA Results of ETO-ETO Coatings

TGA values of ETO-ETO coatings are shown in Table 2. Since the polymerization occurred as a result of the expected ring opening with the homopolymerization of the epoxy resin (Scheme 23), the thermal stability of the coatings was determined by using TGA measurements. There is no big difference between the thermal stability of the coatings realized in the 80-150 ˚C range (Figure 24).

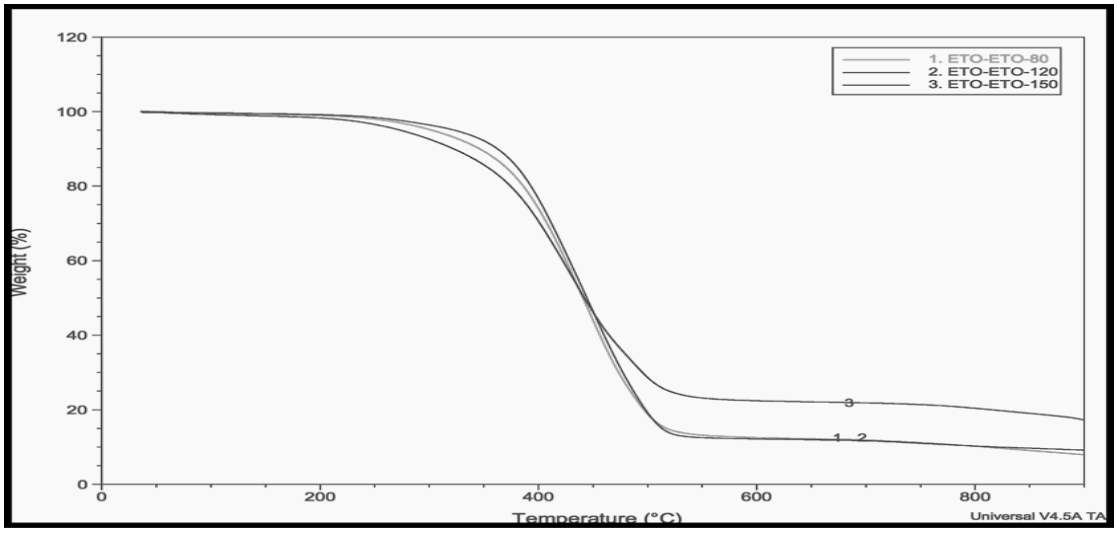

Figure 24. TGA Values of ETO-ETO Coatings

Table 2. TGA Values of ETO-ETO Coatings

ETO-ETO Systems	T (˚C)	%Y (at 900 ˚C)
ETO-ETO (25°C)	-	-
ETO-ETO (80 ˚C)	408	10.26
ETO-ETO (120 ˚C)	412	10.30
ETO-ETO (150 ˚C)	402	20.40

4.3. Results of New Epoxide-Nanocomposite Coatings

In this part of the thesis, new epoxide-nanocomposite coatings for metallic surfaces from the reaction of bio-based epoxide resin (ETO) with a polyetheramines (Jeffamin T403 and ED900) and carbon nanoparticles (carbon nanotubes, graphene and fullerenes) are given. While characterization of cured coatings is evaluated by IR, DSC, TGA, gel content, the mechanical properties of the cured coating are determined by the known tests such as pencil hardness, pendulum hardness, cross-cut resistance, pull-off adhesion, impact/reverse impact resistance tests.

Epoxidation product (ETO) of tung oil in the first stage was carried out using a Diels-Alder reaction of glycidyl methacrylate (GMA) with tung oil (Scheme 21).

The nanocomposites epoxide-amine coatings are synthesized by equimolar ratio a (1:1) of epoxide and amine and 0.1% nanoparticules at 25°C. The epoxide-nanocomposite coatings are cured at different temperatures, starting from 25°C, 80 ˚C, 120 ˚C and 150 ˚C. Bio-based epoxide resin (ETO) was formulated with two different polyetheramines, Jeffamine T403 with triamine functionality and Jeffamine ED900 with diamine functionality, and carbon nanoparticles (carbon nanotubes, graphene, and fullerenes) (Scheme 22).

As a result, epoxide-amine network attached to the surface of carbon nanostructures were coated on aluminum metallic substrates with Graphene/CNT/Fullerene based nanoparticle doped nanocomposites.

ETO underwent cross-linking reaction with various amines, via ring opening reaction at 25°C, as given in Scheme 24 (Cocker et al., 1998).

The second step of the reaction is between the acidic hydrogen of the primary amines and another epoxide molecule to give an alcoholic tertiary amine which undergoes further reaction to give the epoxide- amine network (Scheme 24).

The third step is between the hydrogen remaining in the partially reacted primer amine and a second epoxide ring; this forms a second alcoholic hydroxyl group and a fully reacted tertiary amine. It is at this stage that crosslinking occurs (Cocker et al., 1998). The polymerization between oxirane groups and the amines reaction continuously increases the crosslink density.

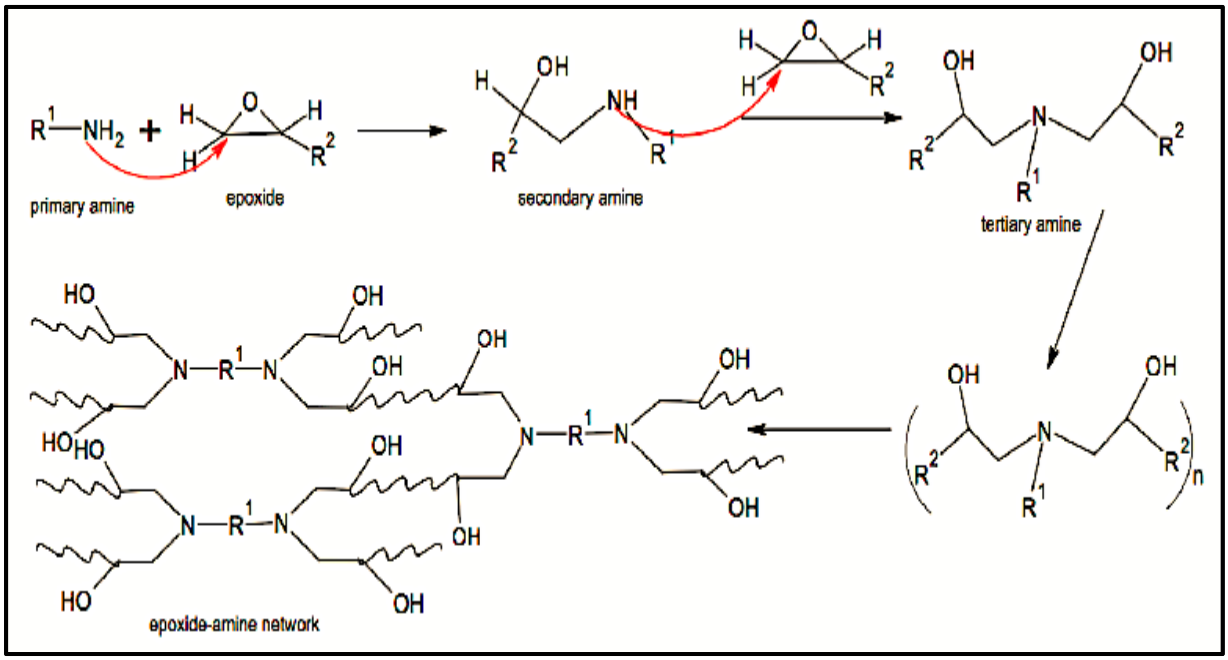

Scheme 24. Formation of The Epoxide-Amine Network

4.3.1. IR Results of New Epoxide-Nanocomposite Systems

The IR values of Epoxide-Triamine (Jeffamine T403) nanocomposite systems are given in Table 3 and Epoxide-Diamine (Jeffamine ED900) nanocomposite systems are given in Table 4. IR spectra of all systems are given in Figures S2-4 in supplementary materials.

The large peaks in the 3292–3464 cm^{-1} region in the IR spectra are related to the –OH groups resulting from the ring opening reaction of the epoxide ring, which is indicative of the polymerization of epoxide resin with Jeffamines. The absence of characteristic peaks in the range

of 3300-3700 cm^{-1} gives an indication of the disappearance of the N-H group due to the reaction with the epoxy group owing to the formation of the epoxide-amine network (Scheme 24).

The significant peaks at 2855–2963 cm^{-1} are attributed to the symmetric and asymmetric stretching of aliphatic-CH bonds (Jebrane, 2007; Wu, 1999). While sp^2-CH bands for double bands are observed at 3009 –3012cm^{-1}, the bond at 1736–1739 cm^{-1} is due to the stretching vibration of the (-C=O) bands (Vijayan, 2017; Wu, 2016; Zahra, 2014). The observed bonds at 1245 cm^{-1} and 1372-1375 cm^{-1} are attributed to the (-CNC-) and -OH groups which result from the curing of epoxide amines. While ether bands (C-O) were observed at 1242-1248 cm^{-1}, ester tension bands appeared in the range of 1096-1102 cm^{-1} (Karadeniz, 2015; Patil, 2017).

When comparing the IR spectra peaks given by the nanocomposite coatings, no significant differences were observed between the epoxide-triamine and epoxide-diamine nanocomposite cured systems. -OH, $-CH_{aliphatic}$, (C=O), (-C-N-C-), (-C-C-N-) and (C-O) tensile bands appeared as expected in epoxy-amine systems and are consistent with literature data (Jebrane, 2007; Karadeniz, 2015; Patil, 2017; Vijayan, 2017; Wu, 1999; Wu, 2016; Zahra, 2014).

Table 3. IR Spectra of the Epoxide-Triamine Systems

Epoxide-Amine Systems	-OH	-sp^2 (-CH) stretch	-sp^3(-CH) stretch.	(C=O) stretch	-sp^3 (C-H) Bend	C-N-C (Ter.Amine) /-OH	C-C-N /(C-O) of ether	(C-O) of ester	C-O-C / Rocking CH_2
ETO-T403-Nano. (Graphene-25°C)	3328	3011	2855-2925	1736	1458	1373	1244	1101	724
ETO-T403-Nano. (Graphene-80 °C)	3329	3011	2857-2925	1737	1459	1373	1245	1102	740
ETO-T403-Nano. (Graphene-120 °C)	3328	3011	2855-2923	1737	1455	1374	1242	1101	726
ETO-T403 (Graphene-150 °C)	3328	3011	2855-2925	1738	1455	1374	1242	1102	726
ETO-T403-Nano. (CNT-25°C)	3342	3011	2855-2960	1739	1455	1373	1243	1103	741
ETO-T403-Nano. (CNT-80 °C)	3342	3011	2855-2960	1739	1457	1373	1244	1103	741
ETO-T403-Nano. (CNT-120 °C)	3342	3011	2855-2960	1739	1457	1373	1243	1102	738
ETO-T403-Nano. (CNT-150 °C)	3342	3011	2855-2960	1738	1456	1374	1243	1102	726
ETO-T403-Nano. (Fullerene-25°C)	3292	3012	2855-2960	1739	1458	1373	1243	1103	741
ETO-T403-Nano. (Fullerene-80 °C)	3292	3012	2855-2961	1736	1456	1374	1248	1101	726
ETO-T403-Nano. (Fullerene-120 °C)	3313	3012	2855-2963	1737	1455	1374	1249	1101	728
ETO-T403-Nano. (Fullerene-150 °C)	3330	3012	2855-2963	1737	1456	1375	1242	1102	727
ETO-ETO (25°C)	-	-	-	-	-	-	-	-	-
ETO-ETO (80 ^{0}C)	3466	3009	2855-2925	1732	1456	-	1238	1099	726
ETO-ETO (120 ^{0}C)	3467	3015	2854-2925	1735	1458	-	1241	1104	726
ETO-ETO (150 ^{0}C)	3459	3008	2858-2927	1735	1455	-	1230	1092	726

Table 4. IR Spectra of the Epoxide-Diamine Systems

Epoxide-Amine Systems	**-OH**	**-sp^2(CH) Stretch.**	**-sp^3(CH) Stretch. CH stretch**	**(C=O) Stretch.**	**-sp^3 (CH) Bend**	**C-N-C (Ter. Amine)/ -OH**	**C-C-N/ (C-O) of ether**	**(C-O) of ester**	**C-O-C/Rocking CH_2**
ER-ED900-Nano. (Graphene-25°C)	3464	3009	2860-2923	1736	1457	1348	1248	1099	725
ER-ED900-Nano. (Graphene-80 °C)	3464	3009	2857-2923	1736	1454	1348	1248	1100	726
ER-ED900-Nano. (Graphene-120 °C)	3463	3009	2856-2922	1737	1457	1348	1247	1100	726
ER-ED900 (Graphene-150 °C)	3463	3009	2857-2922	1737	1454	1349	1247	1100	725
ER-ED900-Nano. (CNT-25°C)	3464	3009	2856-2923	1738	1460	1348	1246	1101	726
ER-ED900-Nano. (CNT-80 °C)	3454	3009	2855-2923	1738	1457	1348	1245	1102	727
ER-ED900-Nano. (CNT-120 °C)	3463	3012	2855-2923	1738	1458	1348	1246	1101	725
ER-ED900-Nano. (CNT-150 °C)	3454	3012	2855-2923	1738	1456	1349	1245	1101	725
ER-ED900-Nano. (Fullerene-25°C)	3445	3012	2858-2923	1737	1456	1349	1247	1098	725
ER-ED900-Nano. (Fullerene-80 °C)	3445	3009	2858-2923	1737	1456	1349	1247	1098	725
ER-ED900-Nano. (Fullerene-120 °C)	3445	3009	2858-2920	1736	1456	1349	1247	1097	725
ER-ED900-Nano. (Fullerene-150 °C)	3444	3009	2857-2923	1736	1456	1349	1247	1099	725
ETO-ETO (25°C)	-	-	-	-	-	-	-	-	-
ETO-ETO (80 ^{0}C)	3466	3009	2855-2925	1732	1456	-	1238	1099	726
ETO-ETO (120 ^{0}C)	3467	3015	2854-2925	1735	1458	-	1241	1104	726
ETO-ETO (150 ^{0}C)	3459	3008	2858-2927	1735	1455	-	1230	1092	726

4.3.2. DSC Results of New Epoxide-Nanocomposite Systems

Differential scanning calorimetry (DSC) measurements were used to determine glass transition temperatures (Tg) of the synthesized coatings. Tg points were determined from the midpoint of the heat capacity change and calculated from after cooling (20 $^{\circ}C\ min^{-1}$) to eliminate the effects of the sample history. Glass transition temperatures of cured epoxide-amine systems and ETO-ETO systems are given in (Tables 5,6).

ETO-ETO systems were prepared at the same temperatures as control samples without any hardeners. Tg points for ETO-ETO systems are observed around 84 $^{\circ}C$. Glass Transition Temperature (T_g) points around 84$^{\circ}C$ are owing to ETO-ETO homopolymerization. It is known that the epoxy prepolymers undergo small percentage of homopolymerization in precence of limited amount of the catalyst during the same period of reaction time (Doring and Arnold, 2009).

Table 5. Tg Points of Epoxide-Triamine Systems

Systems	Tg Points
ETO-T403-Nano. (Graphene-25°C)	-, -
ETO-T403-Nano. (Graphene-80 °C)	-, -
ETO-T403-Nano. (Graphene-120 °C)	-, -
ETO-T403-Nano. (Graphene-150 °C)	-, -
ETO-T403-Nano. (CNT-25°C)	-, -
ETO-T403-Nano. (CNT-80 °C)	-, -
ETO-T403-Nano. (CNT-120 °C)	-, -
ETO-T403-Nano. (CNT-150 °C)	-, -
ETO-T403-Nano. (Fullerene-25°C)	-, -
ETO-T403-Nano. (Fullerene-80 °C)	-, -
ETO-T403-Nano. (Fullerene-120 °C)	-, -
ETO-T4503-Nano. (Fullerene-150 °C)	-, -
ETO-ETO systems (25°C)	It didn't cure
ETO-ETO systems (80 °C)	84
ETO-ETO systems (120 °C)	82
ETO-ETO systems (150 °C)	84

Table 6. Tg points of Epoxide-Diamine Systems

Systems	Tg Points
ETO-ED900-Nano. (Graphene-25°C)	214, 284
ETO-ED900-Nano. (Graphene-80 °C)	191, 253, 279, 297
ETO-ED900-Nano. (Graphene-120 °C)	192, 231, 253, 279
ETO-ED900-Nano. (Graphene-150 °C)	-, -
ETO-ED900-Nano. (CNT-25°C)	-, -
ETO-ED900-Nano. (CNT-80 °C)	-, -
ETO-ED900-Nano. (CNT-120 °C)	-, -
ETO-ED900-Nano. (CNT-150 °C)	-, -
ETO-ED900-Nano. (Fullerene-25°C)	-, -
ETO-ED900-Nano. (Fullerene-80 °C)	-, -
ETO-ED900-Nano. (Fullerene-120 °C)	-, -
ETO-ED900-Nano. (Fullerene-150 °C)	-, -
ETO-ETO systems (25°C)	It didn't cure
ETO-ETO systems (80 °C)	84
ETO-ETO systems (120 °C)	82
ETO-ETO systems (150 °C)	84

Whereas ETO-ETO systems display one Tg point around 84 °C, the new epoxide-nanocomposite systems exhibit no Tg points expect ETO-ED900 systems prepared with graphene nanoparticles. Tg points of ETO-ED900-graphene systems vary from 192-284 °C. These values are also consistent with previously published epoxide cured systems (Darroman et al., 2016; Nikafshar, 2017; Savonnet et al., 2018). When the Tg values of the epoxide-nanocomposites systems were compared, no significant difference was observed between the cured coating systems.

In this study, a known catalyst was used particularly 2,4,6-tris-(dimethylamino-methyl) phenol, as suitable catalyst to achieve homopolymerization of the epoxy prepolymers which attack the epoxy ring to initiate the homopolymerization reaction, (Doring and Arnold, 2009). The second and higher Tg points around 284°C belong to epoxide-amine networks. Tg points are directly related to the mobility of the polymer chain, the performance of the curing process and the resulting epoxy-amine network (Darroman et al., 2016; Nikafshar, 2017; Savonnet et al., 2018).

Jeffamine ED900, a high molecular weight compound, with multy-amino groups was used as curing agent increases the curing rate. Therefore, the crosslinking density of the epoxy amine structure increased and as a result, the Tg points is at higher values. It can be said that ETO-ED900 systems have high Tg points due to their high crosslinking densities, consistent with previous studies (Darroman et al., 2016; Nikafshar, 2017; Savonnet, 2018).

4.3.3 TGA Results of New Epoxide-Nanocomposite Systems

The Thermogravimetric analysis (TGA) was used to evaluate the thermal stability of the synthesized ETO-T403 and ETO-ED900 coatings (Table 7).

Table 7. TGA Values of Epoxide-Nanocomposite Coatings

Epoxide-Triamine Systems	T (^{0}C)	%Yield (at 900°C)	Epoxide-Diamine Systems	T (^{0}C)	%Yield (at 900°C)
ETO-T403-Nano. (Graphene-25°C)	403.3	61.8	ETO-ED900-Nano. (Graphene-25°C)	397.5 603	57.2
ETO-T403-Nano. (Graphene-80 $^\circ$C)	405.5	51.3	ETO-ED900-Nano. (Graphene 80 $^\circ$C)	394.0	72.6
ETO-T403-Nano. (Graphene-120 $^\circ$C)	409.4	55.5	ETO-ED900-Nano.(Graphene-120 $^\circ$C)	394.6	68.8
ETO-T403-Nano. (Graphene-150 $^\circ$C)	402.9	78.8	ETO-ED900-Nano. (Graphene-150 $^\circ$C)	397.0	60.6
ETO-T403-Nano. (CNT-25°C)	402.6	92.5	ETO-ED900-Nano. (CNT-25°C)	415.8	74.5
ETO-T403-Nano. (CNT-80 ^{o}C)	399.5	72.6	ETO-ED900-Nano. (CNT-80 ^{o}C)	413.8	54.7
ETO-T403-Nano. (CNT-120 ^{o}C)	407.1	84.8	ETO-ED900-Nano. (CNT-120 ^{o}C)	418.4	90.1
ETO-T403-Nano. (CNT-150 ^{o}C)	403.5	43.4	ETO-ED900-Nano. (CNT-150 ^{o}C)	420.6	74.6
ETO-T403-Nano. (Fullerene-25°C)	406.9	56.2	ETO-ED900-Nano. (Graphene-25°C)	415.5	71.9
ETO-T403-Nano. (Fullerene-80 ^{o}C)	411.3	89.3	ETO-ED900-Nano. (Fullerene-80 ^{o}C)	405.6	77.0
ETO-T403-Nano. (Fullerene-120 ^{o}C)	401.0	74.2	ETO-ED900-Nano. (Fullerene-120 ^{o}C)	407.2	44.6
ETO-T403-Nano. (Fullerene-150 ^{o}C)	403.4	77.3	ETO-ED900-Nano. (Fullerene-150 ^{o}C)	412.7	51.9
ETO-ETO systems (25°C)	-	-	ETO-ETO systems (25°C)	-	-
ETO-ETO systems (80 $^\circ$C)	408	10.26	ETO-ETO systems (80 $^\circ$C)	408	10.26
ETO-ETO systems (120 $^\circ$C)	412	10.30	ETO-ETO systems (120 $^\circ$C)	412	10.30
ETO-ETO systems (150 $^\circ$C)	402	20.40	ETO-ETO systems (150 $^\circ$C)	402	20.40

When examined the thermograms of TGA, one step decomposition were observed for all systems except ETO-ED900-graphene at 25°C. TGA analysis revealed that the new epoxide-nanocomposite systems displayed thermal stability up to 409 $^\circ$C for epoxide-triamine nanocomposites (ETO-T403-nanoparticules) and 420 $^\circ$C for epoxide-diamine nanocomposites (ETO-ED900-nanoparticules).

The new bio-based nanocomposites coatings exhibited excellent thermal stability with increased char content when compared to previous studies (Ng et al., 2017). More highly cross-linked networks may promote the charring of cured epoxide resin during pyrolysis since there are more chemical bonds present in the cured epoxide resin.

The ETO-ETO coatings showed low Char900 values in comparison of that values related to the ETO-T403 and ETO-ED900 coatings. These results indicated that the epoxy homopolymerization had a positive effect upon the resin decomposition. ETO-T403-nanocomposite systems and ETO-ED900-nanocomposite systems display high residual between %43.4-92.5 yield at 900 ˚C. While ETO-T403-CNT system cured at 150 ˚C show the lowest residual mass with 43.4 % yield at 900 ˚C, ETO-T403-CNT system cured at 25°C has the highest residual mass with 92.5 % yield at 900 ˚C. Therefore, the epoxide-nanocomposite coatings posses good flame retardation properties due the high mass content (Savonnet et al., 2018).

4.3.4 Gel-Content Test of Epoxide-Nanocomposite Networks

The gel content of cured coatings was determined by weighing cured samples accurately and subjecting them to Soxhlet extraction in acetone for 24 h at 25°C. Then coating samples were subsequently dried in a vacuum oven. Gel content of the coatings was estimated using (Eq.3).

Gel content (%) $=[A_{end}/A_0] * 100$……(Eq.3)

The cross-linking degree after curing process can be predicted by using the Gel-content values, therefore, the higher the Gel-content values is the higher cross-linking degree, (Shakil et al., 2015; Thanamongkollitet al., 2012).

The gel content values of epoxy-hardener systems are shown in (Tables 8,9). As shown in the tables, the gel content of the epoxy-amine-nanocomposite systems increased as the temperature increased. Higher temperatures also enhance the curing process, facilitating the formation of three-dimensional, cross-linked networks. The results demonstrate that all cured-coating formulations led to higher gel content, up to 99% with ETO-T403 and ETO-ED900 systems, except the ETO-ED900-fullerene system at 150 °C with 100% led to the highest gel content.

Table 8. Gel Content of Epoxide-Triamine Systems (%)

Systems	Gel Content(%)
ETO-T403-Nano. (Graphene-25°C)	99.4
ETO-T403-Nano. (Graphene-80 °C)	99.2
ETO-T403-Nano. (Graphene-120 °C)	99.7
ETO-DT403-Nano. (Graphene-150 °C)	99.7
ETO-T403-Nano. (CNT-25°C)	98.4
ETO-T403-Nano. (CNT-80 °C)	99.6
ETO-T403-Nano. (CNT-120 °C)	99.6
ETO-T403-Nano. (CNT-150 °C)	99.7
ETO-T403-Nano. (Fullerene-25°C)	99.5
ETO-T403-Nano. (Fullerene-80 °C)	99.6
ETO-T403-Nano. (Fullerene-120 °C)	99.7
ETO-T403-Nano. (Fullerene-150 °C)	99.7
ETO-ETO systems (25°C)	It didn't cure
ETO-ETO systems (80 °C)	87
ETO-ETO systems (120 °C)	92
ETO-ETO systems (150 °C)	98

Table 9. Gel Content of Epoxide-Diamine Systems (%)

Systems	Gel Content(%)
ETO-ED900-Nano. (Graphene-25°C)	99.5
ETO-ED900-Nano. (Graphene-80 °C)	99.7
ETO-ED900-Nano. (Graphene-120 °C)	99.6
ETO-ED900-Nano. (Graphene-150 °C)	94.4
ETO-ED900-Nano. (CNT-25°C)	99.5
ETO-ED900-Nano. (CNT-80 °C)	99.8
ETO-ED900-Nano. (CNT-120 °C)	98.9
ETO-ED900-Nano. (CNT-150 °C)	94.4
ETO-ED900-Nano. (Fullerene-25°C)	99.5
ETO-ED900-Nano. (Fullerene-80 °C)	99.5
ETO-ED900-Nano. (Fullerene-120 °C)	99.8
ETO-ED900-Nano. (Fullerene-150 °C)	100
ETO-ETO systems (25°C)	It didn't cure
ETO-ETO systems (80 °C)	87
ETO-ETO systems (120 °C)	92
ETO-ETO systems (150 °C)	98

4.3.5. General Coating Properties of Epoxide-Nanocomposite Networks

The typical coating properties (pendulum hardness, pencil hardness, cross-hatch adhesion, pull-off adhesion, impact resistance and reverse impact resistance) were measured, and the results are presented in Tables 10-11.

In terms of pendulum hardness for epoxide-triamine systems, it is observed that the highest point is at (120±2) for the ETO-T403-CNT (120 ˚C) system, and the lowest point is at (56± 3) for ETO-T403 (Fullerene-rt). For epoxide-diamine systems the highest point is at (133±3) for the ETO-ED900-CNT (120 ˚C) system, and the lowest point is at (56± 3) for ETO-ED900 (Fullerene-rt). In generally, epoxide-triamine nanocoatings display higher pendulum hardness compared to epoxide-diamine nanocoatings. In both systems, while CNT nanocomposites cured at 120 ºC exhibit highest pendulum hardness values, fullerene nanocomposites cured at 25°C show the lowest pendulum hardness values. ETO-ETO systems show highest value at (35± 3) for pendulum hardness. It can be said that nanocomposites increase the hardness of coatings.

No differences were observed among the systems for pencil hardness. All the systems prepared in this study were shown to have good pencil hardness at 6H, according to ASTM standards. There were also no differences among the systems in cross-hatch adhesion. All the systems prepared in this study showed good cross-hatch adhesion at 5B, according to ASTM standards.

In dry conditions, the prepared coatings displayed adhesion, with pull-off values between (0.67-1.18 Ib/ln^2 x100) for epoxide-triamine nanocoating systems and (0.79-1.16 Ib/ln^2 x100) for epoxide-diamine nanocoating systems. There is no big difference between epoxide-triamine nanocoatings and epoxide-diamine nanocaotings systems in terms of pull-off adhesion. However, epoxide-amine nanocoating decrease the adhesion properties compared to ETO-ETO systems which have pull-off adhesion values with (0.80-2.00 Ib/ln^2 x100). It can be said that carbon nanoparticles decrease the adhesion properties of coatings. Generally, the coating systems, which were cured at 150 ˚C, were shown to have higher pull-off values compared to the other coatings in this study.

Impact resistance was evaluated to study the coating systems' load distribution properties. The results of indirect impact are shown in Tables 10-11. All the prepared coatings in this study

displayed very good impact and reverse impact at > 40. This positive result in the mechanical property can be attributed to the increase in the interface surface interaction between the micro-sized ilmenite particles and epoxy base matrix. Increasing the cross-linking density of Jeffamine resin molecules with the epoxide resin matrix decreased the microvoids between these particles and the coating matrix, thus decreasing the likelihood of cracks forming under mechanical stress.

Table 10. Mechanical Properties of Epoxide-Triamine Nanocomposite Coatings

Epoxide-Triamine Systems	Pendulum Hardn.	Pencil Hardn.	Cross-Hatch Adhes.	Pull-off Adhes (lb/in^2 x100)	Impact Resist. (kg/cm)	Reverse Resist. (kg/cm)
ETO-T403-Nano. (Graphene-25°C)	65±2	5H	5B	1.18	> 40	> 40
ETO-T403-Nano. (Graphene-80 °C)	71±3	6H	5B	1.18	> 40	> 40
ETO-T403-Nano. (Graphene-120 °C)	74±2	6H	5B	1.11	> 40	> 40
ETO-T403-Nano. (Graphene-150 °C)	73±3	6H	5B	1.19	> 40	> 40
ETO-T403-Nano. (CNT-25°C)	62±2	5H	5B	0.69	> 40	> 40
ETO-T403-Nano. (CNT-80 °C)	96±3	6H	5B	1.11	> 40	> 40
ETO-T403-Nano. (CNT-120 °C)	120±2	6H	5B	0.72	> 40	> 40
ETO-T403-Nano. (CNT-150 °C)	112±3	6H	5B	1.02	> 40	> 40
ETO-T403-Nano. (Fullerene-25°C)	56±2	5H	5B	0.67	> 40	> 40
ETO-T403-Nano. (Fullerene-80 °C)	57±2	6H	5B	0.92	> 40	> 40
ETO-T403-Nano. (Fullerene-120 °C)	80±3	6H	5B	0.79	> 40	> 40
ETO-T403-Nano. (Fullerene-150 °C)	98±2	6H	5B	1.00	> 40	> 40
ETO-ETO systems (25°C)	-	-	-	-	-	-
ETO-ETO systems (80 °C)	17±2	3H	5B	0.80	> 40	> 40
ETO-ETO systems (120 °C)	28±3	4H	5B	1.20	> 40	> 40
ETO-ETO systems (150 °C)	35±3	6H	5B	2.00	> 40	> 40

Table 11. Mechanical Properties of Epoxide-Diamine Nanocomposite Coatings

Epoxide-Diamine Systems	Pendulum Hardn.	Pencil Hardn.	Cross-Hatch Adhes.	Pull-off Adhes (lb/in^2 x100)	Impact Resist (kg/cm)	Reverse Resist (kg/cm)
ETO-ED900-Nano. (Graphene-25°C)	34±3	5H	5B	0.96	> 40	> 40
ETO-ED900-Nano. (Graphene-80 °C)	45±2	6H	5B	0.93	> 40	> 40
ETO-ED900-Nano. (Graphene-120 °C)	60±3	6H	5B	0.91	> 40	> 40
ETO-ED900-Nano. (Graphene-150 °C)	85±3	6H	5B	0.95	> 40	> 40
ETO-ED900-Nano. (CNT-25°C)	86±3	6H	5B	1.15	> 40	> 40
ETO-ED900-Nano. (CNT-80 °C)	120	6H	5B	0.97	> 40	> 40
ETO-ED900-Nano. (CNT-120 °C)	133±3	6H	5B	0.79	> 40	> 40
ETO-ED900-Nano. (CNT-150 °C)	98±2	6H	5B	1.16	> 40	> 40
ETO-ED900-Nano. (Fullerene-25°C)	56±3	6H	5B	0.99	> 40	> 40
ETO-ED900-Nano. (Fullerene-80 °C)	67±2	6H	5B	0.82	> 40	> 40
ETO-ED900-Nano. (Fullerene-120 °C)	75±3	6H	5B	0.84	> 40	> 40
ETO-ED900-Nano. (Fullerene-150 °C)	73±2	6H	5B	0.93	> 40	> 40
ETO-ETO systems (25°C)	-	-	-	-	-	-
ETO-ETO systems (80 °C)	17±2	3H	5B	0.80	> 40	> 40
ETO-ETO systems (120 °C)	28±3	4H	5B	1.20	> 40	> 40
ETO-ETO systems (150 °C)	35±3	6H	5B	2.00	> 40	> 40

5. CONCLUSION AND RECOMMENDATIONS

The bio-based epoxied resin was cured with two different amines (Jeffamine T403 and ED900) and carbon nanoparticules (Graphene, CNT and Fullerene). These new epoxide-nanocomposite coatings exhibited excellent thermal stability. All the cured films have good mechanical properties in terms of hardness, adhesion and impact resistance. Among the cured systems in this study, epoxide-amine-CNT (120°C) coatings displayed highest mechanical properties in terms of pendulum hardness. There is no big differences between epoxide-triamine nanocoatings and epoxide-diamine nanocaotings in terms of thermal and mechanical properties.

Epoxide-nano coatings prepared with epoxied tung oil, Jeffamines (T403 and ED900) and nanoparticules can be used instead of BPA-based epoxy coatings in food and beverage industry due to their good thermal and mechanical properties.

REFERENCES

Adachi, T., Araki, W., Nakahara, T., Yamaji, A., Gamou, M. (2002*).* Fracture Toughness of Silica Particulate-Filled Epoxy Composite. *J Appl Polym Sci*, 86(9), 2261–2265.

Ahmadi, Z. (2019). Epoxy In Nanotechnology: A Short Review, *Progress in Organic Coatings*, 132, 445–448.

Al-Saleh, M.H., Sundararaj, U. A. (2009). Review of Vapor Grown Carbon Nanofiber/Polymer Conductive Composites. *Carbon*, 47, 2-22.

Anderson, T. F., Messick, V. B., Pritchard. G. (1980). *(Ed.): Developments in Reinforced Platics 1,* Allied Science Publishers Ltd, London: 29–58,

Argon, A.S., Cohen. R.E. (2003). Toughenability of Polymers. *Polymer*, 44(19), 6013–6032.

Auvergne, R., Caillol, S., David, G., Boutevin, B., Pascault, J.P. (2014). Biobased Thermosetting Epoxy: Present and Future. *Chem. Rev*,114(2), 1082−1115.

Aydin, T., Gurcan, C., Taheri, H., Yilmazer, A. (2018). Graphene Based Materials in Neural in Tissue Regeneration. Adv Exp Med Biol, 1107,129-142.

Babahan, I., Zheng, Y., Soucek, M.D. (2020). New bio based glycidal epoxides. *Progress in Organic Coatings*, 142(2), 105580.

Berhanuddin, N. I.C., Zaman, I., Rozlan, S.A.M., Karim, M.A.A., Manshoor, B., Khalid, A., Chan, S.W., Meng, Q. (2017). Enhancement of mechanical properties of epoxy/graphene nanocomposite, International Conference on Materials Physics and Mechanics, 914, 1-7.

Bottero, J.-Y., Rose, J., Wiesner, M.R. (2006). Nanotechnologies: Tools for Sustainability in A New Wave of Water Treatment Processes. *Integr Environ Assess Manage,* 2(4), 391-395.

Bourbigot, S., Duquesne, S. (2007). Fire retardant polymers: recent developments and opportunities. Journal of Materials Chemistry, 17(22), 2283–2300.

Boyaca, L.A., Beltran, A.A. (2010*). Soybean Epoxide Production with In Situ Peracetic Acid Using Homogeneous Catalysis*. *Ing Invest*, 30(1), 136-140.

Boyle, M. A., Martin, C. J., Neuner, J. D., (2001). *Epoxy resins.* Asm Handbook Volume 21 Composites,78-89.

Camille François, A., Sylvie Pourchet, A., Gilles Boni, A., Sari Rautiainen, B., Joseph Samec, B., Lucie Fournier, C., Carine Robert, C., Christophe, M., Thomas, C., Stephane Fontaine, D., Yves Gaillard, E., Vincent Placet, E., Plasseraud, L. (2017). Design And Synthesis of Biobased Epoxy Thermosets from Biorenewable Resources. *C. R. Chimie*, 20(11-12), 1006-1016.

Campbell, F. C. (2010), *Structural Composite Materials*, Materials Park, Oh, Asm International, 68.

Chen, Y., Zhang, H.B., Huang, Y., Jiang, Y., Zheng, W.G., Yu, Z.Z. (2015). Magnetic and electrically conductive epoxy/graphene/carbonyl iron nanocomposites for efficient electromagnetic interference shielding. *Compos. Sci. Technol.*, 118, 178–185.

Chrysanthos, M., Galy, J., Pascault, J.P. (2011). Preparation and properties of bio-based epoxy networks derived from isosorbide diglycidyl ether. *Polymer*, 52(16), 3611–3620.

Cocker, R.P., Chadwick, D.L., Dare, D.J., Challis, R.E. (1998*).* A low resolution pulsed NMR and ultrasound study to monitor the cure of an epoxy resin adhesive. *International Journal of Adhesion and Adhesives,* 18(5), 319-331.

Corrales, J., Kristofco, L., Steele, W., Yates, B., Breed, C., Williams, E., Brooks, B. (2015). Global Assessment of Bisphenol a In the Environment Review and Analysis of Its Occurrence and Bioaccumulation. *Dose Response,* 13(3), 1-29.

Darroman, E., Durand, N., Boutevin, B., Caillol, S. (2016). Improved Cardanol Derived Epoxy Coatings. Prog. Org. Coat, 91, 9–16.

Deng, J., Liu, X., Li, C., Jiang, Y., Zhu, J. (2015). Synthesis and properties of a bio-based epoxy resin from 2,5-furandicarboxylic acid (FDCA). *Rsc Adv*, 5(21), 15930–15939.

Ding, C., Matharu, A.S. (2014). Acs Sust. *Chem. Eng*, 2(10), 2217–2236.

Doring, M., Arnold, U. (2009). Polymerization of Epoxy Resins Initiated by Metal Complexes, *Polym. Int.*, 58(9), 976 – 988.

Eatemadi, A., Daraee, H., Karimkhanloo, H., Kouhi, M., Zarghami, N., Akbarzadeh, A., Abasi, M., Hanifehpour, Y., Joo, S.W. (2014). Carbon nanotubes: properties, synthesis, purification, and medical applications. *Nanoscale Research Letters*, 9(1), 393.

Ebnesajjad, S. (2011). *Handbook of Adhesives and Surface Preparation: Technology, Applications and Manufacturing.* Elsevier, Oxford, Uk.
Ellis, B. (1993). *Chemistry and Technology of Epoxy Resins,* Springer, Netherlands.

Ferdosian, F., Yuan, Z., Anderson, M., Xu, C. (2016*). Synthesis And Characterization of Hydrolysis Lignin- Based Epoxy Resins. Indust. Crop. Product*, 91, 295-301.

Fink, J.K. (2013). *Reactive Polymers Fundamentals and Applications: A Concise Guide to Industrial Polymers,* William Andrew, Uk.

Fiore, V., Valenza, A. (2013*). 5 - Epoxy Resins as A Matrix Material In Advanced Fiber-Reinforced Polymer (Frp) Composites*, Woodhead Publishing: Sawston: 88-121.

Gallart-Sirvent, P., Li, A., Li, K., Villorbina, G., Canela Garayoa, R. (2017). Preparation of Pressure Sensitive Adhesives from Tung Oil Via Di-Els-Alder Reaction. *International Journal of Adhesion and Adhesives,* 78(10), 67–73.

Gannon, J.A. (1986). *History and Development of Epoxy Resins. In: Seymour R.B., Kirshenbaum G.S. (eds) High Performance Polymers: Their Origin and Development,* Springer, Dordrecht: 299-307.

Garcia, F.G., Leyva, M.E., De Queiroz, A.A.A., Higa, O.Z. (2009). Epoxy networks for medicine applications: Mechanical properties and in vitro biological properties. *Journal of Applied Polymer Science*, 112(3), 1215–1225.

Gibson, G. (2017). *Chapter 27 - Epoxy Resins, In Brydson's Plastics Materials.* (8th ed.). Ed.; Gilbert, M., Elsevier: Oxford, UK: 773–797.

Gonza´Lez, M.C., Cabanelas, J. C., Pozuelo, J., Baselga, J. (2011). Preparation of Cycloaliphatic Epoxy Hybrids. *Journal of Thermal Analysis and Calorimetry,* 103(2), 717–723

Goud, V.V., Patwardhan, A.V., Pradhan, N.C. (2006). Studies on The Epoxidation of Mahua Oil (Madhumica Indica) by Hydrogen Peroxide, *Bioresource Technology*, 97(12), 1365-1371

Goyat, M.S., Ray, S., Ghosh, P.K. (2011*). Innovative Application of Ultrasonic Mixing to Produce Homogeneously Mixed Nanoparticulateepoxy Composite of Improved Physical Properties. Compos. Pt A*, 42(10), 1421–1431.

Gu, H., Tadakamalla, S., Huang, Y., Colorado, H. A., Luo, Z., Haldolaarachchige, N., Young, D.P., Wei S., Guo, Z. (2012). Polyaniline Stabilized Magnetite Nanoparticle Reinforced Epoxy Nanocomposites. *Acs Appl. Mater. Interfaces*, 2012, 4(10), 5613–5624.

Guo, H., Gu, H., Wei, Q., Zhang, N. S., Haldolaarachchige, Y., Li, D. P., Young, S., Wei, Z. Guo, J. (2013*). Magnetite–Polypyrrole Metacomposites: Dielectric Properties and Magnetoresistance Behavior. Phys. Chem. C*, 117(19), 10191–10202.

Guo, J., Long, J., Ding, D., Wang, Q., Shan, Y., Umar, A., Zhang, X., Weeks, B. L., Wei, S., Guo, Z. (2016). Significantly enhanced mechanical and electrical properties of epoxy nanocomposites reinforced with low loading of polyaniline nanoparticles. *Rsc Advances*, 6(25), 21187–21192.

Guo, J., Zhao, M.H., Shin, K.T., Niu, Y.J., Ahn, Y.D., Kim, N.H., Cui, X.S. (2017). The Possible Molecular Mechanisms of Bisphenol A Action on Porcine Early Embryonic Development. *Sci Rep*, 7(1), 8632.

Guo, Q. (2012). *Thermosets Structure, Properties and Applications* (1st ed.). Cambridge: Woodhead Publishing Ltd.

Guo, Z. Henry, L.L., Palshin, V., Podlaha, E.J. 2006. Synthesis of poly (methyl methacrylate) stabilized colloidal zero-valence metallic nanoparticles. *Journal of Materials Chemistry*, 16(18), 1772–1777.

Haddadi, S.A., Mehmandar, E., Jabair, H., Ramazani, S.A., Mohammadkhani, R., Yan, N., Arjmand, M. (2021). Zinc-doped silica/polyaniline core/shell nanoparticles towards corrosion protection epoxy nanocomposite coatings. Composites Part B: Engineering, 212, 108713.

Hergenrother, P.M., Thompson, C. M., Smith Jr, J. G., Connell, J. W., Hinkley, J. A., Lyon, R. E., Moulton, R. (2005). Flame retardant aircraft epoxy resins containing phosphorus. *Polymer*, 46(14), 5012–5024.

Hirose, S. (2011). New Epoxy Resins from Oil Palm Components. *Journal of Oil Palm Researc*, 23, 1110-1114.

Hu, F., La, Scala, J.J., Sadler, J.M., Palmese, G.R. (2014). Synthesis and Characterization of Thermosetting Furan-Based Epoxy Systems. *Macromolecules*, 47(10), 3332–3342.

Hu, F., Yadav, S.K., La Scala, J.J., Sadler, J.M., Palmese, G.R. (2015). Preparation and Characterization of Fully Furan-Based Renewable Thermosetting Epoxy-Amine Systems. *Macromol. Chem. Phys*, 216(13), 1441–1446.

Huang, K., Zhang, Y., Li., M. Lian, J., Yang, X., Xia, J. J. (2012). Preparation of a light color cardanol-based curing agent and epoxy resin composite: Cure-induced phase separation and its effect on properties. *Prog. Org. Coat*, 74(1), 240–247.

Huang, X., Zhi, C., Jiang, P., Golberg, D., Bando, Y., Tanaka, T. (2013). Polyhedral oligosilsesquioxane-modified boron nitride nanotube-based epoxy nanocomposites: an ideal dielectric material with high thermal conductivity. *Advanced Functional Materials*, 23(14), 1824–1831.

Iijima S. (1991). Helical Microtubules of Graphitic Carbon. *Nature*, 354(6348), 56–58.

Iijima, S., Ichihashi, T. (1993). Single-Shell Carbon Nanotubes of 1-Nm Diameter. *Nature*, 363, 603 – 605.

Jana, S., Zhong, W. H. (2007). FTIR Study of Ageing Epoxy Resin Reinforced by Reactive Graphitic Nanofibers. *J Appl Polym Sci*, 106(5), 3555–3563.

Jang, J., Bae, J., Lee, K. (2005). Synthesis and characterization of polyaniline nanorods as curing agent and nanofiller for epoxy matrix composite, *Polymer*, 46(11), 3677–3684.

Jaworski. C., Fox, C. B., Hameed, N. (2020). Multifunctionality In Epoxy Resins, *Polymer Reviews*, 60(1), 1-41.

Jebrane, M., Cai, S., Sandström, C., Terziev, N. (2017). The Reactivity of Linseed and Soybean Oil with Different Epoxidation Degree Towards Vinyl Acetate and Impact of The Resulting Copolymer on The Wood Durability. *Express Poly. Lett.*, 11(5), 383–395.

Jojibabu, P., Zhang, Y.X., Rider, A.N., Wang, J., Wuhrer, R., Prusty, B.G. (2020). High-performance epoxy-based adhesives modified with functionalized graphene nanoplatelets and triblock copolymers. *Int. J. Adhes. Adhes*, 96, 102521.

Kadam, A., Pawar, M., Yemul, O., Thamke, V., Kodam, K. (2015). Biodegradable Biobased Epoxy Resin from Karanja Oil. *Polymer*, 72, 82–92.

Kalia, S., Dufresne, A., Cherian, B.M., Kaith, B., Avérous, L., Njuguna, J., Nassiopoulos, E. (2011). Cellulose-Based Bio-And Nanocomposites: A Review. *Int. J. Polym. Sci.*, 2011, 1-35.

Kamat, P.V., Haria, M., Hotchandani, S. (2004). C60 Cluster as An Electron Shuttle in A Ru (II)- Polypyridyl Sensitizer-Based Photochemical Solar Cell, *J. Phys. Chem. B*, 108(17), 5166 - 5170.

Karadeniz, K., Aki, H., Sen, M.y., Calikoglu, Y. (2015). Ring Opening of Epoxidized Containing Two Different Functional Group, *J. Am. Oil Chem. Soc*, 92, 725-731.

Kavaler, Ar. (1987). Chemical Profile: Bisphenol A. *Chemical Market Reporter*, 232(4), 46.

Kotnarowska, D. (1999). Influence of Ultraviolet Radiation and Aggressive Media on Epoxy Coating Degradation. *Prog Org Coat*, 37(3-4), 149–159.

Kroto, H.W., Heath, J.R, Obrien, S.C., Curl, R.F., Smalley R.E. (1985). C60: Buckminsterfullerene, *Nature*, 318(6042), 162-163.

Kry´Sa, J., Balı´Kb, K., Kr˘enac, J., Gregorb, J. (1998*)*. Corrosion of Carbon–Epoxy Resin (C/E) And Carbon–Carbon (C/C) Composites. *Mater Chem Phys*, 57(2),156–61.

Kwan, K.M., Cheng, K., Benatar, A. (1998). Feasibility Study of Rapid Curing of Structural Adhesives. *Proc Ann Tech Confsoc Plast Eng*, 56(1), 1089-1094.

Lakshmi, B., Shivananda, K.N., Mahendra, K.N. (2010). Synthesis, Characterization and Curing Studies of Thermosetting Epoxy Resin with Amines. *Bull. Kor. Chem. Soc.*, 31(8), 2272–2278.

Lee, H., Neville, K. (1982). *Handbook of Epoxy Resins, Mcgraw-Hill*, Inc., New York 1967, Reprinted 1982.

Levchik, S.V., Weil, E. D. (2004). Thermal decomposition, combustion and flame-retardancy of epoxy resins—a review of the recent literature. *Polym. Int.*, 53(12), 1901–1929.

Li, K., Huo, N., Liu, X., Cheng, J., Zhang, J. (2016). Effects of the furan ring in epoxy resin on the thermomechanical properties of highly cross-linked epoxy networks: a molecular simulation study. *RSC Advances*, 6(1), 769–777.

Lide, D.R., Milne, G.W. (1994). *Handbook of Data on Organic Compounds* (3rd ed.). Florida: Crc Press.

Liu, F., Zhang, Z., Xu, L., Tang, M. (2012). Study on the Resistance of Ultraviolet Radiation of Composite Materials Based on Epoxy Resin. *Adv Mater Res*, (391–392), 812–816.

Liu, J.Q., Bai, C., Jia, D.D., Li, W.L., He, F.Y., Liu, Q.Z., Yao, J.S., Wang, X.Q., Wu, Y.Z. (2014). Design and fabrication of a novel superhydrophobic surface based on a copolymer of styrene and bisphenol A diglycidyl ether monoacrylate. *Rsc Advances.*, 4(35), 18025-18032.

Liu, R., Zhu, J., Luo, J., Liu, X. (2014). Synthesis and application of novel UV-curable hyperbranched methacrylates from renewable natural tannic acid. *Prog. Org. Coat.*, 77(1), 30–37.

Liu, W., Zhou, R., Goh, H.L.S., Huang, S., Lu, X. (2014). From Waste to Functional Additive: Toughening Epoxy Resin with Lignin. *Acs Appl. Mater. Interfaces*, 6(8), 5810–5817.

Liu, Y., Lin, Z., Lin, W., Moon, K.S., Wong, C. P. (2012). Reversible Superhydrophobic–Superhydrophilic Transition of ZnO Nanorod/Epoxy Composite Films. *Acs Appl. Mater. Interfaces*, 4(8), 3959–3964.

Liu, Z., Tabakman, S.M., Chen, Z., Dai, H. (2009). Preparation of Carbon Nanotube Bio Conjugates for Biomedical Applications. *Nat Protocols*, 4,1372-1382.

Ma, Q. Q., Liu, X. Q., Zhang, R. Y., Zhu, J., Jiang, Y. H. (2013). Synthesis and properties of full bio-based thermosetting resins from rosin acid and soybean oil: The role of rosin acid derivatives. *Green Chem*, 15(5), 1300–1310.

Ma, S., Li, T. Liu, X. Zhu, J. (2016). Bio-based shape memory epoxy resin synthesized from rosin acid. *Iranian Polymer Journal*, 25(11), 957–965.

Ma, S., Liu, X., Jiang, Y., Tang, Z., Zhang, C., Zhu, J. (2013). Bio-Based Epoxy Resin from Itaconic Acid and Its Thermosets Cured with Anhydride and Comonomers. *Green Chem*, 15(1), 245–254.

Maiorana, A., Ren, L., Lo Re, G., Spinella, S., Ryu, C.Y., Dubois, P., Gross, R. (2015). Bio Based Epoxy Resin Toughening with Cashew Nut Shell Liquid – Derived Resin. *Green Materials*, 3(3), 80-92.

Manthey, N.W., Cardona, F., Francucci, G., Aravinthan, T. (2013). Thermo-Mechanical Properties of Epoxidized Hemp Oil-Based Bioresins and Biocomposites. *Journal of Reinforced Plastics and Composites*, 32(19), 1444–1456.

Marks, D.W., Larock, R.C. (2002). The Conjugation and Epoxidation of Fish Oil. *J Am Oil Chem Soc.*, 79(1), 65-68.

Mascia, L., Tang, T. (1998). Curing And Morphology of Epoxy Resin-Silica Hybrids. *J. Mater. Chem*., 8(11), 2417–2421.

Masuno. H., Iwanami, J., Kidani, T., Sakayama, K., Honda. K. (2005*). Bisphenol A Accelerates Terminal Differentiation of 3t3-L1 Cells into Adipocytes Through the Phosphatidylinositol 3-Kinase Pathway. Toxicol Sci*, 84(2):319–327.

Matejka, L., Dusek, K., Dobas I. (1985). Curing of Epoxy Resins with Amines. *Polymer Bulletin*, 14(3), 309-315.

May, C.A. (1988). *Epoxy Resins, Chemistry and Technology*, (2 ed.). New York: Marcel Dekker.

May, C.A. (1989). *Epoxy resins: chemistry and technology*. In Engineered Materials Handbook; The Materials Information Society. Asm International: Novelty, Oh, Usa, Volume 1, pp. 66–77.

McDevitt, M.R., Chattopadhyay, D., Kappel, B.J., Jaggi, J.S., Schiffman, S.R., Antczak, C., Njardarson, J.T., Brentjens, R., Scheinberg, D.A. (2007). Tumor Targetting with Antibody-Functionalized, Radiolabeled Carbon Nanotubes. *J Nuclear Med.*, 48(7), 1180-1189.

Mcgrath, M., Parnas, R. S., King, S. H., Schroeder, J. L., Fischer D. A., Lenhart, J. L. (2008).
Investigation of the thermal, mechanical, and fracture properties of alumina–epoxy composites. *Polymer*, 49(4), 999–1014.
Meijer, E. (1989). Polyepoxides: Formation and Properties of Their Network Structure, *Philips Technical Review*, 44(4), 110-121.

Meli, R., Monnolo, A., Annunziata, C., Pirozzi, C., Ferrante, M.C. (2020). Oxidative Stress and Bpa Toxicity: An Antioxidant Approach for Male and Female Reproductive Dysfunction, *Antioxidants*, 9(5), 405.

Mestry, S., Mhaske, S. T. (2019). Synthesis of Epoxy Resins Using Phosphorus-Based Precursors for Flame-Retardant Coating. *J. Coat. Technol. Res.*, 16(3), 807–818.

Mezzenga, R., Boogh, L., Manson, J.A.E. (2001). A Review of Dendritic Hyperbranched Polymer as Modifiers in Epoxy Composites. *Compos Sci Technol,* 61(5),787–795.

Mirmohseni, A., Zavareh, S. (2010). Epoxy/acrylonitrile-butadiene-styrene copolymer/clay ternary nanocomposite as impact toughened epoxy. J Polym Res, 17, 191–201.

Moriyama, K., Tagami, T., Akamizu, T., Usui, T., Saijo, M., Kanamoto, N., Hataya, Y., Shimatsu, A., Kuzuya, H., Nakao, H. (2002). Thyroid Hormone Action Is Disrupted by Bisphenol a As an Antagonist. *J Clin Endocrinol Metab,* 87(11), 5185–5190.

Muroi, S., Ishimura, H. (1988). *Epoxy Resin Introduction.* Polymer Publishing Association, 2.

Muskopf, J.W., Mccollıste, S.B. (1987). *Epoxy Resıns, In Ullmann's Encyclopedıa of Indust Rıal Chemıstry,* Vol. A9, Ed. By Gerhartz, W., Yamamoto, Y.S., Kaudy, L., Rounsavılle, J.F., Schulz, G., Weınheım, Vch, 547–563

Ng, F., Bonnet, L., David, G, Caillol, S. (2017). Novel Biobased and Food Contact Epoxy Coatings for Glass Toughening Applications. *Prog. Org. Coat.,* 109,1–8.

Nguyen, B. H., Nguyen, V. H. (2016). Promising applications of graphene and graphene-based nanostructures. *Advances in Natural Sciences: Nanoscience and Nanotechnology,* 7, 1-15.

Niedermann, P., Szebényi, G., Toldy, A. (2015). Novel High Glass Temperature Sugar-Based Epoxy Resins: Characterization and Comparison to Mineral Oil-Based Aliphatic and Aromatic Resins. *Express Polymer Letters*, 9(2), 85-94.

Nikafshar, S., Zahibi, O., Moradi, Y., Ahmadi, M., Amiri, S. (2017). Chemical Modification of Lignins: Towards Biobased. *Polymers,* 9(7), 266-280.

Njuguna, B.J., Pielichowski, K., Alcock, J.R. (2007). Epoxy-Based Fibre Reinforced Nanocomposites. Advanced Engineering Materials, 9(10), 835-847.

Nouailhas, H., Aouf, C., Guerneve, C.l., Caillol, S., Boutevin, B. (2011). Synthesis And Properties of Biobased Epoxy Resins. Part 1: Glycidylation of Flavonoids by Epichlorohydrin. *Journal of Polymer Science Part A: Polymer Chemistry,* 49(10), 2261-2270.

Okıeımen, F.E., Eromonsele, O.C. (2000). Stabılızıng Effect of Derıvatıves of Khaya Seed Oıl on The Thermal Degradatıon of Poly (Vınyl Chlorıde), *Eur. Polym. J.,* 36, 525–537.

Olad, M., Barati, M., Behboudi, S. (2012). Preparation of PANI/epoxy/Zn nanocomposite using Zn nanoparticles and epoxy resin as additives and investigation of its corrosion protection behavior on iron. *Prog. Org. Coat*, 74(1), 221–227.

Omonov, T.S., Curtis, J.M. (2014). Biobased Epoxy Resin from Canola Oil. *J. Appl. Polym Sci*, 131(8), 40142.

Omran, B., Abdallah, E.A.A., Abdelwahab, M. (2017). Study of Probable Toxic Effects of Bisphenol A & the Protective Role of Vitamin E on Testes and Prostate of Adult Male Albino Rats. *Ain Shams Journal of Forensic Medicine and Clinical Toxicology,* 29(2), 7-18.

O'Neil, M.J. (2006). *The Merck Index: An Encyclopedia of Chemicals, Drugs, And Biologicals,* Whitehouse Station, N J: Merck and Co., Inc.

Ortiz, P., Wiekamp, M., Vendamme, R., Eevers, W. (2019). Bio-Based Epoxy Resins from Biorefinery by Products. *Bioresources,* 14(2), 3200-3209.

Pan, X., Sengupta, P., Webster, D. C. (2015). Novel biobased epoxy compounds: epoxidized sucrose esters of fatty acids. *Green Chemistry,* 13(4), 965-975.

Park, I., Peng, H.G., Gidley, D.W., Xue, S., Pinnavaia, T.J. (2006). Epoxy−Silica Mesocomposites with Enhanced Tensile Properties and Oxygen Permeability. *Chem. Mater*, 18(3), 650–656.

Patil, D.M., Phalak, G.A., Mhaske, S.T. (2017). Enhancement of Anti-Corrosive Performances of Cardanol Based Amine Functional Benzoxazine Resin by Copolymerizing with Epoxy Resins. *Prog. Org. Coat.,* 105, 18-28.

Pin, J.M., Sbirrazzuoli, N., Mija, A. (2015*).* From Epoxidized Linseed Oil to Bioresin: An Overall Approach of Epoxy/Anhydride Cross-Linking. *Chemsuschem*, 8(7), 1232–1243.

Pradhan, S., Pandey, P., Mohanty, S., Nayak, S.K. (2016). Insight on the Chemistry of Epoxy and Its Curing for Coating Applications: A Detailed Investigation and Future Perspectives. *Polymer-Plastics Technology and Engineering,* 2016, 55(8), 862–877.

Pritchard, G. (1998). *Plastics Additives,* (1. ed.). Netherlands: Springer.

Prolongo, S. G., Gude, M. R., Sanchez, J., Ureña, A. (2009). Nanoreinforced Epoxy Adhesives for Aerospace Industry. The Journal of Adhesion, 85(4-5), 180-100.

Qing, Y., Wang, X., Zhou, Y., Huang, Z., Luo, F., Zhou, W. (2014). Enhanced Microwave Absorption of Multi-Walled Carbon Nanotubes/Epoxy Composites Incorporated with Ceramic Particles. *Compos. Sci. Technol.,* 102, 161-168.

Rafiei Hashjin, R., Ranjbar, Z., Yari, H. (2018). Modeling of Electrical Conductive Graphene Filled Epoxy Coatings. *Prog. Org. Coat.,*125, 411-419.

Raquez, J.-M., Deléglise, M., Lacrampe, M.-F., Krawczak, P. (2010). Thermosetting (Bio)Materials Derived from Renewable Resources: A Critical Review. *Progress in polymer science,* 35(4), 487-509.

Ravindra, D., Priya, S.D., Sujay, U.M. (2013). Epoxidation Of Mustard Oil and Ring Opening with 2-Ethylhexanol for Biolubricants with Enhanced Thermo-Oxidative and Cold Flow Characteristics. *Industrial Crops and Products,* 49, 586-592.

Rosca, D., Hoa, S.V. (2011). Method for reducing contact resistivity of carbon nanotube-containing epoxy adhesives for aerospace applications. *Compos. Sci. Technol.,* 71(2), 95–100.

Sahoo, S. K., Mohanty, S., Nayak, S. K. (2015). Toughened Bio-Based Epoxy Blend Network Modified with Transesterified Epoxidized Soybean Oil: Synthesis and Characterization. *Rsc Adv*, 5(18) 13674-13691.

Saithai, P., Lecomte, J., Dubreucq, E., Tanrattanakul, V. (2013). Effects of different epoxidation methods of soybean oil on the characteristics of acrylated epoxidized soybean oil-copoly(methyl methacrylate) copolymer. *Express Polymer Letters, BME-PT Hungary,* 7(11), 910-924.

Saran, N., Parikh, K., Suh, Munõz, E., Kolla, H., Manohar, S.K. (2004). Fabrication And Characterization of Thin Films of Single-Walled Carbon Nanotube Bundles on Flexible Plastic Substrates, *J. Am. Chem. Soc*, 126(14), 4462-4463.

Savonnet, E., Grau, E., Grelier, S.B., Defoort, B., Cramail, H. (2018). Divanillin-Based Epoxy Precursors as Dgeba Substitutes for Biobased Epoxy Thermosets. *Acs Sustainable Chem. Eng.*, 6(8), 11008-11017.

Schneider, R.D.C.S., Lara, L.R.S., Bitencourt, T.B., Nascimento, M.D.G., Dos Santos Nunes, M.R. (2009). Chemoenzymatic Epoxidation of Sunflower Oil Methyl Esters. *Journal Of the Brazilian Chemical Society*, 20(8),1473-1477.

Seretis, G.V., Polyzou, A.K., Manolakos, D.E., Provatidis, C.G. (2018). Tensile performance of graphene nanoplatelets/glass fabric/epoxy nanocomposite laminae, Procedia Structural Integrity, 10, 249–256.

Shakil, M., Akhter, T., Siddiqi, H.M., Akhtar, Z. (2015). The Effect of Even-Odd Methylene Spacer Groups on The Thermal Stability of Epoxy-Amine Polymers. *J. Chem. Soc. Pak.*, 37(1), 92-98.

Sharma, P., Choudhary, V., Narula, A. (2006). Curing of epoxy resin using imide-amines. *Journal of Applied Polymer Science*, 101(5), 3503 – 3510.

Sharma, S., Luzinov, I. (2011). Ultrasonic Curing of One-Part Epoxy System, *J Compos Mater*, 45(21), 2217–2224.

Shehzad, K., Xu, Y., Gao, C., Duan, X. (2016). Three-Dimensional Macro-Structures of Two-Dimensional Nanomaterials. *Chem. Soc. Rev.*, 45(20), 5541–5588.

Sıngh, A.S., Gunasekaran, G., Suryanaraya Na C., Naık, R.B. (2015). Fatty Acıd Based Water Borne Aır Dryıng Epoxy Ester Resın For Coatıng Applıcatıons, *Prog. Org. Coat*, 87, 95–105.

Sinha Ray, S., Okamoto M. (2003). Polymer Layered Silicate Nanocomposites: A Review from Preparation to Processing. *Prog Polym Sci*,28(11), 1539-641.

Srikanta, D., Anand, V.P., Vaibhav, V.G. (2008). Epoxidation of Cottonseed Oil by Aqueous Hydrogen Peroxide Catalysed by Liquid Inorganic Acids. *Bioresource Technology*, 99(9), 3737–3744.

Stemmelen, M., Pessel, F., Lapinte, V., Caillol, S., Habas, J.-P., Robin, J.-J. (2011). A fully biobased epoxy resin from vegetable oils: From the synthesis of the precursors by thiol-ene reaction to the study of the final material. *Journal of Polymer Science*, 49(11), 2434–2444.

Sudha, G.S., Kalita, H., Mohanty, S., Nayak, S.K. (2017). Biobased Epoxy Blends from Epoxidized Castor Oil: Effect on Mechanical, Thermal, And Morphological Properties. *Macromol. Res*, 25, 420–430.

Tachibana, Y., Torii, J., Kasuya, K.I., Funabashi, M., Kunioka, M. (2014). Hardening process and properties of an epoxy resin with bio-based hardener derived from furfural. *Rsc Adv*, 4(99), 55723–55731.

Tang, W.Y., Morey, L.M., Cheung, Y.Y., Birch, L., Prins, G.S., Ho, S.M. (2012). Neonatal Exposure to Estradiol/Bisphenol A Alters Promoter Methylation and Expression of Nsbp1 and Hpcal1 Genes and Transcriptional Programs of Dnmt3a/B and Mbd2/4 In the Rat Prostate Gland Throughout Life. *Endocrinology*, 153(1), 42–55.

Teppala, S., Madhavan, S., Shankar, A. (2012). Bisphenol A and Metabolic Syndrome: Results from Nhanes. *International Journal of Endocrinology,* 2012, 1-5.

Thanamongkollit, N., Soucek, M.D. (2012). Synthesis And Properties of Acrylate Functionalized Alkyds Via a Diels-Alder Reaction. *Prog. Org. Coat.*, 73(4), 382–391.

Thomas, R. (2014). *Christophe Sinturel, Sabu Thomas, And Elham Mostafa Sadek El Akiaby. Micro- And Nanostructured Epoxy/Rubber Blends* (1st ed.). Weinheim: Wiley-Vch Verlag Gmbh and Co. Kgaa.

Thomas, S., Sinturel, C., Thomas, R. (2014). *Micro- And Nanostructured Epoxy/Rubber Blends.* Wiley-Vch Verlag Gmbh and Co, Kgaa: Pp.1-30

Tian, Q., Yuan, Y.C., Rong, M.Z., Zhang, M.Q. (2009). A thermally remendable epoxy resin. *J. Mater. Chem*, 19(9), 1289–1296.

Tripathi, G. Srivastava, D. (2011). Study on the Effect of Carboxyl Terminated Butadiene Acrylonitrile (CTBN) Copolymer Concentration on the Decomposition Kinetics Parameters of Blends of Glycidyl Epoxy and Non-Glycidyl Epoxy Resin. *International Journal of Organic Chemistry*, (1), 105, 112.

Trumbo, Dl., Otto, Jt. (2008). Epoxidized Fatty Acid-Derived Oxazoline in Thermoset Coatings. *Journal of Coatings Technology and Research*, (5), 107-111.

Unnikrishnan, K.P., Thachil, E.T. (2006). Toughening of Epoxy Resins. *Des. Monomers Polym,* 9(2), 129–152.

Unnikrishnan, K.P., Thachil, E.T. (2008). Synthesis andCharacterization of Cardanol-Based Epoxy Systems. *Designed Monomers and Polymers*, 11(6), 593-607.

Vijayan, P., Tanvir, P.A., El-Gawady, Y.H., Al-Maadeed, M. (2017). Cellulose Nanofibers to Assist The Release of Healing Agents In Epoxy Coatings. *Prog. Org. Coat.*, 112 127-132.

Wan, J., Li, C., Bu, Z.Y., Xu, C.J., Li, B.G., Fan, H. (2012*).* A Comparative Study of Epoxy Resin Cured with A Linear Diamine and A Branched Polyamine. *Chemical Engineering Journal*, 188, 160–172.

Wang K, Wang L, Wu J, Chen L, and He C. (2005). Preparation of Highly Exfoliated Epoxy/Clay Nanocomposites by "Slurry Compounding": Process and Mechanisms. *Langmuir*, 21(8),3613-3618.

Wang, D., Kou, R., Choi, D., Yang, Z., Nie, Z., Li, J., Saraf, L. V., Hu, D., Zhang, J., Graff, G. L., Liu, J., Pope M. A., Aksay, I. A. (2010). Ternary Self-Assembly of Ordered Metal Oxide−Graphene Nanocomposites for Electrochemical Energy Storage. *Acs Nano*, 4(3), 1587–1595.

Wang, H., Liu, B., Liu, X., Zhang, J., Xian, M. (2008). Synthesis of biobased epoxy and curing agents using rosin and the study of cure reactions. *Green Chemistry*, 10(11), 1190–1196.

Webster, G. (1997). Chemistry & Technology of Uv and Eb Formulation for Coatings, Inks and Paints. *John Wiley and Sons, Inc*, 2(41), 73.

Wıcks Jr, Z.W., Jones, F.N., Pappas, S.P., Wıcks, D.A. (2007). *Organıc Coatıngs: Scıence And Technology*. (3rd ed.). New Jersey, USA: John Wıley And Amp; Sons, Inc, 2007.

Wu, K.H., Cheng, K.F., Wang, C.R., Yang, C.C., Lai, Y.S. (2016). Study of Thermal and Optical Properties of Epoxy/Organically Modified Silicate Hybrids. *Materials Express*, 6(1), 28-36.

Wu, S., Sears, M.T., Soucek, M.D., Simonsick, W.J. (1999). Synthesis of Reactive Diluents for Cationic Cycloaliphatic Epoxide Uv Coatings. *Polymer*, 40(20), 5675-5686.

Wutticharoenwong, M.D. (2010). Soucek, Synthesis of Tung Oil-Based Reactive Diluents, *Macromol. Mater. Eng.*, 295(12), 1097–1106.

Yeasmin, F., Mallik, A.K., Chisty, A.H., Robel, F.N., Shahruzzaman, M.D., Haque, P., Rahman, M.M., Hano, N., Takafuji, M., Ihara, H. (2021). Remarkable enhancement of thermal stability of epoxy resin through the incorporation of mesoporous silica micro-filler. Heliyon, 7(1), 1-12.

Yu, J., Huang, X., Wang, L., Peng, P., Wu, C., Wu X., Jiang, P. (2011). Preparation of hyperbranched aromatic polyamide grafted nanoparticles for thermal properties reinforcement of epoxy composites. *Polymer Chemistry*, 2(6), 1380–1388.

Yuan, H., Qi, F., Zhao, N., Wan, P., Zhang, B., Xiong, H., Liao, B., Ouyang, X. (2020). Graphene Oxide Decorated with Titanium Nanoparticles to Reinforce the Anti-Corrosion Performance of Epoxy Coating. *Coatings*, 10(2), 129.

Zahra, Y., Djouani, F., Fayolle, B., Kuntz, M., Verdu, J. (2014). Thermo-Oxidative Aging of Epoxy Coating Systems. *Prog. Org. Coat.*, 77(2), 380–387.

Zaman, I., Phan, T. T., Kuan, H.C., Meng, Q., La, L. T. B., Luong, L., Youssf O., Ma, J. (2011). Epoxy/graphene platelets nanocomposites with two level of interface strength, *Polymer*, 52(7), 1603–1611.

Zhang, Q., Chen, C., Chen, W., Pastel, G., Guo, X., Liu, S., Wang, Q., Liu, Y., Li, J., Yu, H., Hu, L. (2019). Nanocellulose-Enabled, All-Nanofiber, High-Performance Supercapacitor. ACS Appl. Mater. Interfaces, 11(6), 5919–5927.

Zhang, W., Li, Y., He, M., Chen, Q. (2007). Synthesis of Bisphenol F by Using Modified Cation Exchange Resin. *Huagong Jinzhan*, 26(7), 1032-1035.

Zhao, R., Torley, P., Halley, P.J. (2008). Emerging Biodegradable Materials: Starch- And Protein-Based Bio-Nanocomposites. *J. Mater. Sci.*, 43, 3058–3071.

Zheng, Y. (2014). *Relationship Between Crosslinking and Ordering for the Fabrication of Soft Templated Mesoporous Carbon Thin Films and Attempts Toward Time Efficient Fabrication of Mesoporous Carbon and Metal Oxides*, Master Thesis, The University of Akron, Department of Polymer Engineering, Akron.

Zhu, J., Wei, S., Haldolaarachchige, N., Young, D. P., Guo, Z. (2011). Electromagnetic Field Shielding Polyurethane NanocompositesReinforced with Core-Shell Fe-Silica Nanoparticles. *J. Phys. Chem. C*, 115(31), 15304–15310.

Zhu, J., Wei, S., Ryu, J., Budhathoki, M., Liang, G., Guo, Z. (2010). In situ stabilized carbon nanofiber (CNF) reinforced epoxy nanocomposites. *Journal of Materials Chemistry*, 20(23), 4937–4948.

Zhu, J., Wei, S., Ryu, J., Sun, L., Luo, Z., Guo, Z. (2010). Magnetic Epoxy Resin Nanocomposites Reinforced with Core−Shell Structured Fe@FeO Nanoparticles: Fabrication and Property Analysis. *Acs Appl. Mater. Interfaces*, 2(7), 2100–2107.

APPENDICES

APPENDIX 1: Supplementary materials

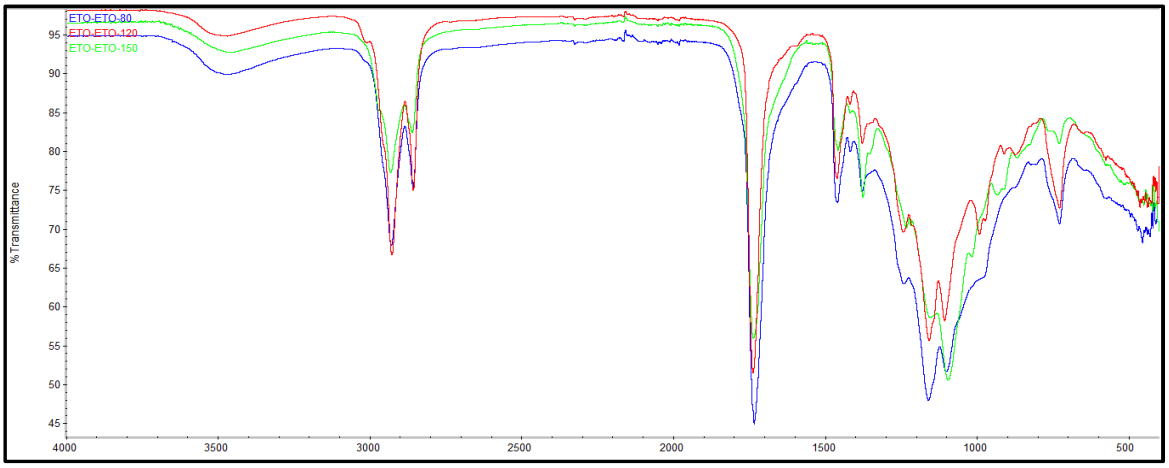

Figure S1. IR spectra for ETO-ETO systems

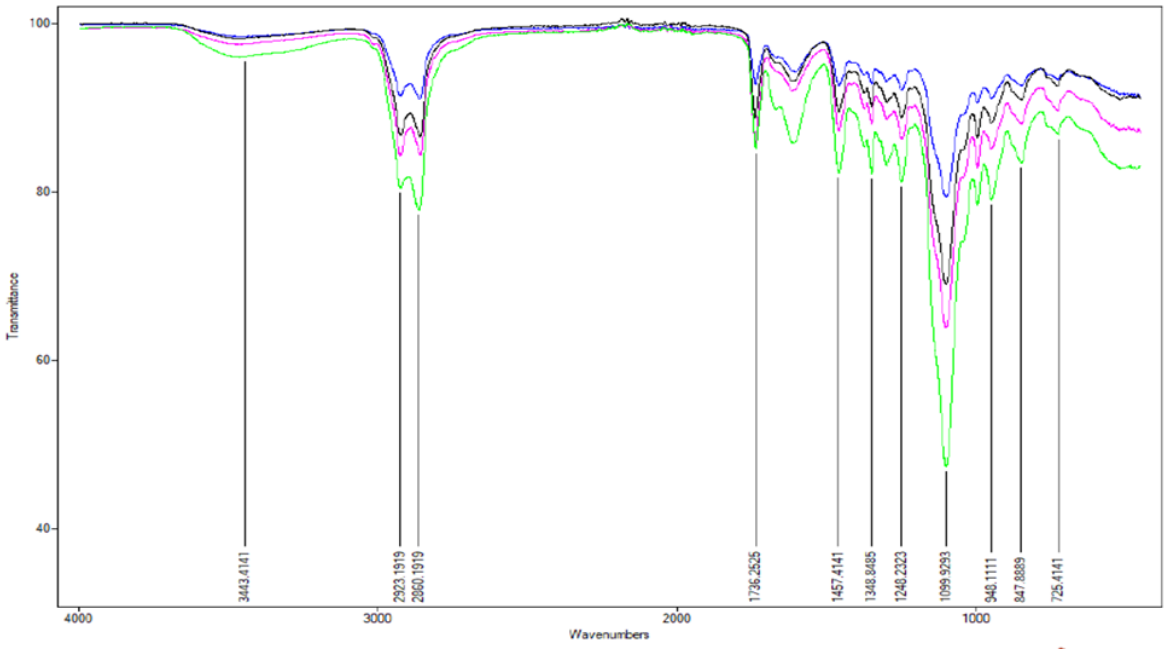

Figure S2. IRs of Jeffamine ED900-Graphene Systems

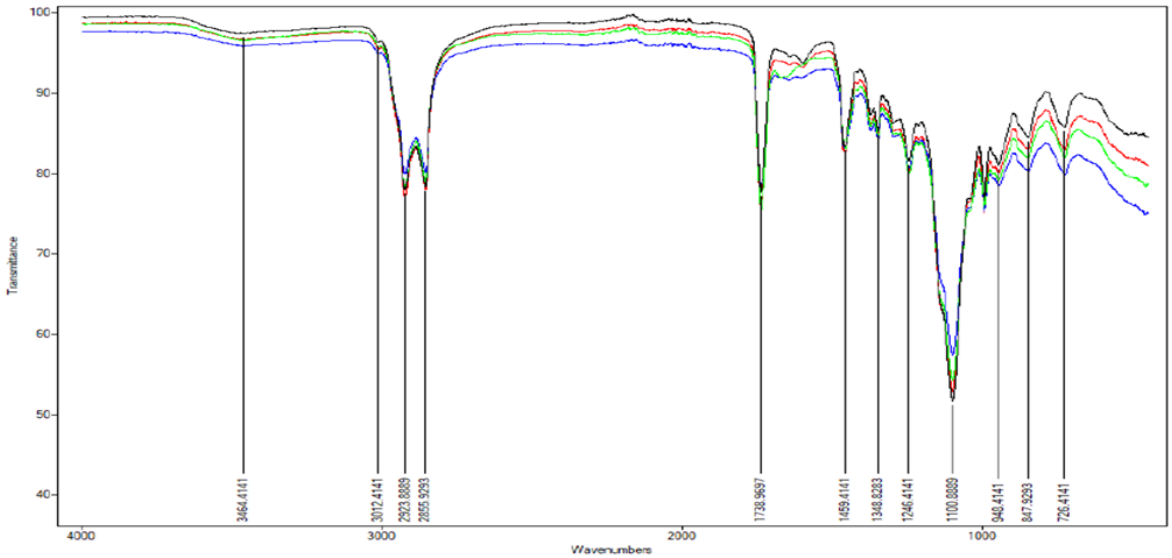

Figure S3. IRs of Jeffamine ED900-CNT Systems

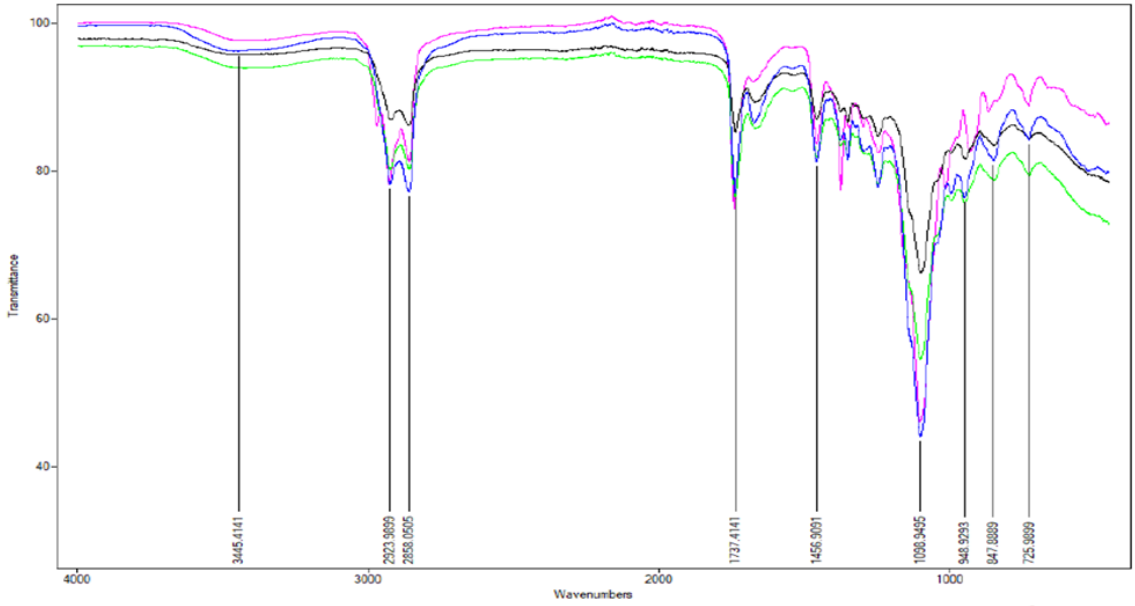

Figure S4. IRs of Jeffamine ED900-Fullerene Systems

T.C.

AYDIN ADNAN MENDERES UNIVERSITY

GRADUATE SCHOOLOF NATURAL AND APPLIED SCIENCES

SCIENTIFIC ETHICAL STATEMENT

I hereby declare that I composed all the information in my master's thesis entitled “Synthesis and Characterization of New Bio-Based Epoxide Nanocomposite Coatings Alternative to Bisphenol-A” within the framework of ethical behavior and academic rules, and that due references were provided and for all kinds of statements and information that do not belong to me in this study in accordance with the guide for writing the thesis. I declare that I accept all kinds of legal consequences when the opposite of what I have stated is revealed.

Samer Obaid Hasan HASAN

03/08/2021